Studies on molecular mechanisms of lipid metabolism in Japanese flounder *Paralichthys olivaceus* and red seabream *Pagrus major*

(ヒラメ ***Paralichthys olivaceus*** およびマダイ ***Pagrus major*** における脂質代謝メカニズムに関する研究**)**

Anurak Khieokhajonkhet

アヌラック キョウカジュンケット

2014

Studies on molecular mechanisms of lipid metabolism in Japanese flounder *Paralichthys olivaceus* and red seabream *Pagrus major*

(ヒラメ *Paralichthys olivaceus* およびマダイ *Pagrus major* における脂質代謝メカニズムに関する研究)

A Thesis

Submitted to

The Graduate School of Agricultural and Life Sciences

The University of Tokyo

in partial fulfillment of the requirements

for the degree of

Doctor of philosophy

in

The Department of Aquatic Bioscience

By

Anurak Khieokhajonkhet

2014

DEDICATION

This thesis is dedicated to my lovable father, mother, elder brother for their enormous support and sacrifices, love and endless support

List of Publications

Parts of work described in this dissertation have been published in the following journals:

Khieokhajonkhet, A., Kaneko, G., Ohara, K., Shirakami, H., Ushio, H. 2014. Hormone-sensitive lipase in Japanese flounder *Palalichthys oilicaceus* function of the inclinator muscle of fin as a lipid storage site. Fisheries Science 80: 1-11.

Acknowledgements

First and foremost I would like to thank and sincere gratitude to all of my advisors who give valuable advises, while I was lucky to have five the best trainer me during my experiment.

First, I would like to deeply gratitude my advisor Professor Shugo Watabe and Dr. Gen Kaneko for accepting me an opportunity to work in an interesting project and to be a student at The University of Tokyo, teaching, guiding and supporting me so much about genetics and molecular techniques, advising to submit my publication.

I would also like deepest to thank Professor Hideki Ushio for supporting and encouraging me during my study and give me much invaluable guidance for my experiment and thesis dissertation.

I would like to show my gratitude to Professor Shuichi Asakawa and Dr. Shigeharu Kinoshita to give me many suggestions and resolutions for better experiment.

I would like to thanks the other members of my thesis committee, Professors Shigeki Matsunaga and Professor Toyoji Kaneko.

My sincere thanks go to Dr. Misako Nakaya, Dr. Hina Satone, Dr. Kazuyuki Ohara, Dr. Muhammad Mehedi Hasan, Ms. Yuki Hirano, Ms. Moemi Oba and Ms. Wang Lu for helping me during the research experiment.

I would like to thank Naresuan University for financially support under the staff development scholarship from Naresuan University, Phitsanulok, Thailand.

There are countless with other peoples in the laboratory of Marine Biochemistry and the laboratory of Marine Biochemistry and Aquatic Molecular Biology members who have helped the author of technically and personally.

Most importantly, I of course cannot forget to thank so much my family who give me tremendous encouragement and support me during living out of my home country.

Contents

List of Abbreviations

ALBP	: Adipose lipid binding protein
ANOVA	: Analysis of variance
ATGL	: Adipocyte triacylglycerol lipase
AUAP	: Abridged universal amplification primer
BLAST	: Basic local alignment search tool
BSA	: Bovine serum albumin
β-AR	: β-adrenergic receptor
cAMP	: Cyclic adenosine monophosphate
cDNA	: Complementary deoxyribonucleic acid
CE	: Cholesteryl ester
cGMP	: Cyclic guanosine monophosphate
DAG	: Diacylglycerol
DDBJ	: DNA data bank of Japan
DIG	: Digoxigenin
DNTP	: Deoxyribonucleotide triphosphate
EMBL	: European molecular biology laboratory
ERK	: Extracellular signal-regulated kinase
FFA	: Free fatty acid
GH	: Growth hormone
HSL	: Hormone-sensitive lipase
kDa	: Kilo Dalton
MAG	: Monoacylglycerol
MAPK	: Mitogen-activated protein kinase

MGL	: Monoacylglycerol lipase
mRNA	: Messenger ribonucleic acid
MEGA 5.1	: Molecular evolutionary genetics analysis 5.1
Mw	: Molecular weight
NEFA	: Non-esterified fatty acids
PAGE	: Polyacrylamide gel electrophoresis
PBS	: Phosphate buffered saline
PBST	: Phosphate buffered saline tween-20
PCR	: Polymerase chain reaction
PFA	: Paraformaldehyde
p*I*	: Isoelectric point
PDE 3B	: Phosphodiesterase 3B
PKA	: Protein kinase A
PKB	: Protein kinase B
PKC	: Protein kinase C
PVDF membrane	: Polyvinylidene difluoride membrane
3'-RACE	: Rapid amplification of cDNA 3'-ends
5'-RACE	: Rapid amplification of cDNA 5'-ends
Real-time PCR	: Real-time polymerase chain reaction
RNA	: Ribonucleic acid
RT-PCR	: Reverse transcription polymerase chain reaction
SDS-PAGE	: Sodium dodecylsulfate-polyacrylamide gel electrophoresis
TAG	: Triacylglycerol

TBS	: Tris-buffered saline
TBST	: Tris-buffered saline tween-20
TLC	: Thin layer chromatography
Tm	: Melting temperature
Tris	: Tris (hydroxymethyl) aminomethane
UTR	: Untranslated region

List of Tables

List of Figures

Abstract

Lipid stored tissue plays a major role in free fatty acid supply for whole body energy homeostasis. The lipid in the form of triacylglycerol (TAG) is hydrolyzed by catalytic enzymes into free fatty acid (FFA) and glycerol. Hormone-sensitive lipase (HSL) is one of those catalytic enzymes which have an important role in lipolysis in mammalian adipose tissue. In fish, lipids are mainly deposited in three organs, adipose tissue, liver and skeletal muscle. Different fish species are likely to deposit lipid in the different types of organs, known as "tissue- and species-specific" manners. However, the process of HSL-mediated lipolysis in fish is poorly documented and remains unclear, which leads to misunderstanding and contradictory in our knowledge of lipid metabolism.

In order to clarify the function of fish HSLs, HSL cDNAs were cloned from two different species: Japanese flounder *Paralichthys olivaceus*, mainly stored their lipid in inclinator muscle of fin, and red seabream *Pagrus major*, mainly in visceral adipose tissue. The full-length cDNAs of two HSL genes were determined and designated as HSL1 and HSL2. In Japanese flounder, HSL1 and HSL2 consisted of 2,922 bp and 2,832 bp, respectively, while 2,955 for HSL1 and 2,723 bp for HSL2 were observed in red seabream. Additionally, proteins encoding HSLs were 702 and 837 amino acids in Japanese flounder, and 710 and 874 amino acids in red seabream, respectively. The molecular mass of Japanese flounder showed that the HSLs protein migrated on SDS-PAGE exhibited an apparent molecular mass of approximately 96 kDa of HSL1 and 125 kDa of HSL2. On the other hand, HSL1 protein of red seabream has molecular

mass of 98 kDa. However, HSL2 protein was not observed in red seabream. The deduced amino acid sequences of HSL1 and HSL2 genes shared 58.7% identity in Japanese flounder and 55% identity in red seabream. The identity of HSL1 and HSL2 in both of Japanese founder and red seabream showed about 57- 89%, and 60-73% with HSLs from rainbow trout *Oncorhynchus mykiss*. The multiple amino acid alignment with other species clearly showed that HSLs of the present study were comprised of two major domains; N-terminal and C-terminal, which were separated by glutamine and aspartate (Gln316 and Asp317 in Japanese flounder HSLs and, Gln322 and Asp323 for HSL1, and Gln355 and Asp356 for HSL2 of red seabream, respectively). Three amino acid residues comprising the catalytic triad were conserved in all HSLs. The multiple alignments also showed that both Japanese flounder and red seabream HSLs also have several serine residues aligned with the potential phosphorylation sites of rainbow trout HSLs, but these were misaligned with the rat and human HSL of phosphorylation sites. Several phosphorylation motifs of mammalian PKA (R/K-R/K-X-pS/T or R/K-R/K-X-X-pS/T) were also conserved to both species.

Tissue distribution of HSLs performed by RT-PCR found that the HSL transcripts of the Japanese flounder genes were abundant in the inclinator muscle of fin, liver, and skeletal muscle, whereas the highest transcripts were observed in adipose tissue and gonad in red seabream. The relative mRNA levels revealed that the transcripts of HSL1 and HSL2 genes were broadly expressed in all tested tissues. The relative mRNA levels of HSL2 were lower than HSL1 in both Japanese flounder and red seabream, suggesting that HSL2 has a minor function in the hydrolysis of stored lipid. In addition, the relative mRNA levels

and HSL proteins were accumulated in the different tissues, being significantly higher in inclinator muscle of fin for Japanese flounder, whereas the highest HSLs mRNA expression was observed in adipose tissue and gonad for red seabream. HSL protein further showed that HSL1 immunoreactive bands were observed in adipose tissue and gonad. The present data confirm that the expression of HSL is tissue- and species-specific.

The present study found that the inclinator muscle of fin contained high amount of lipid in adipocytes aligned along the muscle fiber cells as revealed by oil red O staining. *In situ* hybridization showed that HSL1 transcripts were accumulated in the peripheral region of adipocyte in the inclinator muscle of fin in Japanese flounder. HSL2 of Japanese flounder and HSLs of red seabream were not observed in this study. Total lipid from inclinator muscle of fin and skeletal muscle were subjected to thin layer chromatography (TLC) in order to characterized lipid class compositions in the tissues. Cholesteryl esters and FFA were detected in the inclinator muscle of fin, but were not found in skeletal muscle. Accordingly, the present study suggests that adipocytes in the inclinator muscle of fin are lipid storage sites, which would possibly release FFAs for the fin continuous movement through the HSL-mediated lipolysis in Japanese flounder.

The effects of nutritional and endocrine regulations on HSL mRNA expression were examined using red seabream as a model organism. For nutritional regulation experiment, red seabream were fasted for 7 days and then refed for three days. HSL mRNAs in both adipose and liver tissues of fasted red seabream were rapidly increased from day 4 until day 7. Furthermore, HSL1 and

HSL2 mRNA expressions in adipose tissue was higher than the expression found in liver tissue. Fasting resulted in depletion of stored lipid in mesenteric fat and liver, and this action was reversed to normal state by re-feeding. Fasting condition increased the expression of HSL1 mRNA to a greater extent than that HSL2 mRNA. The present findings indicate that fasting condition associated with lipid depletion is accompanied by increasing HSL expression.

Sliced tissues of three organs including adipose tissue, liver and skeletal muscle of red seabream were incubated with 3 concentrations of insulin and 4 different time ranges. HSL1 and HSL2 mRNA expression levels were suppressed by insulin treatment compared to control in both adipose and liver tissues in concentration and time dependent manners. These results also suggest that HSL would be inhibited during insulin incubation, owing to dephosphorylation of HSL. The suppression of HSL phosphorylation was due to a decrease of cAMP, caused by phosphodiesterase 3B activation via PI-3K activation by insulin. In contrast, the expression of HSL1 was inhibited, whereas HSL2 was dramatically increased in skeletal muscle. To study the induction of GH on HSL mRNA expression, HSL mRNA levels in liver and mesenteric fat were performed under incubation in the presence of 3 concentrations of GH for 1, 4 and 10 h. The results suggest that GH stimulates HSL expressions in liver and adipose tissue and linearly increases until 10 h incubation. The present studies clearly demonstrate that GH stimulates HSL mRNAs in both of time- and concentration-related manners.

In conclusion, Japanese flounder and red seabream possess HSL encoding mRNAs that express tissues in different tissue. Their transcripts and

HSLs protein were ubiquitously expressed in various tissues. The HSL mRNA levels were markedly high in the inclinator muscle of fin for Japanese flounder where TAG, CE, and FFA were accumulated. The transcripts of HSL1 were localized in adipocytes of the inclinator muscle of fin. These results suggest that the adipocyte around the inclinator muscle of fin is a supplier of FFA in Japanese flounder, and that HSL-mediated lipolysis provides FFAs for the continuous and aerobic movement of fins. Fasting condition stimulated the expression of the two HSL mRNAs in major lipid depots in a tissue-specific manner. The HSL mRNAs, HSL1 and HSL2 are differentially expressed within and among tissues, and state of nutrition would modulate the pattern of HSL expression in part via hormonal regulations such as insulin and GH.

General introduction

Lipid distribution and metabolism in fish

Most of animals, including teleost fish, utilize their energy for maintenance, regulation and repair of their life. The main sources of energy are obtained by macromolecules: including, protein, carbohydrate and lipid (De Vlaming and Pardo 1975). These nutrients are utilized for energy generation to maintain their lives. Adipocyte triacylglycerol is a site to store an excess energy in form of triaclyglycerol in lipid droplets (Nicole and Bickel 2008). In poikilothermic vertebrates, the pattern of lipid storage and deposition are more diverse in fish. For example, lipids are accumulated in three major organs, mesenteric fat, liver and skeletal muscle, in a species-specific manner (Oku et al. 2000; Ando et al. 1993; Kaneko et al. 2013).

In fish, adipose tissue is an important site for lipid accumulation, although some species deposit their lipid in liver or muscle as storage site. In salmonids, adipose tissues are found in the abdominal cavity, including mesenteric and pyroric ceaca. Torafugu and Japanese flounder normally accumulated lipid in the liver tissue (Ando et al. 1993). In gilthead seabream and red seabream, lipid is predominantly stored in visceral adipose tissue (Kaneko et al. 2013). It has been known that fish and mammalian adipose tissue is naturally influenced by seasonal changes. High fat content in diet can lead to increase adipocyte mass in Atlantic salmon (Planas et al. 2000). Fish exhibits unique aspects on lipid accumulation and metabolism, and stores lipid in several tissues,

such as mesenteric fat, liver and skeletal muscle, unlike other mammalians that store lipid in adipose tissue (Kittilson et al. 2011). Fish stores lipid in form of triacylglycerol (TAG) and complex free fatty acid (FFA) with long chain length and high degree of unsaturation.

Lipolysis of adipocyte triacylglycerol stores results in the liberation of FFA that will be supplied for other requiring tissues. The release of metabolic energy, in the form of FFAs, is regulated through several hormonal and others biochemical controls. However, the studies of hormonal regulations in fish are limited, and the results are largely controversial. Harmon and Sheridan (1992) found that fasting caused a significant decrease in total body mass, mesenteric fat mass, plasma insulin levels and IGF-I in 45 fasted rainbow trout *Oncorhynchus mykiss*. In addition, fasting for 24 and 72 h resulted in increase lipase activity in rainbow trout (Geromel and Montgomery, 1980). Glucagon is responsible to increase blood glucose levels and simultaneously stimulates the breakdown of stored lipid by increasing cAMP, leading to the phosphorylation and activation of HSL. Glucagon stimulates the lipolytic activity with releasing FFA *in vivo* of reptile tissue. However, catecholamine and glucagon are unable to regulate the release of FFA from adipose tissue of wolf fish, toadfish, and snakefish (Migliorini et al. 1992).

In a fasting state, several organisms show various responses physiologically and behaviorally to maintain their metabolic needs. This process requires the hydrolysis of stored lipids for energy production. It has been documented that blood glucose concentration was generally suppressed in a fasting state, leading to a decrease in insulin secretion and rise in glucagon

secretion (Golay et al. 1986; Chambrier et al. 1990). Fasted rainbow trout is associated with growth retardation and lipid deprivation that mediated by the hydrolysis of HSL (Kitillsen et al. 2011) in accordance with mammalian cases. Fasting also affected the increase of glucagon stimulating lipolysis in liver of rainbow trout (Harmon and Sheridan 1992) and adipose tissue of gilthead seabream (Albala et al. 2005). Further investigations are needed to detail the role of possible lipolytic/antilipolytic hormones in the endocrine control of adipocytes in teleost fish.

In particular, antilipolytic action is mediated by insulin, however; the investigated on the effect of insulin on adipose tissue was rarely documented in fish. Rainbow trout injected with insulin showed that plasma FFA concentration dramatically decreased with the reduction in hepatic triacylglycerol lipase activity (Sheridan and Harmon 1992). In fish, insulin injection had an effect to reduce the concentration of plasma FFA also in goldfish (Minick and Chavin 1972) and northern pike (Ince and Thorpe 1975), indicating that insulin most likely regulates the antilipolytic action. In addition, Sheridan and Harmon (1992) showed the reduction in the insulin activity and the elevation of glucagon-stimulated lipase activity in fasted rainbow trout.

Growth hormone (GH) is a complex hormonal regulator. GH is controlled under the central nervous system (CNS) in a large extent of pituitary by several integrated intracellular signaling. GH directly stimulates adipocyte lipolysis leading to release FFA and glycerol (Carroll et al. 2004; Chavez et al. 2006). GH deficiency shows an increase of body weight and body visceral fat mass (Roemmich et al. 2001) and several studies in GH deficiency showed that

GH induced obesity in mice (Joosten et al. 1975; Meyer et al. 2004; Luque et al. 2006). In fish, the studies on GH regulation in nutrition deprivation and lipolysis are limited. Deng et al. (2004) reported that GH levels are elevated in starved black seabream (Deng et al. 2004). In coho salmon implanted hepatic tissue incubated with GH *in vivo*, GH caused lower fat deposition in liver and increased hepatic lipase activity leading to a hydrolysis of stored lipid in liver (Sheridan 1986). More recently, Bergan et al. (2013) found that GH activates protein kinase C (PCK) and extracellular signal-regulated kinase (ERK), leading to phosphorylation of Ser600 of hormone-sensitive lipase (HSL, see below) and enhancement of the lipolysis in rainbow trout.

Lipolysis of adipocyte

The adipose tissue is an important site for hydrolysis of TAG into FFA and glycerol for whole body energy homeostasis. Adipose tissue stores lipid in the TAG-form, which is hydrolyzed into FFA in response to the following demands of peripheral tissues. These mechanisms take place during high energy requirement, for example hibernation, reproduction, fostering and fasting. Adipose tissue is also an endocrine organ that secretes a variety of hormones to harmonize whole body fuel metabolism (Erin and Jeffrey 2004).

The catalytic process in adipose tissues is mediated by three main enzymes including monoacylglycerol lipase (MGL), HSL, and adipocyte triacylglycerol lipase (ATGL), which complete the adipocyte lipolysis. The degradation of TAG firstly cleaves by ATGL. ATGL preferentially hydrolyzes

TAG to diacylglycerol (DAG), then followed by HSL which hydrolyzes DAG to form MAG and monoacylglycerol lipase (MGL) which finally cleaves MAG to FFA and glycerol (Lampidonis et al. 2011). HSL is a ubiquitous enzyme and has broad substrate specificity, since HSL preferentially hydrolyzed long-chain fatty acyl chain esters in forms of TAG, DAG and MAG, as well as cholesteryl- and retinyl-esters (Kraemer et al. 2002; Fig 0-0-1B). The hydrolytic activity of HSL against DAG is higher than those of against TAG and MAG, 10 to 12 fold and 5-10 fold, respectively, indicated that HSL catalyze DAG better than TAG. HSL preferentially cleaves TAG at *sn*-1 or *sn*-3 ester position in its structure. HSL activity against *sn*-3 ester bond is 3 to 4 folds higher than the *sn*-2 ester bond (Kreamer and Shen, 2002). In addition, the participations of MGL and ATGL are needed to complete the adipocyte lipolysis (Lass et al. 2011).

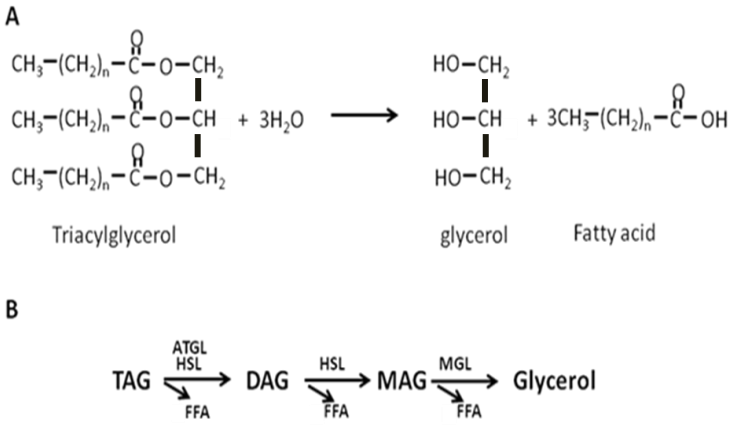

Figure 0-0-1. Hydrolysis of triacylglycerol (TAG) into three molecules of free fatty acid and one molecule of glycerol (A). The flow scheme represents hydrolysis of triacylglycerol (TAG) into diacylglycerol (DAG) and monoacylglycerol (MAG) with responsible catalytic enzymes (B; cited from Lampidonis et al. 2011).

Regulation of HSL

HSL has a unique feature to differentiate among the others lipases groups with against TAG and cholesteryl ester substrates regulated by phosphorylation as explained briefly in the above. HSL constitutes a highly regulated enzyme that mediates lipolysis in adipocytes. HSL activity appears to be regulated by site-specific phosphorylation of serine residues. Several studies demonstrate that HSL can be phosphorylated through protein kinase A (PKA), leading to increases the catalytic activity of HSL (Holm et al. 2003; Krintel et al. 2009). Phosphorylation sites have been found with five serine residues (Ser563, Ser565, Ser600, Ser659 and Ser660 for rat numbering). These sites are also conserved in human, corresponding to Ser552, Ser554, Ser589, Ser649 and Ser650, respectively. Catecholamine is a hormonal control that stimulates HSL activity by increasing an intracellular cyclic AMP (cAMP) concentration through β-adrenergic receptor (β-AR), leading to an activation of protein kinase A (PKA) (Contreras et al. 1998; Watt et al. 2006). Three major sites of HSL phosphorylation, Ser563, Ser569 and Ser660, activated through PKA have been reported (Martin et al. 2009). It has been reported that Ser659 and Ser660 were required for HSL activity, whereas phosphorylation of Ser563 did not have a direct effect on the catalytic activity (Lampidonis et al. 2011).

The regulatory site is considered to have an important role in HSL activation. HSL lipolytic activity is activated by the catecholamine hormone through β-AR, whereas insulin has the reverse effect on HSL phosphorylation, reducing HSL enzymatic activity (Fig. 0-0-2). In contrast to phosphorylation, dephosphorylation by phosphatase plays an important role in HSL suppression

(Martin et al. 2009). Some studies clearly showed that phosphatase has the critical regulating role in the anti-lipolytic effect of insulin. Ser565 is a major site for dephosphorylation (Kraemer and Shen, 2002).

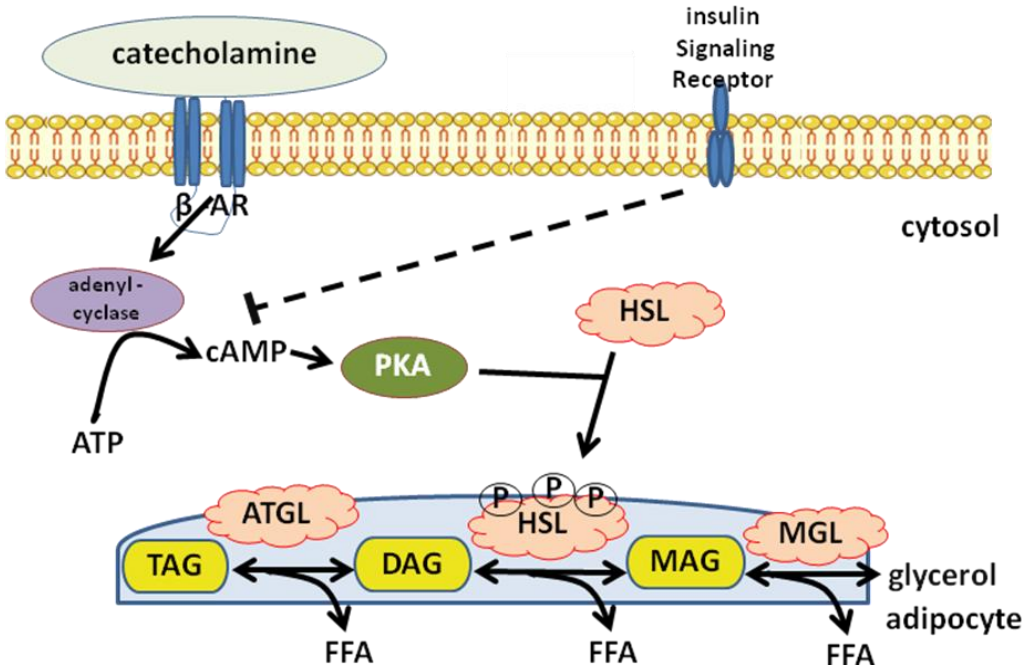

Figure 0-0-2. Regulation of stimulated hormone-sensitive lipase (HSL). HSL is located in the cytosol in an unstimulated condition. Catecholamines bind to β-adrenergic receptors (β-AR) in a stimulation condition, activating a G protein-mediated signaling, followed by cyclic AMP (cAMP) release by adenylate cyclase. The cAMP stimulates protein kinase A (PKA), resulting to phospholylate HSL.

Structure of HSL

The primary structure of HSL is unrelated to any other mammalian lipases, including lipoprotein lipase, pancreatic lipase and hepatic lipase. HSL had no homology found with any biological protein in mammal. However, HSL shows a homology similar to HSL of Antarctic bacterium, *Moraxella sp*. (TA144). HSL could have cold tolerance adaptability, indicating that HSL could probably have high activity at low temperature (Langin et al. 1993). An extensive study on HSL found that HSL is a member of lipase family and also belongs to esterase subfamily of a newly described superfamily of lipase/esterases (Cygler et al. 1993; Shen et al. 2001). The molecular weight of rat HSL protein is 84,000 Da, corresponding to 768 amino acids. Human HSL cDNA encoded 775 amino acid proteins corresponding to 84,032 Da and showed 88 kDa immunoreactive proteins. HSL molecular mass has been reported from several protein species of non-adipose and adipose tissues ranging from 26 to 130 kDa (Casado et al. 2012; Kraemer et al. 1993). HSL has at least three isoforms mainly found in adipose tissue and testis. In testis, it appears to have 2 isoforms and the molecular mass is approximately 120-130 kDa, which is larger than HSL protein in adipose tissue, where 88 kDa for human slightly larger than 84 kDa for rat adipose tissue and 82 kDa for mouse and guinea-pig (Holm et al. 1989; Chung, et al. 2001). HSL amino acid shares catalytic sequence at the similar sites of other lipases, representing G-X-S-X-G motif, which is a consensus lipid binding sequence. The catalytic sequence of rat HSL is conserved between 421 and 425 (Holm et al. 1994).

HSL sequence analysis and molecular modeling have been extensively studied in various species, suggesting that HSL contains 2 major domains, N-

terminal and C-terminal domains. The N-terminal portion of the adipocyte enzyme apparently comprises approximately 320 residues, mediates protein–protein interactions, and possibly binds together with lipid (Yeaman 2004). Moreover some studies have identified residues 192-200 as being critical for the interaction with fatty acid binding protein 4 (FABP4), with site-specific mutagenesis, indicating a specific role of His194 and Glu199. The C-terminal is comprised of 450 amino acids, which are similar to the secondary structure of acetylcholinesterase, bile salt-simulated lipase and fungal lipase from *Geotrichum candidum* and *Candida rugosa*. It was reported that Ser423, Asp703 and Ser733 represent as the catalytic triad for HSL in C-terminal domain (Lampidonis et al. 2011).

Lipolysis is known to be enhanced by the increase of intracellular cAMP levels and subsequent PKA-dependent phosphorylation of HSL. Phosphorylation on Ser563 Ser659 and Ser660 are required for the activation of rat HSL. Since fish HSLs probably have lipolytic functions, they might be activated by the cAMP/PKA pathway as well. In fish, the recent study showed that HSL of rainbow trout sequences have a sequence gap around AA530-570 of both HSL isoforms, leading to be shorter than of mammalian HSLs (Kitillsen et al. 2011). Based on the multiple alignments, amino acids of catalytic triad were conserved of Ser424, Asp698 and His723 in rainbow trout. Three of four phosphorylation sites were further identified to Ser541, Ser543, Ser592 and Ser594 which conserved to Ser552, Ser554 and Ser660 of human HSL. The putative PKA phosphorylation sites have been investigated in fish HSLs, and found serine residues probably correspond to Ser563 of rat HSL. However, no

other putative PKA phosphorylation site was found in fish HSLs, suggesting the regulation of other signaling pathways. Alternatively, the PKA in fish cannot rule out the possibility that PKA recognizes the amino acid sequence different from the mammalian PKA.

Objective of this study

As stated above, TAG in stored tissues mainly found in adipose tissue, liver and skeletal muscles are hydrolyzed into glycerol and three free fatty acids. This occurs when energy is needed in term of fasting or stress. In general, stored lipid is influenced by de novo lipid synthesis and by deposition from various plasma lipoproteins. Lipolysis is mainly modulated by the action of HSL. So far, the HSL cDNA sequence has been documented for human (Langin et al. 1993), rat (Holm et al. 1988), mouse HSLs (Li et al. 1994) and rainbow trout HSL, which is the first study in fish species (Kittillson et al. 2011). However, the molecular mechanism regarding to their distribution and the effect of hormonal controls on lipid metabolism in fish remains largely unclear. In order to understand the molecular mechanism and hormonal control of HSL, Japanese flounder and red seabream were investigated. The purposes involved in the present study are as follows:

1. Genetical characterization of HSL genes in Japanese flounder and red seabream.

2. Elucidation of tissue distribution and its expression pattern of HSL genes in Japanese flounder and red seabream.

3. Effects of nutritional state and cytokines on HSL mRNA expression in red seabream.

Synopsis of chapters

This thesis consists of general introduction and four chapters. Chapter I deal with molecular cloning and characterization of HSL in Japanese flounder and red seabream. The tissue distribution of HSL and localization of adipose tissue were investigated in Chapter II. The effects of nutritional state and cytokine on HSL mRNA expression in red seabream were performed in chapter III. Chapter V was dedicated for general discussion based on the results obtained in each chapter.

In chapter I, cDNA encoding two isoforms of HSLs have been cloned and characterized in Japanese flounder, *Paralichthys olivaceus* and red seabream, *Pagrus major*. The HSL cDNAs of two HSL genes from Japanese flounder were cloned from inclinator muscle of fin and adipose tissue and gonad of red seabream using degenerate primer. The full-length cDNAs of two HSL genes, designated HSL1 and HSL2, consisted of 2,922 bp and 2,832 bp of HSL1 and HSL2, respectively in Japanese flounder, while 2,955 and 2,723 bp of HSL1 and HSL2, respectively in red seabream. Proteins encoding HSLs were 702 and 837 amino acids in Japanese flounder, and 710 and 874 amino acids in red seabream, respectively. The molecular masses of Japanese flounder were performed in skeletal muscle and inclinator muscle using immunoprecipitation. In red seabream, the molecular mass of HSL1 protein was detected in adipose and gonad using immunoblot analysis whereas, HSL2 protein was not observed. The multiple amino acid alignment from various species, including Japanese flounder, red seabream, rainbow trout, rat and human HSLs showed that the basic

constitutions were conserved. Three amino acid residues of catalytic triad sites and phosphorylation sites were conserved to all HSLs. The phylogenetic analysis reveals that HSLs from Japanese flounder and red seabream were distinctly separated to mammalian organisms and located at the same clade as HSLs from bony fish.

Chapter II deals with localization of adipose tissue, tissue distribution of HSLs genes and proteins, lipid classification and *in situ* hybridization. To localize adipose tissues, oil red O was used to perform in Japanese flounder fillet. Oil red O was stained in the inclinator muscle of fin and highly observed in the subcutaneous layer of the blind side. Tissue distributions were amplified by RT-PCR using HSL specific primers in nine tissues including the fin, gill, heart, intestine, liver, skeletal muscle, inclinator muscle of fin, skin and gonad from Japanese flounder, and adipose tissue, fin, gill, heart, intestine, liver, muscle, skin and gonad from red seabream. Their expressions were further studies by more accurate quantitative real-time PCR. The abundance of each HSL mRNA was varied by tissues. HSLs were most abundant in the inclinator muscle of the fin in Japanese flounder, while HSL1 and HSL2 mRNA expression were highly expressed in adipose tissue and gonad in red seabream. Immunoblot analysis was further performed to clarify on HSL protein expression pattern. *In situ* hybridization was performed to localize the transcripts of HSL1 in Japanese flounder and red seabream. HSL1 transcripts were accumulated in the peripheral region of adipocyte cells of the inclinator muscle of fin in Japanese flounder. Meanwhile, HSL1 transcripts were detected in the bone, gill, intestine and gonad in red seabream. In order to evaluate the FFA releasing through the HSL mediates

lipolysis, the lipid classification in inclinator muscle of fin and skeletal muscle was investigated by using thin layer chromatography (TLC). TLC detected CE and FFA in the lipid extracted from the inclinator muscle of fin, suggesting that the inclinator muscle of fin is a site of lipid storage which releases FFAs mediated by HSL lipolysis in Japanese flounder.

Chapter III deals with the effects of nutritional state and cytokines on HSL mRNA expression in red seabream were studied. The first experiment is to understand their expression levels of HSL genes at several sampling points of fasting and re-feeding in the adipose tissue and liver. The nutritional state was carried out totally 10 consecutive days, including 4 day fasted, 7 days fasted, 8 days re-feeding and 10 day re-feeding. Fasted for 4 days resulted in elevation of HSL1 and HSL2 and continued increasing in day 7, an action that was reversed by refeeding in both tissues. The effects of insulin on HSL expression levels in adipose tissue, liver and skeletal muscle incubated with 3 different concentrations of insulin. The results revealed that insulin suppressed HSL mRNA expression in both HSL1 and HSL2 of red seabream in adipose tissue and liver but not in the skeletal muscle. To study the effects of GH mediates HSLs lipolysis in adipose tissue and liver. The results showed that GH mediated lipolysis by elevating HSL mRNAs expression levels. Relative mRNA levels of the target genes were determined by a comparative Ct method with reference to that of β-actin genes as internal control and the normalized Ct values.

Finally, Chapter IV is culminated with general discussion based on the present study to identify a possible aspect of applications and scope to the future studies.

Chapter 1

Molecular cloning and characterization of hormone-sensitive lipase in Japanese flounder *Paralichthys olivaceus* and red seabream *Pagrus major*

The cDNA encoding HSL was firstly isolated from rat adipose tissue in 1988 (Holm et al. 1988). After that HSL genes were cloned from several eukaryotic organisms including human (Holst et al. 1996), rat and mice (Holm et al. 1988), swine (Harbitz et al. 1999) and ovine (Lampidonis et al. 2008). Interestingly, Antarctic bacteria, *Moraxella* TA144 also have lipases homologous to HSL family protein (Choo et al. 1998). This finding suggests that prokaryotic organisms would be an origin of lipolysis mediated by HSL.

According to the amino acid alignment, HSL protein can be divided into two main domains. The N-terminal domain of rat and human HSLs is composed of 1-315 amino acids and the rest is the C-terminal region. The N-terminal region is linked to the adipose lipid binding protein (ALBP) and is distinctly different among each species (Holm et al. 2000; Shen et al. 1999). The rat and human HSLs share only 44% sequence identity in the N-terminal domain. On the other hand, the C-terminal region, which is absent in HSLs of prokaryotic organisms, consisted of two parts: regulatory module and catalytic core (GXSXG). The regulatory module contains the serine residues phosphorylated by protein kinase A (PKA). The HSL phosphorylation occurs at least five serine residues including Ser563, Ser565, Ser600, Ser659 and Ser660 of rat amino acid

sequence numbering. Ser563, Ser659, and Ser660 are the major sites for PKA phosphorylation, whereas Ser563 indirectly affects the catalytic activity (Lampidonis et al. 2011). Ser565 is phosphorylated by AMP-activated protein kinase and Ca^{2+}/calmodulin-dependent protein kinase II, and this site may decrease phosphorylation leading to suppression of human HSL activity (Daval et al. 2005; Lampidonis et al. 2011). The Ser600 is phosphorylated by extracellular signal-regulated kinase (ERK) in 3T3-L1 adipocytes, resulting in the increased activity of HSL (Green berg et al. 2001). In fish, HSL sequences from rainbow trout were elucidated and the multiple alignments showed that some basic structures including catalytic triad and phosphorylation sites were conserved in comparison with human HSL (Kitillsen et al. 2011). However, the HSL characterizations in fish have to be further investigated.

The purpose of this chapter is to clone HSL genes from Japanese flounder and red seabream. The deduced amino acid sequence of HSLs from both Japanese flounder and red seabream were analyzed from multiple alignment and phylogenetic analyses.

Section 1

cDNA cloning

In this section, the full-length cDNAs encoding HSLs were cloned and characterized from Japanese flounder and red seabream. In addition, molecular weight (Mw), multiple alignment, and evolutionary relationship were investigated.

Materials and Methods

Materials

Specimens of Japanese flounder (900-1,800 g) and red seabream (1,500-2,500 g) were purchased from a commercial dealer (Fish Interior, Tokyo, Japan). Fish were reared in fiber glass tanks. Experimental fish were fed with commercial diets *ad libitum* twice a day at 20°C under a 12 h light/dark cycle in indoor experimental facilities of The University of Tokyo. Fish were anesthetized with ice cold water for approximately 20 min prior to sampling. From Japanese flounder, fin, gill, heart, intestine, liver, skeletal muscle, inclinator muscle of fin, skin and gonad were sampled. Adipose tissue, fin, gill, heart, intestine, liver, skeletal muscle, skin and gonad were excised out from red seabream. The collected tissues were placed in RNAlater (Ambion, Cambridgeshire, UK) and immediately stored at -20°C until analysis.

RNA extraction and cDNA synthesis

Total RNA was extracted using Isogen (Nippon Gene, Tokyo, Japan) according to the manufacturer's protocol. Purification of mRNA containing poly (A) tail was carried out using Oligotex-dT30 Super (Takara, Otsu, Japan). The quantity RNA was measured from the absorbance at 260 and 280 nm using spectrophotometer, whereas the quality was checked by gel electrophoresis. The total RNA was reversely transcribed to first-strand cDNA using enzyme SuperScript III reverse transcriptase according to the manufacturer's protocols. The reaction was performed at 48^{o}C for 90 min, and then was stopped by heating at 70^{o}C for 15 min. RNase H treatment was performed to remove the RNA template from cDNA/RNA hybrid molecule at 37^{o}C for 60 min.

Rapid Amplification of cDNA Ends (RACE)

Japanese flounder

PCR was performed with degenerate primers shown in Table 1-1-1. The PCR mixture of 20 µl contained 1 µl of the cDNA solution, 10 pmol of forward primer (HSLC1F_JF or HSLC2F_JF), 10 pmol of reverse primer (HSLC1R_JF or HSLC2R_JF), 0.2 µl of Ex *Taq* DNA polymerase (Takara, Otsu, Japan), 2 µl of 10X Ex *Taq* buffer, 4 nmol of dNTP mixture, and 14.2 µl of sterile and distilled water. PCR was carried out at 94°C for 2 min, followed by 40 cycles of 94°C for 30 s, 65°C for 45 s, and 72°C for 1.5 min with a final extension at 72°C for 5 min. The PCR products were separated by electrophoresis using 2% agarose

gels, purified from the gel using a FastGene gel/PCR extraction kit (Nippon genetics, Tokyo, Japan), and subcloned into pCR®4-TOPO vector using a TOPO TA cloning kit (Invitrogen). Sequencing was performed using an ABI PRISM 3130 genetic analyzer (Applied Biosystems, Foster City, CA, USA). Degenerate primers were designed based on the conserved region of other full-length and partial HSL of other species. The HSL gene sequences obtained from the first amplification will be used to determined 3'-RACE and 5'-RACE.

For 3'-RACE, total RNAs were extracted from the inclinator muscle of fin by using the RNeasy lipid tissue mini kit (Qiagen). First-strand cDNAs were synthesized with the SuperScript III reverse transcriptase and 10 pmol of Oligo-d(T) primer (Invitrogen). First PCR was carried out with the forward primer (HSLC1F1_JF3' or HSLC2F1_JF3') and GeneRacer 3' primer (Table 1-1-1). The positions of primers are showed in figure 1-1-1. The mixed solution contained Ex *Taq* DNA polymerase (Takara) as described previously. The PCR cycle consisted of 94°C for 2 min followed by 40 cycles at 94°C for 30 s, 60°C for 30 s, and 72°C for 30 s with a final extension at 72°C for 5 min. In the nested PCR, the 20 µl reaction mixture contained 1 µl of the first PCR products, 10 pmol the forward primer (HSLC1F2_JF3' or HSLC2F2_JF3'), 10 pmol of GeneRacer 3' nested primer (Invitrogen), 0.2 µl of Ex *Taq* DNA polymerase (Takara), 2 µl of 10X Ex *Taq* buffer, 4 nmol of dNTP mixture, and 14.2 µl of sterile and distilled water. The PCR was conducted at 94°C for 2 min of denaturation, followed by 40 cycles of 94°C for 30 s, 64°C for 30 s, and 72°C for 30 s with a final extension at 72°C for 5 min.

The 5'- end sequences of the HSL genes were determined using the GeneRacer kit (Invitrogen) and total RNAs extracted from liver. PCR was performed using Ex *Taq* DNA polymerase. The first PCR was carried out with the cDNA template, the gene-specific primer (HSLC1R1_JF5' or HSLC2R1_JF5'), and the GeneRacer 5' primer (Table 1-1-1). The nested PCR was conducted under the same conditions with either of HSLC1R2_JF5' or HSLC2R2_JF5' primer (Table 1-1-1), GeneRacer 5' nested primer (Invitrogen), and the first PCR product as the template. To ensure the sequences of open reading frame by a single PCR, two primer sets, HSLC1F3_JF and HSL1R3_JF for HSL1, and HSLC2F3_JF and HSLC2R3_JF of HSL2 were designed from 5'- and 3'- untranslated regions of Japanese flounder HSL1 and HSL2 (Table 1-1-1). The PCR was performed under the same condition as described above but with the annealing temperatures at 64°C and 60°C for HSL1 and HSL2 genes, respectively. The PCR products were purified and subcloned into pCR®4-TOPO vector using the TOPO TA cloning kit (Invitrogen), and subsequently sequenced as described previously.

Figure 1-1-1. Schematic diagram of the primer designs for HSL1 and HSL2 of Japanese flounder *Paralichthys olivaceus* and red seabraeam *Pagrus major*. The boxed area consists of white and gray colored ones, corresponding to the HSL open reading frame, 5' untranslated region (5'UTR) and 3' untranlated region (3'URT), respectively. The black arrows indicate the position of the first HSL amplification. The red and gray arrows show the position of primer used for 5'-RACE and 3'-RACE amplifications. An orange arrows show position of primers used for single amplification.

Red seabream

Total RNA extraction and first-strand cDNA syntheses were performed as described above using red seabream tissues. The first PCR was performed under the same condition with forward primer (HSLC1F_SB or HSLC2F_SB) and reverse primer (HSLC1F_SB or HSLC2F_SB). The 3'-end sequence of HSL genes were sequenced using GeneRacer 3' primer (Table 1-1-1). The PCR cycle consisted at 94°C for 2 min followed by 35 cycles at 94°C for 30 s, 59°C for 45 s and 72°C for 1.0 min with a final extension at 72°C for 5 min. In the nested PCR, 10 pmol of forward primer (HSLC1F1_SB3' and HSLC2F2_SB3'), and GeneRacer 3' nested primer (Invitrogen) were used. The PCR was conducted

at 94°C for 2 min followed by 40 cycles of 94°C for 30 s, 52°C for 30 s, and 72°C for 30 s with a final extension at 72°C for 5 min.

The 5'-end sequences of the HSL genes were determined using total RNAs extracted from liver and the GeneRacer kit (Invitrogen). PCR was performed using Ex *Taq* DNA polymerase under conditions described previously using the cDNA template, the gene-specific primer (HSLC1R1_SB5' or HSLC2R_SB5'), and the GeneRacer 5' primer (Table 1-1-1). The nested PCR was conducted under the same conditions with the combination of either HSLC1R2_SB5' or HSLC2R2_SB5' primer (Table 1-1-1), and GeneRacer 5' nested primer (Invitrogen). To ensure the sequences of open reading frame by a single PCR, two primer sets, HSLC1F3_SB and HSL1R3_SB, and HSLC2F3_SB and HSLC2R3_SB were designed from 5'- and 3'- untranslated regions (3'-and 5'-UTR) of red seabream HSL1 and HSL2 (Table 1-1-1). The PCR was performed under the same condition by changing the annealing temperatures to 62°C and 60°C for HSL1 and HSL2 genes, respectively. The PCR products were purified, subcloned into pCR®4-TOPO vector using the TOPO TA cloning kit (Invitrogen).

Subcloning and DNA sequencing

The PCR products were purified and ligated in the pGEM-T Easy Vector (Promega). After ligated, the *E. coli* (JM 109) competent cells were transformed by heat shock at 42°C for 30 s, plated on the LB plate and incubated at 37°C overnight. Inserted cDNA was confirmed by colony PCR using GoTaq Master Mix (Promega) with universal primers (SP6 and T7). Positive clones were

cultured in LB broth at 37°C for 18-24 h. The plasmids were extracted using Fast Gene Plasmid mini kit (Nippon genetics Europe GmbH, Tokyo, Japan). The labeling PCR was carried out with the extracted plasmid as template, a gene-specific primer or a universal primer, BigDye buffer and BigDye (Applied Biosystem, Warrington, UK). The PCR cycle consisted at 96°C for 2 min followed by 27 cycles at 96°C for 10 s, 50°C for 5 s and 60°C for 2 min without a final extension. The PCR products were purified with sequencing solution mixture containing 1.5 ml NaOAC (3 M), 31.25 ml 100% ethanol and 7.25 ml distilled water. The PCR product was added 40 µl of the sequencing solution and centrifuged at 5000 g for 30 min. The DNA pellets were then rinsed with 70% ethanol centrifuged for 15 min, and dried for 5 min after the supernatant was discarded. Finally, the PCR produce was added 15 µl HI-DI formamide (Life-Technology, USA), treated at 94°C for 3 min and immediately placed on ice for 3 min. The purified PCR products were subsequently sequenced by ABI Prism 3130 Genetic analyzer (Applied Biosystem).

Table 1-1-1. Nucleotide sequence of primers used for cDNA cloning.

Sequences 5'-3'	genes	Purpose
CCARGCGCYTGGTSACATG	HSL1	1st amplification
GGCTYAGGAAGCCATGWGG	HSL1	1st amplification
CCAGKGGTGATGGWCACCAARGC	HSL2	1st amplification
TKACACACCCCTATRGGTCC	HSL2	1st amplification
CACGCGCCGGCGGAACAT	HSL1	1st amplification
CACTATGTGTACAGGCGGCAGGCC	HSL1	1st amplification
CGGCCCTGTACAGCGTGTGC	HSL2	1st amplification
GAACCCTCCTCTCCACCAGGG	HSL2	1st amplification
GTTTACCCACAGGGCTTTGAGCC	HSL1	3'-NEST
GACGCCTTGCTGGATGAC	HSL1	3'-NESTED
GAAGAGCCAGACTTGCCAGGACTTGG	HSL2	3'-NEST
CAGTGGCCATACCACCACCTGCTG	HSL2	3'-NESTED
CCTTCTCGAAGCTCATAGGAGATCAGTC	HSL1	5'-NEST
GGTCTGAGGCCAGAGGAAGGCGTAGAGG	HSL1	5'-NESTED
GAGCTGTTGTCATGTAGCATGCGC	HSL2	5'-NEST
TCCAGACTGCGAGCGTGCTCCTGG	HSL2	5'-NESTED
GTTTACCCACAGGGCTTTGAGCC	HSL1	3'-NEST
GACGCCTTGCTGGATGAC	HSL1	3'-NESTED
GAAGAGCCAGACTTGCCAGGACTTGG	HSL2	3'-NEST
CAGTGGCCATACCACCACCTGCTG	HSL2	3'-NESTED
CATGGGAGATAAGGCGCATG	HSL1	5'-NEST
CATACGTCTCTCCATATGAACC	HSL1	5'-NESTED
GAGCCACGCAAGCACCGCAAG	HSL2	5'-NEST
CCCTGGTGGAGGAGGGTTC	HSL2	5'-NESTED
GTACAACGCAGAGTACATTGGG	HSL1	Single amplification
CAATACCGCCAGCATCAGTG	HSL1	Single amplification
CAACGCAGAGTACATGGGG	HSL2	Single amplification
GCCACAGCAACTAAGTCCTC	HSL2	Single amplification
CACGCGCCGGCGGAACAT	HSL1	Single amplification
GGTCGGGCTGGTTATGGTG	HSL1	Single amplification
GCAGAGTACATGGGGAAAAGG	HSL2	Single amplification
GCAATTTTAGCTCCTTTCCCG	HSL2	Single amplification

5'- and 3'- RACE anchored primers	
	GCTGTCAACGATACGCTACGTAACGCCATG ACAGTG(T)24
GeneRacer 3'	GCTGTCAACGATACGCTACGTAACG
GeneRacer 3' nested	CGCTACGTAACGGCATGACAGTG
GeneRacer 5'	CGACTGGAGCACGACGAGGACACTGA
GeneRacer 5' nested	GGACACTGACATGGACTGAAGGAGTA
GSPHSLC1F	CGCTACGTAACGGCATGACAGTG

Results

Japanese flounder

The PCR using degenerate primers, HSLC1F_JF and HSLC1R_JF (Table 1-1-1), amplified DNA fragments of 1,887 bp, homologous to HSL genes from other species. 5'-RACE and 3'-RACE added 172 and 863 bp to the Japanese flounder HSL gene, respectively. On the other hand, PCR using primers HSLC2F_JF and HSLC2R_JF resulted in the amplification of cDNA fragments of 2,373 bp, which was also similar to HSL genes of other species. 5'-RACE and 3'-RACE further added 236 and 223 bp sequences to this gene, respectively. The full-length sequences of the Japanese flounder HSL1 and 2 cDNAs, consisted of 2,922 and 2,832 bp, respectively (Fig 1-1-2 and Fig 1-1-3, respectively). These genes encoded 702 and 837 amino acids, respectively, and their deduced amino acid sequences shared 58.7% identity to each other. The sequence of open reading frame was confirmed by a single PCR for the HSL1 gene (data not shown), but it was not possible for the HSL2 gene probably due to their low mRNA level.

```
                                                                                                                    GCGGGCGCCGGGAGGACAAAAAGAGAAAAAAAAAGAAAGGAAAAAAAAAAGAGGGAGGAGCGGGGTCCCTTCAGAT

ATG GAT TAC AAG GTT GTG TTT GCA GCC TTG GAG ACG GTG TGT GAA GAC AAC AAT TCG CCC TTG TGT GGG CCT TCT GAT TTG CCG TAC GGC    90
Met Asp Tyr Lys Val Val Phe Ala Ala Leu Glu Thr Val Cys Glu Asp Asn Asn Ser Pro Leu Cys Gly Pro Ser Asp Leu Pro Tyr Gly    30

ACT GTC GCC AAG CGC CTG GTC ACA TGT TTG AGA GAA ATT CAG GAG CAC GGC CAT GCG CTG GAG CCT GTG GTC GCC AGC CTC ACC GCC GTT   180
Thr Val Ala Lys Arg Leu Val Thr Cys Leu Arg Glu Ile Gln Glu His Gly His Ala Leu Glu Pro Val Val Ala Ser Leu Thr Ala Val    60

TAC CAC CAC TAC GAC TTT GAC GCA CAA ACG CCT GGG AAC GGC TAC CGC ACC CTG GTC AAA GTC TTG CAC GCC TGC ATT TTG CAC ATC ATA   270
Tyr His His Tyr Asp Phe Asp Ala Gln Thr Pro Gly Asn Gly Tyr Arg Thr Leu Val Lys Val Leu His Ala Cys Ile Leu His Ile Ile    90

CAC AAG GGC CGT TAC ATT GCC GAC AAC TGC AAC GGT GCT TTC TTC AGG GCC GAG CAC AAT GCG TCT GAG ATG GAG GCG TAC TGC AGC GCC   360
His Lys Gly Arg Tyr Ile Ala Asp Asn Cys Asn Gly Ala Phe Phe Arg Ala Glu His Asn Ala Ser Glu Met Glu Ala Tyr Cys Ser Ala   120

CTG TGC CAG CTG CGT GCC CTG GTC CAC CTC GCC CAG CGG CTG ATC AAC GAC AAC GAA TGC GGC CAG CTG TAC TCC CAG CAG GAC GGG GAC   450
Leu Cys Gln Leu Arg Ala Leu Val His Leu Ala Gln Arg Leu Ile Asn Asp Asn Glu Cys Gly Gln Leu Tyr Ser Gln Gln Asp Gly Asp   150

CTG ACC CGC AGG TTT GTG CAG GAG TAC AGC TCC ATG CAC AAG GCG TGT TTC TAC GGA CGC TGT CTT GGC TTT CAG TTC TCT CCA GCT CTT   540
Leu Thr Arg Arg Phe Val Gln Glu Tyr Ser Ser Met His Lys Ala Cys Phe Tyr Gly Arg Cys Leu Gly Phe Gln Phe Ser Pro Ala Leu   180
```

```
CGT CCA TTC CTC CAG ACT GTT GTC ATA AGC ATG ATT TCA TAC GGA GAG ACG TAC GGT AAA CAG CAG TCA CGG TTT GGT ATG GCG GCC CTG   630
Arg Pro Phe Leu Gln Thr Val Val Ile Ser Met Ile Ser Tyr Gly Glu Thr Tyr Gly Lys Gln Gln Ser Arg Phe Gly Met Ala Ala Leu   210

TCT CTC CTC ACA TCA GGG AAG TAC GTC ATT GAT CCA GAG ATG CGG GGC ACT GAG TTT GAA CGC ATA ACC CAG AAC CTG GAT TTA CAT TTC   720
Ser Leu Leu Thr Ser Gly Lys Tyr Val Ile Asp Pro Glu Met Arg Gly Thr Glu Phe Glu Arg Ile Thr Gln Asn Leu Asp Leu His Phe   240

TGG AAG TCT TTC TGG AAC CTC ACA GAG TCC GGC CTT ATA ACA GGT TTA AAC AGA ATA GCT TCT AAC ACA GTG CAG GTG AAC CTC ACC TTG   810
Trp Lys Ser Phe Trp Asn Leu Thr Glu Ser Gly Leu Ile Thr Gly Leu Asn Arg Ile Ala Ser Asn Thr Val Gln Val Asn Leu Thr Leu   270

ACT GTG CCT CCT CTC CCT CTA CGC CTT CCT CTG GCC TCA GAC CCA AAT CTA ACG GCC ACT GTG TCG CCT CCA ATC GCT CAC TCG GGC CCC   900
Thr Val Pro Pro Leu Pro Leu Arg Leu Pro Leu Ala Ser Asp Pro Asn Leu Thr Ala Thr Val Ser Pro Pro Ile Ala His Ser Gly Pro   300

GGG CCT GTC CAC ATG CGA CTG ATC TCC TAT GAG CTT CGA GAA GGA CAA GAC AGT GAG GAG CTG CTG GCT TTT TCC CGA ACT GAC CCT CAT   990
Gly Pro Val His Met Arg Leu Ile Ser Tyr Glu Leu Arg Glu Gly Gln Asp Ser Glu Glu Leu Leu Ala Phe Ser Arg Thr Asp Pro His   330

CCC ATC ACC ACG TCT CAT CTC CCT GGG GTA CAG AAG CTG CCT CAT TCA CCC TGG CTG CTC ATC CAC TTC CAC GGA GGA GGT TTT GTA GCC   1080
Pro Ile Thr Thr Ser His Leu Pro Gly Val Gln Lys Leu Pro His Ser Pro Trp Leu Leu Ile His Phe His Gly Gly Gly Phe Val Ala   360

CAG ACA TCC AGA TCT CAT GAG AGT TAT CTT CGG AGC TGG TCG AAG GAG CTG AAC GTC CCC ATC CTG TCT GTC GAC TAC TCT TTG TCA CCT   1170
Gln Thr Ser Arg Ser His Glu Ser Tyr Leu Arg Ser Trp Ser Lys Glu Leu Asn Val Pro Ile Leu Ser Val Asp Tyr Ser Leu Ser Pro   390

GAA GCG CCT TTT CCC AGA GCT CTG GAG GAG TGT TTC TAC GCC TAC TGC TGG GCA CTG AAA AAC TGT CAC CTC CTG GGC TCC ACA GCG GAG   1260
Glu Ala Pro Phe Pro Arg Ala Leu Glu Glu Cys Phe Tyr Ala Tyr Cys Trp Ala Leu Lys Asn Cys His Leu Leu Gly Ser Thr Ala Glu   420

CGA GTT TGT CTG GCG GGG GAC AGT GCT GGA GGA AAC CTC TGC ATC ACT GTG TCC ATG AAG GCC ATG ACC TGC GGC ATC CGA GTC CCT GAC   1350
Arg Val Cys Leu Ala Gly Asp Ser Ala Gly Gly Asn Leu Cys Ile Thr Val Ser Met Lys Ala Met Thr Cys Gly Ile Arg Val Pro Asp   450

GGC ATG ATG ACC GCC TAC CCC GCC ACC CTG CTC ACC ACA GAC GCC TCG CCC TCT CGC CTG CTC ACA CTC ATC GAC CCA CTG TTG CCT TTA   1440
Gly Met Met Thr Ala Tyr Pro Ala Thr Leu Leu Thr Thr Asp Ala Ser Pro Ser Arg Leu Leu Thr Leu Ile Asp Pro Leu Leu Pro Leu   480

GGT GTT CTT GCC AAG TGC CTC AAT ACC TAT GCA GGT ATA GAC TAT CAC ACG GTG CAG CCG GCA GTG GGA AGC AAC AGT CTG AGC ACT CTG
Gly Val Leu Ala Lys Cys Leu Asn Thr Tyr Ala Gly Ile Asp Tyr His Thr Val Gln Pro Ala Val Gly Ser Asn Ser Leu Ser Thr Leu   510

GGC AGA GAC ACA GCC GTG CTG CTC GGT GAT CTC ACC CAG GGA GCC TCC AAC TGG ATC CAC TCA TTT CTG GAC CCC ATG CTG AGT TCA GGT   1620
Gly Arg Asp Thr Ala Val Leu Leu Gly Asp Leu Thr Gln Gly Ala Ser Asn Trp Ile His Ser Phe Leu Asp Pro Met Leu Ser Ser Gly   540

GGA GCC CAC TCC CAG TCG CCG TTA GAG AGG AGG TCC CAG AGC AGT GAA ACC CGC AGG ACA TCA ACT CGC ACC TCC ACG CAA ACA TCT GGG   1710
Gly Ala His Ser Gln Ser Pro Leu Glu Arg Arg Ser Gln Ser Ser Glu Thr Arg Arg Thr Ser Thr Arg Thr Ser Thr Gln Thr Ser Gly   570

GAT CAC GTG GTT TAC CCA CAG GGC TTT GAG CCC CTG CGC GCC GAG TGC CTG GCT GTT GTT CAC CAG ACC TCC TCT CCT GTT TTT AGG AAC   1800
Asp His Val Val Tyr Pro Gln Gly Phe Glu Pro Leu Arg Ala Glu Cys Leu Ala Val Val His Gln Thr Ser Ser Pro Val Phe Arg Asn   600

CCC TTT GTG TCA CCT TTA CTG GCT CCG GAC AAC ATG CTG AGA GGT CTG CCG CCT GTA TAC ATC GTG GCC TCT GCT CTG GAC GCC TTG CTG   1890
Pro Phe Val Ser Pro Leu Leu Ala Pro Asp Asn Met Leu Arg Gly Leu Pro Pro Val Tyr Ile Val Ala Ser Ala Leu Asp Ala Leu Leu   630

GAT GAC TCT GTG ATG TTT GCC AAG AAA CTG CGA GAC ATG GGC CAG CCC GTG AGT CTG ACG GTG GTG GAA GAC CTG CCT CAT GGC TTC CTC   1980
Asp Asp Ser Val Met Phe Ala Lys Lys Leu Arg Asp Met Gly Gln Pro Val Ser Leu Thr Val Val Glu Asp Leu Pro His Gly Phe Leu   660

AGC CTC GGA CAG CTC GCC AAG GAG ACG GAG GTC GCT ACA GAA ATC TGC GTT GCG CGA ATT AGG GAG ATT TTT GAG CAA GAA AAC CCA ACG   2070
Ser Leu Gly Gln Leu Ala Lys Glu Thr Glu Val Ala Thr Glu Ile Cys Val Ala Arg Ile Arg Glu Ile Phe Glu Gln Glu Asn Pro Thr   690

CCT GCT CTT CGC AGT CGG CCA AAG CGG GAA GTG GCG TAA   2109
Pro Ala Leu Arg Ser Arg Pro Lys Arg Glu Val Ala *   703

CAGAGAATCAAGCCATGACCTATTTATCTGTCATTCCAGCTGTTTTTGGATAAAGAAGAGAACTGACGTTTTGTTGTGCAATAAGTTAAAGGAAACAAATCAGGGAGAATAATGAA
GATGCACCAAAAACTGAAGGAAGCTTAGAGGGAAACTGCACTTGAAACCTTCACTGCACAACGAAAATGTTCAAGAGAGCCACTAAAACTTTTAACTTTCTACATCTATAATCTAA
AATGATCTGATGTGATGACAGAAATGAAAGTAGTATTTTTCTATTAAGATTTCCATGTTGAAGAAGCAGATTAAACGCACATTCATAATTTTACAAGCTGACTAAAACAAAAAGAT
CACTATAACCAGCACTGGTTGAGATACATATCAGTAACAGAAGCTGTTGTGCTTGAATTTAAAGCATTGCTGTATTTGCATATGACCAAAGTTAAAGGTTAACTTGAACAGAGAAC
ACTTTTCCGATGTGTTGTATTGTTATTATATAATTTAGATAAATAGTTTTACCTGGTTTTGCCAGTTTGTCACATGTTTACAGCGTTTTGATGAGGAGGCCTTTACCTTGTGTTTA
CCGGCAGTATGTGGATGTGACTTGTTCTACTGAAGGGGCGGAATTTCGTTAAAACCCTAAATTCATTCTTTATATCTCTAATTATAAATATTTAACACAGTTTATTTAAAACCTGT
ATTAAATCAAAACTCCAAAAAAAAAAAAAAAAAAAAAAAAAA
```

Figure 1-1-2. Nucleotide and deduced amino acid sequences of cDNA encoding HSL1 gene in Japanese flounder. Bold faced letters and asterisk indicate the initiation and stop codon, respectively.

ACACGGGGGAGTAGAATCGGTGATCACAAGGCTGACATACTAAGGATTACGTACATAGGTGGGAGCAGTGGTGTCAACTCAGCGCTCCCAGGCAGGTAGGTCGGTGGTAAGTTGATAG
GCGGCGCGAGCTCCTCTGTCCGGAGCACTGGGCGAAGAGGGCGTCGAACAAGAAGGGCGGCGGGAGCAGGCTGGAGAAGGGAGTGTCCGGAAGACGCTCGTCCAAACACAGATAGGGT
CCAGTGGTG

ATG GAC ACC AAG GCA GTG TTT GCG GCC CTG TAC AGC GTG TGC GAA GAA AAT GCC ACT TTC TTC TCA GGA GGA GCC AAA GGA ACA CAG GGT 90
Met Asp Thr Lys Ala Val Phe Ala Ala Leu Tyr Ser Val Cys Glu Glu Asn Ala Thr Phe Phe Ser Gly Gly Ala Lys Gly Thr Gln Gly 30

GAC GCG GCG CGG CGG CTG GTG GAT ACA ATG AAC TTG ATC CAG GAG CAC GCT CGC AGT CTG GAG CCA GTC ATC TCT GGC TTC GCT TCA GTT 180
Asp Ala Ala Arg Arg Leu Val Asp Thr Met Asn Leu Ile Gln Glu His Ala Arg Ser Leu Glu Pro Val Ile Ser Gly Phe Ala Ser Val 60

TAC CAT CAT TTT GAC TTT GAC CCA CAC ATA CCT GCT AAT GGC TAT CGT TCG CTG GTC AAG GTG GTG CGT TGC TGC ATT CTC CAC ATC ATC 270
Tyr His His Phe Asp Phe Asp Pro His Ile Pro Ala Asn Gly Tyr Arg Ser Leu Val Lys Val Val Arg Cys Cys Ile Leu His Ile Ile 90

CAC AAG GGG CGC TAC ATA AGC GCC AAT CGC CGC AGC ATC TTT TTT AGA GTA GCG CAC AAT GCA GGG GAG ATG GAG GCA TAC TGC AGC GCC 360
His Lys Gly Arg Tyr Ile Ser Ala Asn Arg Arg Ser Ile Phe Phe Arg Val Ala His Asn Ala Gly Glu Met Glu Ala Tyr Cys Ser Ala 120

CTG TGT CAG CTG CGT GCC CTG CTC TAC TTG GCT CAG CGC ATG CTA CAT GAC AAC AGC TCT GGC AAC TTG TTT TTC CAG GAC GAA AGT GGC 450
Leu Cys Gln Leu Arg Ala Leu Leu Tyr Leu Ala Gln Arg Met Leu His Asp Asn Ser Ser Gly Asn Leu Phe Phe Gln Asp Glu Ser Gly 150

CTC AGC GAG AGC TTT GTC CGC GAG TAC TCA TCT ATG CAC AAG GGA TGC TTC TAT GGC CGT TGC CTG GGC TTT CAG TTT ACT CCA TCT ATC 540
Leu Ser Glu Ser Phe Val Arg Glu Tyr Ser Ser Met His Lys Gly Cys Phe Tyr Gly Arg Cys Leu Gly Phe Gln Phe Thr Pro Ser Ile 180

CGA CCC TGT CTC CAG ACC ATT GCT ATC GGC CTT GTG GCC TTT GGA GAG AAC TAC AAG CGC CAT CAG TCA GGA ATA GGG GTG GCA GCC AGC 630
Arg Pro Cys Leu Gln Thr Ile Ala Ile Gly Leu Val Ala Phe Gly Glu Asn Tyr Lys Arg His Gln Ser Gly Ile Gly Val Ala Ala Ser 210

TCG CTC TTT ACC TCA GGG AAG TAC GCC ATT GAC CCT GAG TTG AGA GGG GCG GAA TTT GAA CGC ATC ACC CAG AAC CTG GAC GTC CAT TTT 720
Ser Leu Phe Thr Ser Gly Lys Tyr Ala Ile Asp Pro Glu Leu Arg Gly Ala Glu Phe Glu Arg Ile Thr Gln Asn Leu Asp Val His Phe 240

TGG AAG ACC TTC TGG AAC ATT ACT GAG ACT GAA CTC CCG TCG AGT CTG GCC AGT ATG ACA TCC ACT CAG GTT AAG GTG AAC CGG CCT CTC 810
Trp Lys Thr Phe Trp Asn Ile Thr Glu Thr Glu Leu Pro Ser Ser Leu Ala Ser Met Thr Ser Thr Gln Val Lys Val Asn Arg Pro Leu 270

TCT GTG CCC CCT GTG CCC TTT GAC CTT CCC TTG GCG GCC AAC CAC AGA GTA TCT GTA ACC ATT TCT CCA CCG TCT GCG CAC ATT GGC ACT 900
Ser Val Pro Pro Val Pro Phe Asp Leu Pro Leu Ala Ala Asn His Arg Val Ser Val Thr Ile Ser Pro Pro Ser Ala His Ile Gly Thr 300

GCT CCA GTT CAG ATG AGG CTC ATC TCT TAT GAC TTG CGT GAA GGA CAG GAC AGT GAA ACC CTG CTA TCT CTC TCC CGC TCT GAG GGA GGA 990
Ala Pro Val Gln Met Arg Leu Ile Ser Tyr Asp Leu Arg Glu Gly Gln Asp Ser Glu Thr Leu Leu Ser Leu Ser Arg Ser Glu Gly Gly 330

TCC ATC TCT CTG TCG CTG GGG TTG AAG GCC AAG CGA CTC CCC TCT TCT CCT TGC TTG CTG ATC CAC TTC CAT GGA GGG GGC TTT GTG GCC 1080
Ser Ile Ser Leu Ser Leu Gly Leu Lys Ala Lys Arg Leu Pro Ser Ser Pro Cys Leu Leu Ile His Phe His Gly Gly Gly Phe Val Ala 360

CAG ACG TCC AAG TCC CAT GAG CCC TAT CTG AAG AGT TGG TCC CAG GAC CTT GGT GTC CCC GTC TTG TCA ATT GAC TAC TCC CTG GCC CCT 1170
Gln Thr Ser Lys Ser His Glu Pro Tyr Leu Lys Ser Trp Ser Gln Asp Leu Gly Val Pro Val Leu Ser Ile Asp Tyr Ser Leu Ala Pro 390

GAA GCC CCC TTT CCG AGG GCC TTG GAG GAG TGC TTC TAT TCC TAC TGC TGG GCT CTG AGA AAC CAC CAC CTA CTG GGA TGG ACC GGA GAG 1260
Glu Ala Pro Phe Pro Arg Ala Leu Glu Glu Cys Phe Tyr Ser Tyr Cys Trp Ala Leu Arg Asn His His Leu Leu Gly Trp Thr Gly Glu 420

AAA GTA TGT CTG GCT GGG GAT AGT GCG GGA GGC AAT TTG TGT CTG ACG ACA TCG ATG CGA GCG GCT GCC TTT GGT GTT CGA ATG CCA GAT 1350
Lys Val Cys Leu Ala Gly Asp Ser Ala Gly Gly Asn Leu Cys Leu Thr Thr Ser Met Arg Ala Ala Ala Phe Gly Val Arg Met Pro Asp 450

GGC ATC GTG GCA GCC TAC CCG GCT ACC CTG CTG ACT GCC TAC GCA TCT CCC TCC CGT CTG CTT TCA CTT ATG GAT CCC CTG CTT CCG CTC 1440
Gly Ile Val Ala Ala Tyr Pro Ala Thr Leu Leu Thr Ala Tyr Ala Ser Pro Ser Arg Leu Leu Ser Leu Met Asp Pro Leu Leu Pro Leu 480

AGT GTG CTC TCT AGG TGT CTC AGT GCC TAC GCA GGC AAT GAG CCA CAG ACT GAG AAG CAG GTA GAG AAA GTG AGC ACA CTG AGC CTG GTG 1530
Ser Val Leu Ser Arg Cys Leu Ser Ala Tyr Ala Gly Asn Glu Pro Gln Thr Glu Lys Gln Val Glu Lys Val Ser Thr Leu Ser Leu Val 510

AGA AGA GAC ACG GCG CTG ATG CTG CGA GAT TTC CGA CAG GGA GCC TCC AAC TGG ATC CAC TCT CTG CTG GAT CAC AAC AGA GCT CCA GCT 1620
Arg Arg Asp Thr Ala Leu Met Leu Arg Asp Phe Arg Gln Gly Ala Ser Asn Trp Ile His Ser Leu Leu Asp His Asn Arg Ala Pro Ala 540

TCT TCT GGC GCA GCT GCA GAG GTG CCA CCA GGA GCC ACT GAT GCA GTG AGG AAG AGC ATA TCA GAG GCG TCC ATC TCT TCT CCT CAC GCT 1710
Ser Ser Gly Ala Ala Ala Glu Val Pro Pro Gly Ala Thr Asp Ala Val Arg Lys Ser Ile Ser Glu Ala Ser Ile Ser Ser Pro His Ala 570

GAT CCC CCT GTG CCC TCC GAA CTC TCA GAG TTC CCC ACC AGG AAA TTA TCT GTG AAG AGC CAG ACT TGC CAG GAC TTG GGA TCT CAC AGC 1800
Asp Pro Pro Val Pro Ser Glu Leu Ser Glu Phe Pro Thr Arg Lys Leu Ser Val Lys Ser Gln Thr Cys Gln Asp Leu Gly Ser His Ser 600

AGC TCC ACT TTG CAC AGC ACA CCA CTG CTG TCT GAG CGC ACT CCA GAG GAT GTG AAT TTC TTC TTC TGC AAG GAT GCA GAT CCC TCC ATG 1890
Ser Ser Thr Leu His Ser Thr Pro Leu Leu Ser Glu Arg Thr Pro Glu Asp Val Asn Phe Phe Phe Cys Lys Asp Ala Asp Pro Ser Met 630

TCC AGT GAC CTG TCT TCA GTG GCC ATA CCA CCA CCT GCT GGA GAG GAG GGA TCA GAG CTG GGG CAC TGC AGG GAG TTC CCC CTT GGG TTT 1980
Ser Ser Asp Leu Ser Ser Val Ala Ile Pro Pro Pro Ala Gly Glu Glu Gly Ser Glu Leu Gly His Cys Arg Glu Phe Pro Leu Gly Phe 660

GAA CCT CTG CGT TCA GAG CAG CTG GCT GAG ATG AAG TTG AAT AGC TCT CCA GTG GTC AAG GAT CCT TTC TGC TCA CCT CTT CTG GCC CCT 2070
Glu Pro Leu Arg Ser Glu Gln Leu Ala Glu Met Lys Leu Asn Ser Ser Pro Val Val Lys Asp Pro Phe Cys Ser Pro Leu Leu Ala Pro 690

GAT AGC ATG TTG ACA GGC CTG CCA CCT GTA CAT ATA GTG GCT TGT GCA TTA GAC CCC ATG CTG GAT GAC TCT GTG ATG TTT GCC AAG CGT 2160
Asp Ser Met Leu Thr Gly Leu Pro Pro Val His Ile Val Ala Cys Ala Leu Asp Pro Met Leu Asp Asp Ser Val Met Phe Ala Lys Arg 720

TTG AGG AAC TTG GAC CAG CCT GTC ACT CTG TGT GTG GTG GAC GAC CTC CCC CAC GGC TTC CTC AGC CTA TCG CAG CTC TCC AAG GAG ACG 2250
Leu Arg Asn Leu Asp Gln Pro Val Thr Leu Cys Val Val Asp Asp Leu Pro His Gly Phe Leu Ser Leu Ser Gln Leu Ser Lys Glu Thr 750

AGA GAG GCT GCC AAC GTC TGC GTG GAG CGT ATC CGC GCT GTC TTC ACC CAG AAG GAC ACC CCC CCA GAG CCG CGC AAG CAC CGA AAG CTG 2340
Arg Glu Ala Ala Asn Val Cys Val Glu Arg Ile Arg Ala Val Phe Thr Gln Lys Asp Thr Pro Pro Glu Pro Arg Lys His Arg Lys Leu 780

GAA CGG ACC GAT AGG GGT GTG TCA GCC TCT TCT GGG GAG GGT GCC TCC CTC TTT ACT GGT CCT ATC GAG GAA GAG GAG CAA GAT GTC GGG 2430
Glu Arg Thr Asp Arg Gly Val Ser Ala Ser Ser Gly Glu Gly Ala Ser Leu Phe Thr Gly Pro Ile Glu Glu Glu Glu Gln Asp Val Gly 810

```
CGT GGG GTC AAA ATT GCT GAT GGG GAG GAC TTA GTT ACT GTG GCA GCT CAG AAT AGC ACT GAT GCT GGC GGT ATT GGA GCT TAA   2514
Arg Gly Val Lys Ile Ala Asp Gly Glu Asp Leu Val Thr Val Ala Ala Gln Asn Ser Thr Asp Ala Gly Gly Ile Gly Ala  *   838

GTAAGGATAGATTAAAAAAACCAGGGATGGTGTTCCCCCCAAGGAAAAAAAAAAAAAAAAAAAAAAAAAAAA
```

Figure 1-1-3. Nucleotide and deduced amino acid sequences of cDNA encoding HSL2 gene in Japanese flounder. Bold faced letters and asterisk indicate the initiation and stop codon, respectively.

Red seabream

The degenerate primers amplified a part of red seabream HSL1 gene of 1,913 bp. 5'RACE and 3'RACE added 41 and 982 bp to the HSL1 gene, respectively. A 1,921 DNA fragment encoding red seabream HSL2 was also amplified using degenerate primers. 5'-RACE and 3'-RACE further added 160 and 643 bp, respectively. The full-length of sequence of red seabream HSL1 and HSL2 were 2,955 and 2,723 bp (Fig 1-1-4 and Fig 1-1-5, respectively). HSL1 and HSL2 genes of red seabream encoded 710 and 874 amino acids, respectively. The red seabream HSLs shared 57.5% identity to each other. The sequences of red seabream HSLs were confirmed by a single PCR using primer shown in Table 1-1-1.

GCAGTGGTATCAACGCAGAGTACATGGGGCATTCTGCGGGACACGCGCCGGCGGAACATCAAGGAAGAGG

```
ATG GAT TAC ACA GTT GTG TTC GCA GCC TTG GAA ACA GTA TGT GAA GAC AAC ATT GCT ATT ATG TGT GGG CCT TCT GAT TTG CCG TAC GGC   90
Met Asp Tyr Thr Val Val Phe Ala Ala Leu Glu Thr Val Cys Glu Asp Asn Ile Ala Ile Met Cys Gly Pro Ser Asp Leu Pro Tyr Gly   30

AAT GTT GCC AAT CGC CTG GTC ACG TGT ATG AGG CAG ATT CAG GAG CAC GGC CGA GCC CTG GAG CCT GTG GTC GGC AGC TTC ACC GCC GTC   180
Asn Val Ala Asn Arg Leu Val Thr Cys Met Arg Gln Ile Gln Glu His Gly Arg Ala Leu Glu Pro Val Val Gly Ser Phe Thr Ala Val   60

TAC CAC CAT TAC GAC TTT GAC GAA CAA ACG CCT GGG AAT GGC TAC CGC ACC TTG GTT AAG GTC TTG CAG TCT TGC CTC TTG CAC ATC ATT   270
Tyr His His Tyr Asp Phe Asp Glu Gln Thr Pro Gly Asn Gly Tyr Arg Thr Leu Val Lys Val Leu Gln Ser Cys Leu Leu His Ile Ile   90

CAC AAG GGC CGT TAC ATC GCT TCT AAT TAC AAC AGT GCC TTC TTC AGG GCC GAG CAC AAC GCC TCT GAG ATG GAG GCG TAC TGC AGC GCT   360
His Lys Gly Arg Tyr Ile Ala Ser Asn Tyr Asn Ser Ala Phe Phe Arg Ala Glu His Asn Ala Ser Glu Met Glu Ala Tyr Cys Ser Ala   120

CTA TGT CAG CTG CGT GCC CTT CTC CAC CTC GCC CAG CAG CTC ATC AAC GAC AAC GAG TGC GGC CAG CTG TAC TCC CTG CAG GAC AGG GAC   450
Leu Cys Gln Leu Arg Ala Leu Leu His Leu Ala Gln Gln Leu Ile Asn Asp Asn Glu Cys Gly Gln Leu Tyr Ser Leu Gln Asp Arg Asp   150

CTG AGC CGC AAG TTT GTG CAG GAG TAC AGC TCC ATG CAC AAA GCC TGT TTC TAC GGA CGC TGT CTG GGC TTT CAG TTC TCG CCA ACT CTA   540
Leu Ser Arg Lys Phe Val Gln Glu Tyr Ser Ser Met His Lys Ala Cys Phe Tyr Gly Arg Cys Leu Gly Phe Gln Phe Ser Pro Thr Leu   180

CGT CCC TTC CTC CAG ACT GTT GTC ATA AGC ATG GTT TCA TAT GGA GAG ACG TAT GGA AAA CAG CAG TCT GGC TTG GGT ATG GCC GCC CTC   630
Arg Pro Phe Leu Gln Thr Val Val Ile Ser Met Val Ser Tyr Gly Glu Thr Tyr Gly Lys Gln Gln Ser Gly Leu Gly Met Ala Ala Leu   210

TCC CTC CTC ACA TCA GGG AAG TAC GTC ATG GAT CCA GAG CTG CGG GGT GCA GAG TTT GAA CGC ATC ACC CAG AAC CTG GAC ATG CAG TTC   720
Ser Leu Leu Thr Ser Gly Lys Tyr Val Met Asp Pro Glu Leu Arg Gly Ala Glu Phe Glu Arg Ile Thr Gln Asn Leu Asp Met Gln Phe   240

TGG AAG TCC TTC TGG AAC CTC ACA GAG TCC GGC CTT ATA GCA GGC TTC AGC AGA ATA GCC TCT TGC CCA GTG CAG ATG AAT TTC ACC CTG   810
Trp Lys Ser Phe Trp Asn Leu Thr Glu Ser Gly Leu Ile Ala Gly Phe Ser Arg Ile Ala Ser Cys Pro Val Gln Met Asn Phe Thr Leu   270

ACG TTG CCT CCT GTC ACT CTA CAC CTC CCA CTG GCC TCA GAT CCC AGT CTA ACA GCC ACC GTG TCT CCT CCG ATA GCC CAC TGG GGT CCC   900
Thr Leu Pro Pro Val Thr Leu His Leu Pro Leu Ala Ser Asp Pro Ser Leu Thr Ala Thr Val Ser Pro Pro Ile Ala His Trp Gly Pro   300

GGG CCA GTC CAC ATG CGC CTT ATC TCC CAT GAG CTG CGA GAA GGA CAG GAC AGT GAA GAG CTG CTA TCA TTT TCT CGA GAC GAT CCT CCC   990
Gly Pro Val His Met Arg Leu Ile Ser His Glu Leu Arg Glu Gly Gln Asp Ser Glu Glu Leu Leu Ser Phe Ser Arg Asp Asp Pro Pro   330

CCC ATC ACC GCG TCC CAT CTC CCC TGG GTG CAG AAG CAG CCT CGC TCC CCC TGG CTG CTC ATC CAC TTC CAT GGA GGG GGC TTC GTA GCC   1080
Pro Ile Thr Ala Ser His Leu Pro Trp Val Gln Lys Gln Pro Arg Ser Pro Trp Leu Leu Ile His Phe His Gly Gly Gly Phe Val Ala   360

CAG ACT TCC AGA TCC CAT GAG AAT TAT CTT CGA AGT TGG TCA AAG GAG CTG AAC GTA CCA ATA CTC TCC GTG GAC TAC TCT CTG TCA CCC   1170
Gln Thr Ser Arg Ser His Glu Asn Tyr Leu Arg Ser Trp Ser Lys Glu Leu Asn Val Pro Ile Leu Ser Val Asp Tyr Ser Leu Ser Pro   390

GAA GCG CCC TTT CCC AGA GCT CTG GAG GAA TGT TTC TAC GCC TAC TGT TGG GCT CTG AAT AAC TGT CAT CTA CTG GGC TCC ACA GCT GAG   1260
Glu Ala Pro Phe Pro Arg Ala Leu Glu Glu Cys Phe Tyr Ala Tyr Cys Trp Ala Leu Asn Asn Cys His Leu Leu Gly Ser Thr Ala Glu   420

CGG GTT TGT CTG GCC GGG GAC AGC GCT GGA GGA AAC CTC TGC GTC ACC GTG TCC ATG AAG GCC ATA TCC AAC GGC ATC CGA GTC CCT GAC   1350
Arg Val Cys Leu Ala Gly Asp Ser Ala Gly Gly Asn Leu Cys Val Thr Val Ser Met Lys Ala Ile Ser Asn Gly Ile Arg Val Pro Asp   450

GGC ATC ATG GCC GCC TAC CCC GCC ACC TTG CTC ACC ACT GAC GCC TCG CCC TCC CGC CTG CTC ACG CTC ATT GAC CCG CTG TTG CCT CTG   1440
Gly Ile Met Ala Ala Tyr Pro Ala Thr Leu Leu Thr Thr Asp Ala Ser Pro Ser Arg Leu Leu Thr Leu Ile Asp Pro Leu Leu Pro Leu   480

GGT GTT CTC ACA AAG TGC CTC AAT GCC TAT GCA GGC GCA GAC TGT CAG ACG GTG CAG CCT GTG GTG GGA AGC AGC AGT CTG AGC TCT CTG   1530
Gly Val Leu Thr Lys Cys Leu Asn Ala Tyr Ala Gly Ala Asp Cys Gln Thr Val Gln Pro Val Val Gly Ser Ser Ser Leu Ser Ser Leu   510

GGC AGA GAC ACT GCT GTG CTG CTC AGT GAT CTC ACA CAG GGA GCC TCC AAC TGG ATC CAG TCC TTT CTG GAC CCC ATG AGG ACT TCA GGT   1620
Gly Arg Asp Thr Ala Val Leu Leu Ser Asp Leu Thr Gln Gly Ala Ser Asn Trp Ile Gln Ser Phe Leu Asp Pro Met Arg Thr Ser Gly   540

GGA ACA CGC TCG CTA TCA TCA GCG CCG ATG AGG TCT CAG AGC AAC AAC ACC CGC GGG ACA TCC ACT CAC GCC TCT ACA CCA AAC CGC GAA   1710
Gly Thr Arg Ser Leu Ser Ser Ala Pro Met Arg Ser Gln Ser Asn Asn Thr Arg Gly Thr Ser Thr His Ala Ser Thr Pro Asn Arg Glu   570

GAT CAC ATG GAT TAC CCA GAG GGC TTT GAG CCC ATG CGC TCC GAG TGC CTG GCT TTT GTT CGG CCA ACT TCA TCC CCC GTT ATC AGG AAC   1800
Asp His Met Asp Tyr Pro Glu Gly Phe Glu Pro Met Arg Ser Glu Cys Leu Ala Phe Val Arg Pro Thr Ser Ser Pro Val Ile Arg Asn   600

CCC TTT GTG TCG CCC CTG CTG TCT CCT AAC AAC CTG CTG AGA GGC CTG CCG CCT GTA CAC ATA GTG GCC TCT GCT CTG GAC GCC TTG CTG   1890
Pro Phe Val Ser Pro Leu Leu Ser Pro Asn Asn Leu Leu Arg Gly Leu Pro Pro Val His Ile Val Ala Ser Ala Leu Asp Ala Leu Leu   630

GAT GAC TCG GTG ATG TTT GCC AAG AAG CTT CGA GAC ATG GGC CAG CCT GTG AAT CTG ACG GTG GTG GAG GAC CTG CCT CAC GGC TTC CTC   1980
Asp Asp Ser Val Met Phe Ala Lys Lys Leu Arg Asp Met Gly Gln Pro Val Asn Leu Thr Val Val Glu Asp Leu Pro His Gly Phe Leu   660

AGC CTG TCG CAA CTC GCC AAG GAG ACG GAG GTG GCT TCA GAA ATC TGC GTG GAG CAA ATG AGG AAG ATT TTT CAG CAG GAA AAC CCG ACG   2070
Ser Leu Ser Gln Leu Ala Lys Glu Thr Glu Val Ala Ser Glu Ile Cys Val Glu Gln Met Arg Lys Ile Phe Gln Gln Glu Asn Pro Thr   690

CCC GCT CTT AGC AAA CGG CCC AAG CTG GAA GAT ACT CAT CAG AGT ACG AAT CCA TCC GGC TGA   2133
Pro Ala Leu Ser Lys Arg Pro Lys Leu Glu Asp Thr His Gln Ser Thr Asn Pro Ser Gly *     710
```

TGAAGCTGATGATCTTGGGGTGAAAAAGAGACGTGAGAGTATGTGGTGAGAGATGCAATGCATTCGAGAAAAGGAAACAATTGAGGGAGAATAATGAAGATGT
ACAAAAACTGTCTAACTGGAAGCTTAGGGATCCTGCACTCGAAACCTTTACTGCACAAAATTCCTGTAGGCAATAATGATCGAGAGAGACGTTAAAACTCTCTTT
AACCAGCTCTAAAATTATCCTCAACGATGACAAAATAGGAAACAATGAAGTATTTTTCTACCAAGATCCTAATCCAGACCAAGCGCACATTTGACAATATAACGG
ACTGACAGAACGTTCACCATAACCAGCCCGAGCCAGTATGTCTTTCTGATCACGTCAGAGATGTAAGCTTTTGTGCCTTGAATTTAAAGCGCTGCTGTATTTGCAT
TGAACGAAACATAGTTTTGCCTACGTTACCAAACTGACCAGGATTAAAGGTTTACTTACTGGAAACAGTCCAGATACACTGTAGTGTTATTATATTTGGATTTAAT
GTTGAACCTGGTTGTGTAAGTGTTTACATCAAACTGACAAGGAGGCCTTCATGTTGTGTCTACCAGCACTATGTGGGTGTGAATGTAACTTGTAAAACTGTAAAAT
AATTCTTATTATTTCTTAATGTCAATATTTATCAGTTTTGTTTTATTTAAAGTCTGGATTAAATCAAAACTGCAAAAAAAAAAAAAAAAAAAAAAAAAAAAAAA

Figure 1-1-4. Nucleotide and deduced amino acid sequences of cDNA encoding HSL1 gene in red seabream. Bold faced letters and asterisk indicate the initiation and stop codon, respectively.

AAGCAGTGGTATCAACGCAGAGTACATGGGGAAAAGGGGGCGAAG

ATG GCG TCG AAC AAG AAG AGT AGT GGG AAT AGC AGA TTT GAG AAA AGT GTG AAT GGA AGA CGC TCG TCG AAA CAC AAA GAA GGT CCA GTG 90
Met Ala Ser Asn Lys Lys Ser Ser Gly Asn Ser Arg Phe Glu Lys Ser Val Asn Gly Arg Arg Ser Ser Lys His Lys Glu Gly Pro Val 30

GTG ATG GAC ACC AAG GCA GTG TTC GCG GCC CTG TAC AGC GTG TGC GAA GAG AAT GCC ACT TTC TTC TCA GGA GGA GCC AAG GGG TCG CAG 180
Val Met Asp Thr Lys Ala Val Phe Ala Ala Leu Tyr Ser Val Cys Glu Glu Asn Ala Thr Phe Phe Ser Gly Gly Ala Lys Gly Ser Gln 60

GGT GAT GCC GCG CGG CGG CTG GAG GAT GTC ATG AAG ATG ATC CAG GAG CAT GCT CGC AGT CTG GAG CCT GTT ATC TCC AGC TTT GCT TCA 270
Gly Asp Ala Ala Arg Arg Leu Glu Asp Val Met Lys Met Ile Gln Glu His Ala Arg Ser Leu Glu Pro Val Ile Ser Ser Phe Ala Ser 90

GTT TAC CAC CAT TTC GAC TTT GAC CCG CAC ATA CCT GCT AAT GGA TAT CGT TCC CTG GTC AAG GTC GTG CGC TGC TGC CTT CTC CAC ATC 360
Val Tyr His His Phe Asp Phe Asp Pro His Ile Pro Ala Asn Gly Tyr Arg Ser Leu Val Lys Val Val Arg Cys Cys Leu Leu His Ile 120

ATC CAG AAG GGT CGC TAC ATC ACC GCA AAC CGC CGC AGC ATC TTC TTT CGA GTA GCA CAC AAT GCG GGG GAG ATG GAG GCT TAC TGC AAC 450
Ile Gln Lys Gly Arg Tyr Ile Thr Ala Asn Arg Arg Ser Ile Phe Phe Arg Val Ala His Asn Ala Gly Glu Met Glu Ala Tyr Cys Asn 150

GCT CTG TGC CAG ATG CGC GCC CTG CTC TAC CTG GCT CAG CGC ATG CTA CAT GAC AAC AGC CAT GGC AAC CTT TTC TTC CAG GAT GAA AGC 540
Ala Leu Cys Gln Met Arg Ala Leu Leu Tyr Leu Ala Gln Arg Met Leu His Asp Asn Ser His Gly Asn Leu Phe Phe Gln Asp Glu Ser 180

GGG CTC AGC GAG AGC TTC GTC CGC GAA TAC TCC TCC ATG CAC AAG GGC TGC TTC TAC GGC CGT TGC CTT GGT TTT CAG TTC ACT CCG GCC 630
Gly Leu Ser Glu Ser Phe Val Arg Glu Tyr Ser Ser Met His Lys Gly Cys Phe Tyr Gly Arg Cys Leu Gly Phe Gln Phe Thr Pro Ala 210

ATC CGA CCC TGT CTC CAG ACC ATC GCT ATC GGC CTT GTG GCC TTT GGA GAA AAC TAC AGG CGC CAT CAG TCA GGA ATA GGT GTT GCA GCC 720
Ile Arg Pro Cys Leu Gln Thr Ile Ala Ile Gly Leu Val Ala Phe Gly Glu Asn Tyr Arg Arg His Gln Ser Gly Ile Gly Val Ala Ala 240

AGC TCT TTC TTT ACC TCA GGG AAG TAT GCC ATC GAC CCA GAG TTG AGA GGG GCA GAA TTT GAA CGA ATC ACG CAG AAC CTG GAC GTG CAT 810
Ser Ser Phe Phe Thr Ser Gly Lys Tyr Ala Ile Asp Pro Glu Leu Arg Gly Ala Glu Phe Glu Arg Ile Thr Gln Asn Leu Asp Val His 270

TTC TGG AAG AGC TTC TGG AAC ATC ACA GAG ACC GAA GTC CTG TCG AGT CTT GCC AGT ATG ACA TCC ACT CAA GTA AAG GTG AAC CGG GCT 900
Phe Trp Lys Ser Phe Trp Asn Ile Thr Glu Thr Glu Val Leu Ser Ser Leu Ala Ser Met Thr Ser Thr Gln Val Lys Val Asn Arg Ala 300

CTT TCT GTG CCC CCT GTG CCC TTT GAC CTT CCC CTG GCG GCC AAC CAC AGA GCA TCT GTT ACT ATA GCT CCT CCA TCA GCG CAC ATC GGC 990
Leu Ser Val Pro Pro Val Pro Phe Asp Leu Pro Leu Ala Ala Asn His Arg Ala Ser Val Thr Ile Ala Pro Pro Ser Ala His Ile Gly 330

CCA GCC CCG GTT CAG ATG AGG CTC ATC TCT TAT GAC TTA CGT GAA GGA CAG GAC AGC GAG ACT CTG CTT TCT CTT TGC CGC TCT GAG GGG 1080
Pro Ala Pro Val Gln Met Arg Leu Ile Ser Tyr Asp Leu Arg Glu Gly Gln Asp Ser Glu Thr Leu Leu Ser Leu Cys Arg Ser Glu Gly 360

GGA GCC ATC TCT CTG TCG CTG GGG CTG AAG ACC AAG CGC CTC CCC TCG TCT CCC TGC CTC CTG ATC CAC ATC CAC GGG GGA AGC TTT GTC 1170
Gly Ala Ile Ser Leu Ser Leu Gly Leu Lys Thr Lys Arg Leu Pro Ser Ser Pro Cys Leu Leu Ile His Ile His Gly Gly Ser Phe Val 390

GCC CAT ACC TCC AAG TCC CAT GAG CCC TAT TTG AAG AGC TGG TCC CAG GAC CTG GGT GTC CCC ATC CTG TCA GTG GAC TAC TCT CTG GCC 1260
Ala His Thr Ser Lys Ser His Glu Pro Tyr Leu Lys Ser Trp Ser Gln Asp Leu Gly Val Pro Ile Leu Ser Val Asp Tyr Ser Leu Ala 420

CCT GAA GCC CCT TTC CCG AGG GCC CTG GAA GAG TGT TTC TAT GCC TAC TGC TGG GCT CTG AGA AAT CAC CAC CTA CTA GGT TGG ACT GGA 1350
Pro Glu Ala Pro Phe Pro Arg Ala Leu Glu Glu Cys Phe Tyr Ala Tyr Cys Trp Ala Leu Arg Asn His His Leu Leu Gly Trp Thr Gly 450

GAG AAA GTA TGT CTG GCC GGC GAC AGT GCG GGA GGC AAC TTG AGT GTG ACG ACA TCT ATG CGC GCT GCT GCC TTT GGT GTG CGA ATG CCA 1440
Glu Lys Val Cys Leu Ala Gly Asp Ser Ala Gly Gly Asn Leu Ser Val Thr Thr Ser Met Arg Ala Ala Ala Phe Gly Val Arg Met Pro 480

GAT GGC ATC GTG GCA GCC TAC CCG GCT ACC CTG CTG ACT GCC TAC GCT TCA CCC TCC CGT CTG CTA ACA CTT ATG GAT CCC CTG CTG CCG 1530
Asp Gly Ile Val Ala Ala Tyr Pro Ala Thr Leu Leu Thr Ala Tyr Ala Ser Pro Ser Arg Leu Leu Thr Leu Met Asp Pro Leu Leu Pro 510

CTC AGT GTG CTC TCC AGG TGT CTC AGC GCC TAC GCT GGC AAT GAG CCG CAG ACA GAG ACA CAG GTA GAG AAA GTG AGC ACA CTG AGC CTG 1620
Leu Ser Val Leu Ser Arg Cys Leu Ser Ala Tyr Ala Gly Asn Glu Pro Gln Thr Glu Thr Gln Val Glu Lys Val Ser Thr Leu Ser Leu 540

GTG AGG AGA GAC ACG GCG CTG ATG CTC AGA GAT TTT CGA CAG GGA GCC TCC AAC TGG ATC CAC TCT CTG CTG GAT TCC AAC AGA GCC TCG 1710
Val Arg Arg Asp Thr Ala Leu Met Leu Arg Asp Phe Arg Gln Gly Ala Ser Asn Trp Ile His Ser Leu Leu Asp Ser Asn Arg Ala Ser 570

GCC TCC CCC AGC ACA GCT GCA GAG GCA CCG CCA GGA CCC CCT GAC ACA GTG AGG AAG AGC ATT TCA GAG GCA TCC ATC TCC TCT CCT CAC 1800
Ala Ser Pro Ser Thr Ala Ala Glu Ala Pro Pro Gly Pro Pro Asp Thr Val Arg Lys Ser Ile Ser Glu Ala Ser Ile Ser Ser Pro His 600

```
GCT GAC CCC CCT GTA CCG TCA GAG CCT TCA GAA TTC CCC AGC AGG AAA TTA TCT GTG AAG AGC CAG ACT TGC CAG GAC TTG GGA TCC CAG   1890
Ala Asp Pro Pro Val Pro Ser Glu Pro Ser Glu Phe Pro Ser Arg Lys Leu Ser Val Lys Ser Gln Thr Cys Gln Asp Leu Gly Ser Gln   630

CAC AAT GCC ACC TCT CAC AGT GCA CCA CTG CTC TCT GAG CGC ACC CCA GAA GAT GTG AAT TTC TTC CTC GCC AAG GAT GCA GAT CCC TTC   1980
His Asn Ala Thr Ser His Ser Ala Pro Leu Leu Ser Glu Arg Thr Pro Glu Asp Val Asn Phe Phe Leu Ala Lys Asp Ala Asp Pro Phe   660

ATG TCC AGC AAC CTG TCT TCG GTA GCC ATA CCA CCC CCT GGT GGA GAG GAG GGT TCA GAG CAC GAG CAC CCG AGG GAG TTT CCC CTG GGG   2070
Met Ser Ser Asn Leu Ser Ser Val Ala Ile Pro Pro Pro Gly Gly Glu Glu Gly Ser Glu His Glu His Pro Arg Glu Phe Pro Leu Gly   690

TTT GAG CCG CTG CGT TCA GTG CAG CAA ACA GAG ATG AGG TTG CAG AGT TCT CCA GTG GTC AAG GAT CCT TTC TGC TCT CCT CTT CTG GCT   2160
Phe Glu Pro Leu Arg Ser Val Gln Gln Thr Glu Met Arg Leu Gln Ser Ser Pro Val Val Lys Asp Pro Phe Cys Ser Pro Leu Leu Ala   720

CCT GAT AGC ATG CTG AAA GGG CTG CCA CCT GTA CAT ATA GTG GCT TGT GCA TTA GAC CCC ATG CTG GAT GAC TCT GTG ATG TTT GCC AAG   2250
Pro Asp Ser Met Leu Lys Gly Leu Pro Pro Val His Ile Val Ala Cys Ala Leu Asp Pro Met Leu Asp Asp Ser Val Met Phe Ala Lys   750

CGT TTG AGG AAC ATA GAC CAG CCT GTC ACT CTG TGC GTG GTG GAC GAC CTC CCC CAT GGC TTC CTC AGC CTA TCG CAG CTC TCC AGG GAG   2340
Arg Leu Arg Asn Ile Asp Gln Pro Val Thr Leu Cys Val Val Asp Asp Leu Pro His Gly Phe Leu Ser Leu Ser Gln Leu Ser Arg Glu   780

ACG AGG GAA GCT GCC AAC GTC CTG CGT GGA GAG AAT TCG CGC TGT CTT CAC CCA GTC TGA   2400
Thr Arg Glu Ala Ala Asn Val Leu Arg Gly Glu Asn Ser Arg Cys Leu His Pro Val  *    800

CACACCCCCAGAGCCACGCAAGCACCGCAAGCTGGAACGGACCGATAGGGGTGTGTCGGCCTCTTCTGGGGAAGCAGGTACTCTCTTCGTCGGCCCCATTGAGGGAGTGGAGCTTACA
GCCGGGAAAGGAGCTAAAATTGCTGATGGGGAGGACTTAGTTGCTGTGGCGGCCCAGAATAACACCGACTCTGGTGGGCCTTAAATAAGGTTTAAAAAAGAATAAGACTGCAGTCACC
CAAGGAGTGAAAAAAAAAAAAAAAAAAAAAAAAAAAAAAAAAA
```

Figure 1-1-5. Nucleotide and deduced amino acid sequences of cDNA encoding HSL2 gene in red seabream. Bold faced letters and asterisk indicate the initiation and stop codon, respectively.

Section 2

Sequence analysis

The bioinformatics analysis is a method often used in interdisciplinary field to analyze the biological data by using computer. In this section, the multiple alignment, phylogenetic analysis and estimation of isoelectric point were performed for HSLs of Japanese flounder and red sea bream to understand the characteristics and evolutionary relationship of these HSLs.

Materials and methods

Multiple aliments analysis

The deduced amino acid sequences of HSL were aligned by Mega 5.1 softwares using ClustalW method. The phylogenetic tree was produced by maximum-likelihood method with best-fit substitution model (WAG+G) (Thompson et al. 1994; Tamura et al. 2007). Bootstrap resampling analysis from 1000 replicates was used to evaluate the internal branch. The sequences in comparison were obtained from GenBank (with accession numbers) and Ensembl (protein ID numbers). Accession number of amino acid sequences of HSL are as follows: *Homo sapiens* HSL (AAA69810); *Mus musculus* HSL (NM010719); *Rattus norvegicus* HSL (U40001); *Sus scrofa* HSL (AY686759); *Spermophilus*

tridecemlineatus HSL (Q9R101.1); *Cricetulus griseus* HSL (Predicted: XM_003508874.1); *Pan troglodytes* HSL (Predicted: XM_003316383.2); *Papio Anubis* HSL (predicted: XM_003915627.1); *Nomascus leucogenys* HSL (predicted: XM_003280983.2); *Canis lupus* HSL (Predicted: XM_533655.4); *Loxodonta africana* HSL (Predicted: XM_003406403.1); *Oreochromis niloticus* HSL (FJ601660); *Oncorhynchus mykiss* HSL1 (HQ225622); *O. mykiss* HSL2 (HQ225623); *Sparus aurata* HSL (EU254478); *Salmo salar* HSL (NP_001167134); *Danio rerio* HSL1 (ENSDARP 00000086193), *D. rerio* HSL2 (ENSDARP 00000104226).

Sequence analysis

The theoretical isoelectric point (p*I*) and molecular weight (Mw) of Japanese flounder and red seabream was computed base on the amino acid sequences by Compute p*I* and MW ExPASy (http://www.expasy.ch/cgi-bin/pi_tool).

Results

Overall structure of HSLs

The overall structures of Japanese flounder and red seabream HSLs were similar to those of HSLs from rainbow trout, rat, and human (Fig. 1-2-1). The deduced amino acid sequence of Japanese flounder HSL1 showed 68.1, 72.8, 49.3 and 51.6% identities, respectively. The deduced amino acid sequence of Japanese flounder HSL2, on the other hand, showed 60.8, 62.4, 55.2 and 57.7% identities, respectively. On the other hand, red seabream HSL1 showed 69.8, 71.1, 50.3 and 51.1% identities, respectively. The deduced amino acid sequence of red seabream HSL2 showed 59.5, 61.0, 54.3 and 57.2% identities with those of rainbow trout HSL1, rainbow trout HSL2, rat HSL, and human HSL, respectively.

Phosphorylation sites and catalytic sites of HSLs

HSLs of both Japanese flounder and red seabream possess an N-terminal and C-terminal catalytic domains, separated by glutamine and aspartate (Gln316 and Asp317 in Japanese flounder HSLs, and Gln322 and Asp323, and Gln355 and Asp356 in Japanese flounder HSL1 and HSL2, respectively). In addition, HSLs of Japanese flounder were also conserved in three sites of catalytic triad (Asp427, Asp610 and His657 for HSL1 and Asp427, Asp691 and His738 for HSL2), and in red seabream similar conserved regions were also observed (Asp433, Asp616 and His663 for HSL1 and Asp466, Asp730 and His778 for HSL2). Three phosphorylation sites of rainbow trout HSLs were conserved to

Japanese flounder HSLs (Ser544, Ser546 and Ser594 for HSL1, and Ser590, Ser675 and ser676 for HSL2). The phosphorylation sites were conserved (Ser560, Ser562 and Ser600 for HSL1, and Ser629 and Ser715 for HSL2) in red seabream.

```
Seabream1          ----------------------------------------MDYTVVFAALETVCEDNIAIM 21
Seabream2          MGKRGRRWLRQVRVWANSRFEKSVNGRRSSKHNEGPVCRWTPRRCSTALYSVCKRMPPFF 60
Flounder1          ----------------------------------------MDYKVVFAALETVCEDNNSPL 21
Flounder2          ----------------------------------------MDTKAVFAALYSVCEENATFF 21
Rainbowtrout1      ----------------------------------------MDWIAVFTSLEAVCKENITAL 21
Rainbowtrout2      ----------------------------------------MAWRAVFTALEAVCEENITAL 21
Rat                ----------------------------------------MDLRTMTQSLVALAEDNMAFF 21
Human              ----------------------------------------MDLRTMTQSLVTLAEDNIAFF 21
                                                                  *
Seabream1          CGPSDLPYGNVANRLVTCMRQIQEHGRALEPVVGSFTAVYHHYDFDEQTPGNGYRTLVKV 81
Seabream2          SGGAKGSQGDAARRLVDVMKLIQEHARSLEPVISGFASVYHHFDFDPHIPANGYRSLVKV 120
Flounder1          CGPSDLPYGTVAKRLVTCLREIQEHGHALEPVVASLTAVYHHYDFDAQTPGNGYRTLVKV 81
Flounder2          SGGAKGTQGDAARRLVDTMNLIQEHARSLEPVISGFASVYHHFDFDPHIPANGYRSLVKV 81
Rainbowtrout1      SGPPDLPYGDVSRRLVTCMRKIQDHGRALEPVVSGITAVYHHYDFDSDTPGNGYRTLVKV 81
Rainbowtrout2      SGPTDLLCGNASGRLLTCMRKIQDHGRALEPVVAGFTAVYHHYDFDADTPGNGYRTLVKV 81
Rat                SSQGP---GETARRLSNVFAGVREQALGLEPTLGQLLGVAHHFDLDTETPANGYRSLVHT 78
Human              SSQGP---GETAQRLSGVFAGVREQALGLEPALGRLLGVAHLFDLDPETPANGYRSLVHT 78
                           *    **            ***       * *  * *   * **** **
Seabream1          LQSCLLHIIHKGRYIASNYNSAFFRAEHNASEMEAYCSALCQLRALLHLAQQLINDNECG 141
Seabream2          VRCCLLHIIQKGRYITANRRSIFFRVAHNAGEMEAYCNALCQLRALLYLAQRMLHDNSHG 180
Flounder1          LHACILHIIHKGRYIADNCNGAFFRAEHNASEMEAYCSALCQLRALVHLAQRLINDNECG 141
Flounder2          VRCCILHIIHKGRYISANRRSIFFRVAHNAGEMEAYCSALCQLRALLYLAQRMLHDNSSG 141
Rainbowtrout1      LQSCLLHIIHNGRYIASNCHRAFFRADHNASEMEAYGSVLCQLRALLYIAQGMLHDNSPG 141
Rainbowtrout2      LQSCLLHIIHKGRYIASNCHRAFFRANHNASEMEAYSSALCQLRALLYLAQRLIHDNSHG 141
Rat                ARCCLAHLLHKSRYVASNRRSIFFRASHNLAELEAYLAALTQLRALAYYAQRLLTINRPG 138
Human              ARCCLAHLLHKSRYVASNRRSIFFRTSHNLAELEAYLAALTQLRALVYYAQRLLVTNRPG 138
                      *  *     **   *    ***  **  * ***   * *****   **     *  *
Seabream1          QLYSLQDRDLSRKFVQEYSSMHKACFYGRCLGFQFSPTLRPFLQTVVISMVSYGETYGKQ 201
Seabream2          NLFFQDESGLSESFVREYSSMHKGCFYGRCLGFQFTPAIRPCLQTIAIGLVAFGENYRRH 240
Flounder1          QLYSQQDGDLTRRFVQEYSSMHKACFYGRCLGFQFSPALRPFLQTVVISMISYGETYGKQ 201
Flounder2          NLFFQDESGLSESFVREYSSMHKGCFYGRCLGFQFTPSIRPCLQTIAIGLVAFGENYKRH 201
Rainbowtrout1      QLYGEQDGELSRWLVREYASMHKACFYGRCLGFQFSSSLRPILQSLIISMVSFGESYEKQ 201
Rainbowtrout2      QLYSLQNGELSRRFVREYTSMHKACFYGRCLGFQFSPTLRPFLQTVVISMVSFGESYGKQ 201
Rat                VLFFEGDEGLSADFLQDYVTLHKGCFYGRCLGFQFTPAIRPFLQTLSIGLVSFGEHYKRN 198
Human              VLFFEGDEGLTADFLREYVTLHKGCFYGRCLGFQFTPAIRPFLQTISIGLVSFGEHYKRN 198
                    *       *       *   ** ***********    ** **   *     ** *
Seabream1          QSGLGMAALSLLTSGKYVMDPELRGAEFERITQNLDMQFWKSFWNLTESGLIAGFSRIAS 261
Seabream2          QSGIGVAASSFFTSGKYAIDPELRGAEFERITQNLDVHFWKSFWNITETEVLSSLASMTS 300
Flounder1          QSRFGMAALSLLTSGKYVIDPEMRGTEFERITQNLDLHFWKSFWNLTESGLITGLNRIAS 261
Flounder2          QSGIGVAASSLFTSGKYAIDPELRGAEFERITQNLDVHFWKTFWNITETELPSSLASMTS 261
Rainbowtrout1      HSGLGMAAFSLLTSGKYVIDPELRGEEYERITQNLDMKFWKSFWNLTESELVSGFASLTS 261
Rainbowtrout2      QSGLGMAAFSFLTSAKYVIDPELRGAEFERITQNLDMKFWKSFWNLTESELLSGLASVAS 261
Rat                ETGLSVTASSLFTGGRFAIDPELRGAEFERIIQNLDVHFWKAFWNITEIEVLSSLANMAS 258
Human              ETGLSVAASSLFTSGRFAIDPELRGAEFERITQNLDVHFWKAFWNITEMEVLSSLANMAS 258
                         * *  *      *** ** * *** ****  *** *** **          *
Seabream1          CPVQMNFTLTLPPVTLHLPLASDPSLTATVSPPIAHWGPGPVHMRLISHELREGQDSEEL 321
Seabream2          TQVKVNRALSVPPVPFDLPLAANHRASVTIAPPSAHIGPAPVQMRLISYDLREGQDSETL 360
Flounder1          NTVQVNLTLTVPPLPLRLPLASDPNLTATVSPPIAHSGPGPVHMRLISYELREGQDSEEL 321
Flounder2          TQVKVNRPLSVPPVPFDLPLAANHRVSVTISPPSAHIGTAPVQMRLISYDLREGQDSETL 321
Rainbowtrout1      TLVQVNLTLTIPPEPLLLPLVSDPRLSTPVSPPVAHWGPGPVNMRLISYELREGQDSKEL 321
Rainbowtrout2      NLVQLNLTLTIPPEPLRLPLASDPRLFAPVSPPVAHWGPGPVNVRLISYELREGQDSDEL 321
Rat                TTVRVSRLLSLPPEAFEMPLTSDPKLTVTISPPLAHTGPGPVLARLISYDLREGQDSKML 318
Human              ATVRVSRLLSLPPEAFEMPLTADPTLTVTISPPLAHTGPGPVLVRLISYDLREGQDSEEL 318
                     *     *  **     **          *** ** *  **  ****  *****  **  *
```

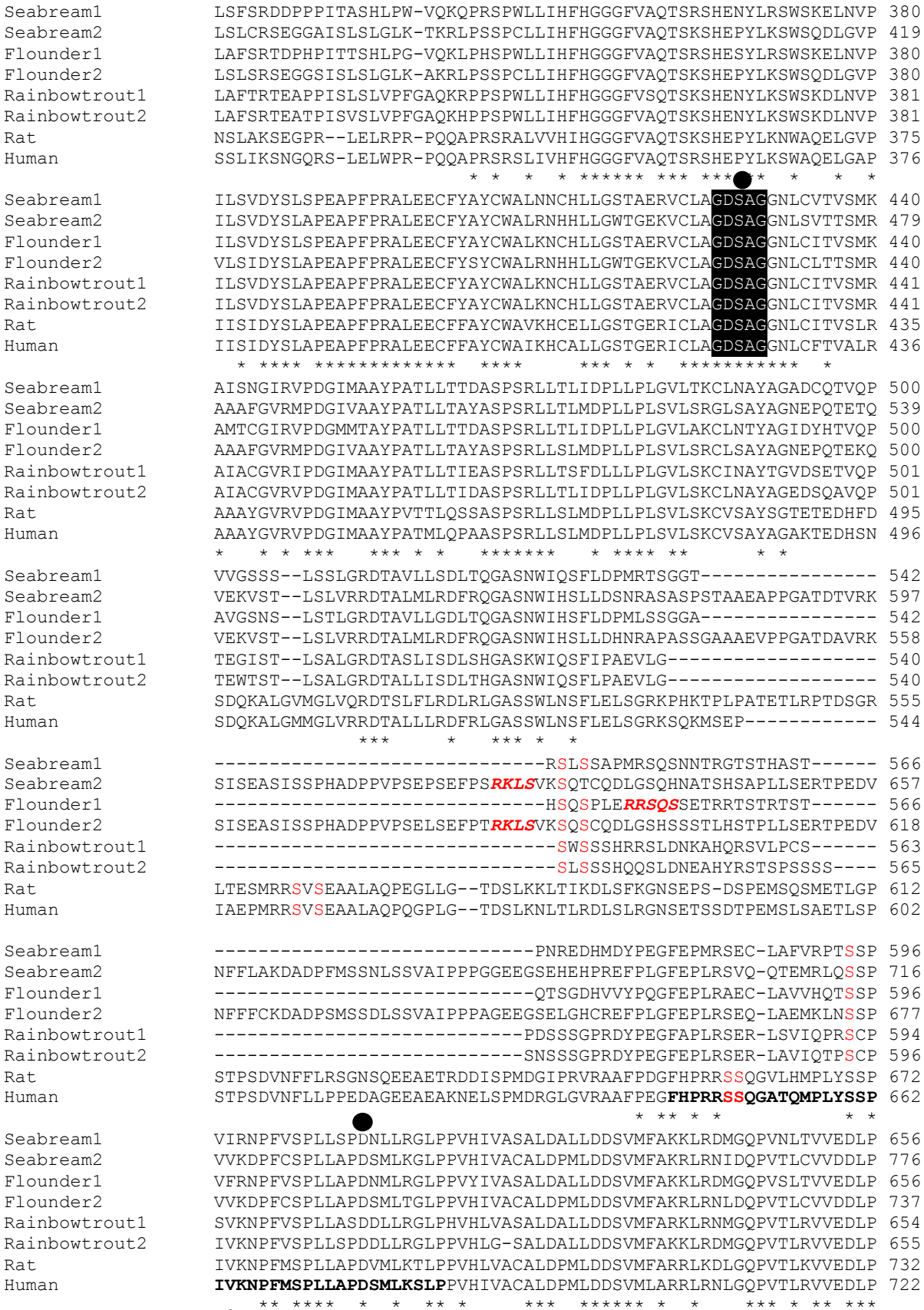
Seabream1 LSFSRDDPPPITASHLPW-VQKQPRSPWLLIHFHGGGFVAQTSRSHENYLRSWSKELNVP 380
Seabream2 LSLCRSEGGAISLSLGLK-TKRLPSSPCLLIHFHGGGFVAQTSKSHEPYLKSWSQDLGVP 419
Flounder1 LAFSRTDPHPITTSHLPG-VQKLPHSPWLLIHFHGGGFVAQTSRSHESYLRSWSKELNVP 380
Flounder2 LSLSRSEGGSISLSLGLK-AKRLPSSPCLLIHFHGGGFVAQTSKSHEPYLKSWSQDLGVP 380
Rainbowtrout1 LAFTRTEAPPISLSLVPFGAQKRPPSPWLLIHFHGGGFVSQTSKSHENYLKSWSKDLNVP 381
Rainbowtrout2 LAFSRTEATPISVSLVPFGAQKHPPSPWLLIHFHGGGFVAQTSKSHENYLKSWSKDLNVP 381
Rat NSLAKSEGPR--LELRPR-PQQAPRSRALVVHIHGGGFVAQTSKSHEPYLKNWAQELGVP 375
Human SSLIKSNGQRS-LELWPR-PQQAPRSRSLIVHFHGGGFVAQTSRSHEPYLKSWAQELGAP 376
Seabream1 ILSVDYSLSPEAPFPRALEECFYAYCWALNNCHLLGSTAERVCLAGDSAGGNLCVTVSMK 440
Seabream2 ILSVDYSLAPEAPFPRALEECFYAYCWALRNHHLLGWTGEKVCLAGDSAGGNLSVTTSMR 479
Flounder1 ILSVDYSLSPEAPFPRALEECFYAYCWALKNCHLLGSTAERVCLAGDSAGGNLCITVSMK 440
Flounder2 VLSIDYSLAPEAPFPRALEECFYSYCWALRNHHLLGWTGEKVCLAGDSAGGNLCLTTSMR 440
Rainbowtrout1 ILSVDYSLAPEAPFPRALEECFYAYCWALKNCHLLGSTAERVCLAGDSAGGNLCITVSMR 441
Rainbowtrout2 ILSVDYSLAPEAPFPRALEECFYAYCWALKNCHLLGSTAERVCLAGDSAGGNLCITVSMR 441
Rat IISIDYSLAPEAPFPRALEECFFAYCWAVKHCELLGSTGERICLAGDSAGGNLCITVSLR 435
Human IISIDYSLAPEAPFPRALEECFFAYCWAIKHCALLGSTGERICLAGDSAGGNLCFTVALR 436
Seabream1 AISNGIRVPDGIMAAYPATLLTTDASPSRLLTLIDPLLPLGVLTKCLNAYAGADCQTVQP 500
Seabream2 AAAFGVRMPDGIVAAYPATLLTAYASPSRLLTLMDPLLPLSVLSRGLSAYAGNEPQTETQ 539
Flounder1 AMTCGIRVPDGMMTAYPATLLTTDASPSRLLTLIDPLLPLGVLAKCLNTYAGIDYHTVQP 500
Flounder2 AAAFGVRMPDGIVAAYPATLLTAYASPSRLLSLMDPLLPLSVLSRCLSAYAGNEPQTEKQ 500
Rainbowtrout1 AIACGVRIPDGIMAAYPATLLTIEASPSRLLTSFDLLLPLGVLSKCINAYTGVDSETVQP 501
Rainbowtrout2 AIACGVRVPDGIMAAYPATLLTIDASPSRLLTLIDPLLPLGVLSKCLNAYAGEDSQAVQP 501
Rat AAAYGVRVPDGIMAAYPVTTLQSSASPSRLLSLMDPLLPLSVLSKCVSAYSGTETEDHFD 495
Human AAAYGVRVPDGIMAAYPATMLQPAASPSRLLSLMDPLLPLSVLSKCVSAYAGAKTEDHSN 496
Seabream1 VVGSSS--LSSLGRDTAVLLSDLTQGASNWIQSFLDPMRTSGGT---------- 542
Seabream2 VEKVST--LSLVRRDTALMLRDFRQGASNWIHSLLDSNRASASPSTAAEAPPGATDTVRK 597
Flounder1 AVGSNS--LSTLGRDTAVLLGDLTQGASNWIHSFLDPMLSSGGA---------- 542
Flounder2 VEKVST--LSLVRRDTALMLRDFRQGASNWIHSLLDHNRAPASSGAAAEVPPGATDAVRK 558
Rainbowtrout1 TEGIST--LSALGRDTASLISDLSHGASKWIQSFIPAEVLG---------- 540
Rainbowtrout2 TEWTST--LSALGRDTALLISDLTHGASNWIQSFLPAEVLG---------- 540
Rat SDQKALGVMGLVQRDTSLFLRDLRLGASSWLNSFLELSGRKPHKTPLPATETLRPTDSGR 555
Human SDQKALGMMGLVRRDTALLLRDFRLGASSWLNSFLELSGRKSQKMSEP---------- 544
Seabream1 ----------RSLSSAPMRSQSNNTRGTSTHAST------ 566
Seabream2 SISEASISSPHADPPVPSEPSEFPSRKLSVKSQTCQDLGSQHNATSHSAPLLSERTPEDV 657
Flounder1 ----------HSQSPLERRSQSSETRRTSTRTST------ 566
Flounder2 SISEASISSPHADPPVPSELSEFPTRKLSVKSQSCQDLGSHSSSTLHSTPLLSERTPEDV 618
Rainbowtrout1 ----------SWSSSHRRSLDNKAHQRSVLPCS------ 563
Rainbowtrout2 ----------SLSSSHQQSLDNEAHYRSTSPSSSS---- 565
Rat LTESMRRSVSEAALAQPEGLLG--TDSLKKLTIKDLSFKGNSEPS-DSPEMSQSMETLGP 612
Human IAEPMRRSVSEAALAQPQGPLG--TDSLKNLTLRDLSLRGNSETSSDTPEMSLSAETLSP 602
Seabream1 ----------PNREDHMDYPEGFEPMRSEC-LAFVRPTSSP 596
Seabream2 NFFLAKDADPFMSSNLSSVAIPPPGGEEGSEHEHPREFPLGFEPLRSVQ-QTEMRLQSSP 716
Flounder1 ----------QTSGDHVVYPQGFEPLRAEC-LAVVHQTSSP 596
Flounder2 NFFFCKDADPSMSSDLSSVAIPPPAGEEGSELGHCREFPLGFEPLRSEQ-LAEMKLNSSP 677
Rainbowtrout1 ----------PDSSSGPRDYPEGFAPLRSER-LSVIQPRSCP 594
Rainbowtrout2 ----------SNSSSGPRDYPEGFEPLRSER-LAVIQTPSCP 596
Rat STPSDVNFFLRSGNSQEEAETRDDISPMDGIPRVRAAFPDGFHPRRSSQGVLHMPLYSSP 672
Human STPSDVNFLLPPEDAGEEAEAKNELSPMDRGLGVRAAFPEGFHPRRSSQGATQMPLYSSP 662
Seabream1 VIRNPFVSPLLSPDNLLRGLPPVHIVASALDALLDDSVMFAKKLRDMGQPVNLTVVEDLP 656
Seabream2 VVKDPFCSPLLAPDSMLKGLPPVHIVACALDPMLDDSVMFAKRLRNIDQPVTLCVVDDLP 776
Flounder1 VFRNPFVSPLLAPDNMLRGLPPVYIVASALDALLDDSVMFAKKLRDMGQPVSLTVVEDLP 656
Flounder2 VVKDPFCSPLLAPDSMLTGLPPVHIVACALDPMLDDSVMFAKRLRNLDQPVTLCVVDDLP 737
Rainbowtrout1 SVKNPFVSPLLASDDLLRGLPHVHLVASALDALLDDSVMFARKLRNMGQPVTLRVVEDLP 654
Rainbowtrout2 IVKNPFVSPLLSPDDLLRGLPPVHLG-SALDALLDDSVMFAKKLRDMGQPVTLRVVEDLP 655
Rat IVKNPFMSPLLAPDVMLKTLPPVHLVACALDPMLDDSVMFARRLKDLGQPVTLKVVEDLP 732
Human IVKNPFMSPLLAPDSMLKSLPPVHIVACALDPMLDDSVMLARRLRNLGQPVTLRVVEDLP 722

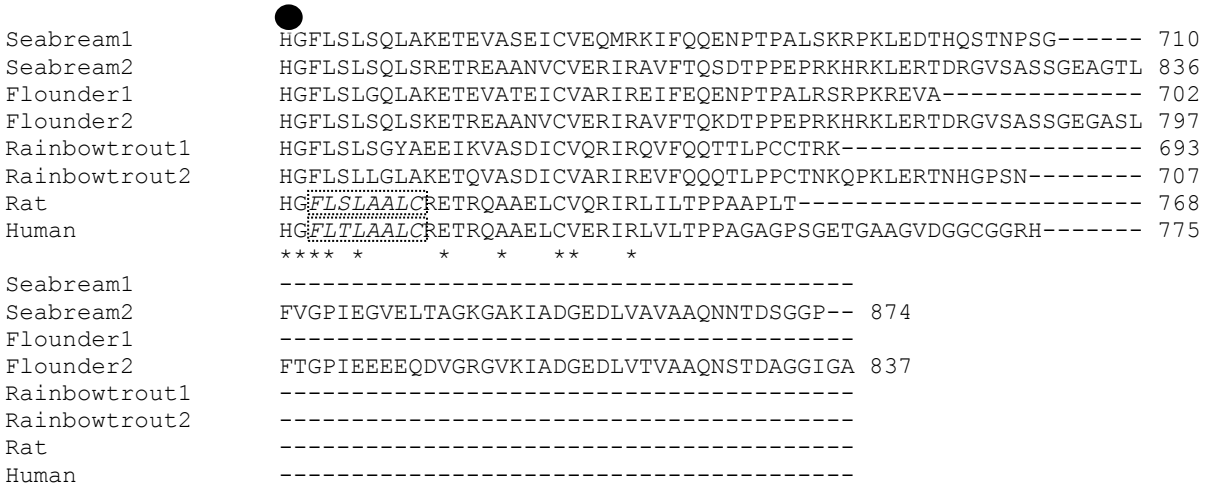

Figure 1-2-1. Multiple alignments of deduced amino acid sequences of HSL 1 and 2 genes from Japanese flounder *Paralichthys olivaceus* and red seabream *Pagrus major* with those from other animals. Gap introduced to optimize alignment are represented by (-). Conserved residues were potted with asterick (*). The catalytic triad determined according to rainbow trout, rat and human HSLs is marked by black circles. Red alphabets shown phosphorylation sites of rat and human HSLs, putative phosphorylation sites of rainbow trout HSLs (Kittilson et al. 2011), and serine residues of Japanese flounder and red seabream HSLs aligned with the rainbow trout putative phosphorylation sites. Putative phosphorylation motif of human protein kinase A (Smith et al. 2011) in Japanese flounder HSLs are shown in red bold italic. Conserved boundary between N- and C-terminal regions is indicated by a vertical line. Crucial regulatory module for the activity of human HSL is shown in bold broaken line box. The catalytic cores of HSL protein represented by GXSXG were highlighted with black box. Putative lipid-binding region of rat and human are shown in box with italic (Lampidonis et al. 2011).

Sequence analysis

The theoretical p*I* and Mw of HSL1 were 6.2 and 77253 and 6.0 and 90954 of HSL2 of Japanese flounder, and 5.88 and 78882.86, and 8.40 and 95556.69, for HSL1 and HSL2 of red seabream, respectively. The DNA nucleotide sequences of Japanese flounder HSL1 and HSL2 genes were registered in the DDBJ/EMBL/GenBank databases with accession numbers AB828672 and AB828673, respectively.

Phylogenetic analysis

Deduced acid sequences of HSL from mammals and teleost including, Japanese flounder and red seabream were used to construct the phylogenetic tree. HSLs from Japanese flounder and red seabream were distinctly separated to mammalian organisms and located at the same clade as HSLs from bony fish. Within the fish clade, HSLs of Japanese flounder and red seabream belonged to HSL1 and HSL2 clusters, respectively. However, in this study, we found that rainbow trout HSL1 and HSL2 belonged to the HSL1 cluster in contrast to the previous report by Kittilson et al. (2011).

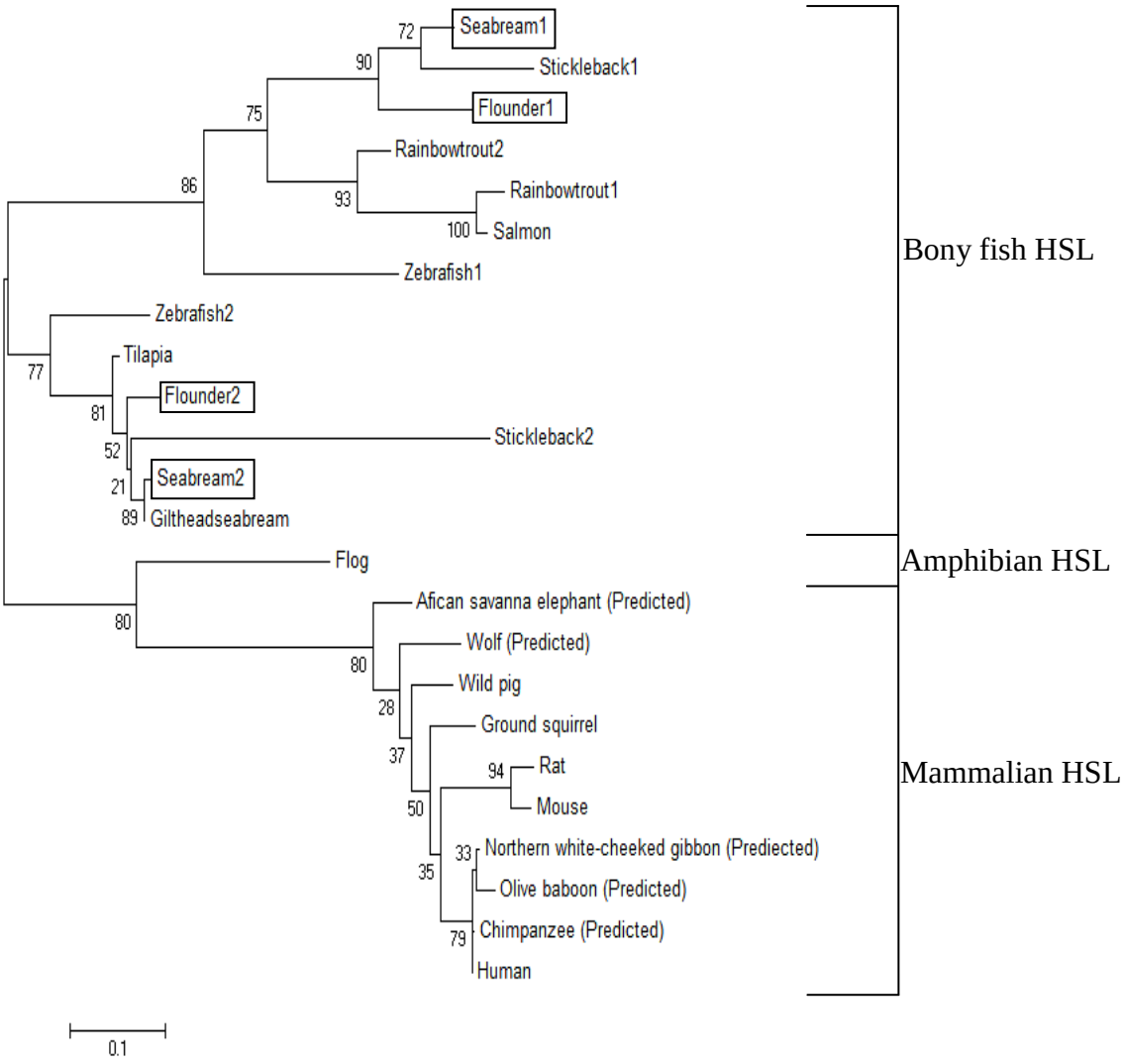

Figure 1-2-2. Maximum-likelihood tree of HSL family proteins from various species constructed with the best-fit substitution model (WAG+G). The boostrap values from 1,000-replicate analysis are given at the nodes in percentage. The sequences in comparison were obtained from GenBank (with accession numbers) and Ensembl (protein ID numbers) as follows: human, *Homo sapiens* HSL (AAA69810); mouse, *Mus musculus* HSL (NM010719); rat, *Lattus norvegicus* HSL (U40001); Wild pig, *Sus scrofa* HSL (AY686759); ground squirrel, *Spermophilus tridecemlineatus* HSL (Q9R101.1); Chimpanzee, *Pan troglodytes* HSL (Predicted: XM_003316383.2); olive baboon, *Papio Anubis* HSL (predicted:

XM_003915627.1); northern white-cheeked gibbon, *Nomascus leucogenys* HSL (predicted: XM_003280983.2); wolf, *Canis lupus* HSL (Predicted: XM_533655.4); Afican savanna elephant, *Loxodonta africana* HSL (Predicted: XM_003406403.1); tilapia *Oreochromis niloticus* HSL (FJ601660); rainbow trout1 (HSL1), *Oncorhynchus mykiss* (HQ225622); rainbow trout2 (HSL2), *O. mykiss* (HQ225623); gilthead seabream, *Sparus aurata* HSL (EU254478); zebrafish1 (HSL1), *Danio rerio* (ENSDARP 00000086193), zebrafish2 (HSL2), *D. rerio* (ENSDARP 00000104226); stickleback1 (HSL1), *Gasterosteus aculeatus* (ENSGACP00000003188), stickleback1 (HSL2), *G. aculeatus* (ENSGACP 00000004226), Japanese flounder1 (HSL1), *Paralichthys olivaceus* (AB828672), Japanese flounder2 (HSL2), *P. olivaceus* (AB828673), red seabream1 (HSL1), *Pagrus major* and red seabream2 (HSL2), *P. major*.

Discussion

In this section, full-length of cDNA encoding HSL was isolated, cloned and sequenced from inclinator muscle of fin and adipose tissue of Japanese flounder and red seabream, respectively. In addition, the theoretical isoelectric point (p*I*) and molecular weight (Mw) were determined. So far, the full-length of HSL cDNA has been cloned from several species such as 3,255 bp in human (Langin et al. 1993), 3,226 bp in rat (Holm et al. 1988), 2,277 bp in nile tilapia (Han et al. 2011), 2,679 bp in orange-spotted grouper (Unpublished data), 2,562 bp HSL1 and 2,887 bp HSL2 in rainbow trout. Multiple nucleotide sequence alignment analysis with deduced of HSLs amino acid sequences from human, rat, and rainbow trout shown that HSLs of Japanese flounder and red seabream are similar and have the same basic organization as previously reported. Notably, HSLs sequences of Japanese flounder, red seabream and other fish are shorter than the mammalian and were misaligned with the rat and human at basic conserved sites. The misaligned of serine residues caused by HSL1 sequences from fish species are shorter than HSLs from mammal which may mispositioning when aligning to longer sequences either human or mouse (Kittilsen et al. 2011). Furthermore, rainbow trout HSL1 and HSL2 have the deletion in the C-terminal region (AA530-570, see Fig. 1-2-1), which is found in Japanese flounder and red seabream HSL1 but not in HSL2. We found phosphorylation motifs of mammalian PKA (R/K-R/K-X-pS/T or R/K-R/K-X-X-pS/T) in deduced amino acid sequences of both Japanese flounder and red seabream HSLs (Fig. 1-2-1).

Phylogenetic analysis further confirmed that the obtained sequences from Japanese flounder and red seabream are the member of HSL family. The results revealed that the phylogenetic tree was distinctly divided into three different ancestor species including primate, bony fish and amphibian. This result suggests that HSLs of Japanese flounder and red seabream sequences clustered with HSL proteins and relatedness was shown of this sequence to other fish species, firmly establishing the encoded protein as the hormone-sensitive lipase family. However, HSL1 and HSL2 of rainbow trout were not separated and located at the same clade with HSL1 of salmonid fish. At present the reason for this discrepancy is not clear, but it might be related to the whole-genome duplication event in salmonid fish (Kitillsen et al. 2011).

Summary

HSL cDNAs were cloned from Japanese flounder *Paralichthys olivaceus* and red seabream *Pagrus major*. The full-length cDNAs of two HSL genes from both Japanese flounder and red seabream, designated HSL1 and HSL2, consisted of 2,922 bp and 2,832 bp, and 2,955 bp and 2,723 bp of Japanese flounder and red seabream, respectively. HSLs encoding with 702 and 837 amino acids for Japanese flounder and 710 and 874 amino acid for red seabream, respectively. A phylogenetic analysis revealed that both fish HSLs were distinctly separated into three different ancestor species. Within teleost fish, HSLs of Japanese flounder and red seabream clustered in the bony fish clade with the same

branch to bony fish. HSL1 and HSL2 from Japanese flounder were distinctly separated to HSL1 and HSL2 clade. Whereas, the multiple HSL protein alignment showed that both fish has the basic organization of HSLs as found in rat and human HSLs. The present study suggests that HSLs from Japanese flounder and red seabream are member of HSL family of lipase.

Chapter 2

Tissue distribution of hormone-sensitive lipase

Currently, lipid accumulation in fish has been studied and interested by many researchers. The topic on lipid accumulation study in teleost fish represents a good model for investigation on lipid metabolism and over all energy mobilization. Teleost fish metabolize their stored lipid for energy production and differ from mammal using carbohydrate for energy production (Yang et al. 2011) except for some species using energy for hibernation, for example polar bear and hibernate bat. Furthermore, lipid content in fish is the major determinant to determine the quality of fish meat (Kaneko et al. 2013). Fish has three major sources to store their excess lipid including liver, skeletal muscle and adipose tissue. Lipid accumulation in fish is specific to fish species; for torafugu *Takifugu rubripes* and Japanese flounder *Paralichthys olivaceus*, their lipid are mainly accumulated in their liver. In contrast, in red seabream *Pagur major* nearly 50% of body lipid is mainly accumulated in visceral adipose tissues (Oku and Ogata 2000).

Several studies have investigated the HSL mRNA expression in various species. The expression of HSL mRNA was abundant not only in the lipid store tissues such as, adipose tissue, liver and skeletal muscle, but also distributed with low levels in the non lipid store tissues. For example, heart (Small et al. 1989), human cancer cell (Lampidonis et al. 2008), macrophages (Contreras et al. 1994), and pancreatic β-cells (Klannemark et al. 1998). Furthermore, the tissue-

specific manner for HSL mRNA expression has shown that HSL expression is detected in white and brown adipose tissues, gonad, and pancreas by northern blot analysis in human and rat (Holm et al. 1990; 1994), indicating that HSL is distributed widely in various tissues in mammal.

In fish, the first cDNA encoding HSL genes was cloned and clarified their molecular mechanism only from rainbow trout. HSL mRNA expression patterns in rainbow trout showed that the highest HSL expression was observed in mesenteric fat for HSL1 and in the pyloric caeca for HSL2, followed by the brain and liver (Kittilsen et al. 2011). The expression levels of HSL mRNAs were observed with low levels in red muscle but higher than the case of white muscle. In contrast, the expression and the function of HSL were limited and poorly clarified in adipose tissue and non-adipose tissue. The relationships of HSL gene expression with lipid storage patterns specific to fish species have not been clarified. In the present study, two models of fish, Japanese flounder, depositing lipid in the skeletal muscle, and red seabream, highly accumulating lipid in the visceral organ, were investigated from the view point of the relationships between HSL gene and protein expression patterns on lipid metabolism.

Section 1

Localization of adipose tissue in Japanese flounder *Paralichthys olivaceus*

Adipose tissue is the main source of lipid reserved for maintenance of energy homeostasis, in term of lipid storing energy in the form of TAG. The adipocyte lipolysis is hydrolyzed during fasting and life activities by releasing FFA and glycerol. The released FFAs are taken up and metabolized to responsible their requirement in peripheral tissues. Several studies in fish found that lipids are species-specific to fish (Oku et al. 2006, Kaneko et al. 2013). Kaneko et al. (2013) has demonstrated that red seabream accumulates lipid in myosepta in the skeletal muscle, while no lipid accumulation was observed in the skeletal muscle of torafugu. They also observed that both species preferentially accumulate lipid in their liver, and that the size of lipid droplets in the liver of torafugu was larger than that of red seabream (Kaneko et al. 2013). The results suggest that teleost fish accumulate lipid in a species- and tissue- specific manner.

Since HSL hydrolyzes TAG and DAG and releases FFA, HSL will be responsible for species- and tissue- specific lipid accumulation patterns as described above. The localization of adipocyte and lipid classification are also essential to understand HSL physiological functions. It is generally accepted that the inclinator muscle of fin, *engawa* tissue in Japanese, of Japanese flounder is rich in lipid, but that very little lipid is accumulated in the skeletal muscle in body

trunk. In this section, oil red O staining was performed to localize adipocytes in Japanese flounder.

Material and methods

Materials

Oil red O was purchased from Nacalai Tesque (Kyoto, Japan). The oil red O stock solution was prepared by mixing 0.5 g oil red O in 100 ml isopropanol under vigorous agitation with magnetic stirrer. After mixed well with isopropanol, the stock solution was filtrated through a No. 2 filter membrane paper (Advantec, Tokyo, Japan). To prepare working solution, the oil red O stock solution was diluted with dH_2O (dH_2O: oil red O stock solution 3:2, v/v).

Sample preparation

Three individuals of Japanese flounder (approximately 1-2 kg in body weight) were cut in vertical direction to the backborne and divided into 2 parts including abdominal and ventral part. The fish fillets were washed with Tris-buffered saline buffer (TBS) to remove blood clotting and then fixed with 4% paraformaldehyde (PFA) in phosphate buffer solution (PBS) at 4°C for 1 week.

Oil red O staining

After fixation with 4% PFA/PBS, the fish fillets were rinsed with flow through tap water for 15 min and washed 3 times with PBS for 15 min. The fish fillets were stained with a working solution as described above at room temperature at 4°C for overnight. The fillets were briefly rinsed with 60% isopropanol, washed twice with distilled water, and photographed using a commercial digital camera and a BZ-9000 microscope (Keyense, Osaka, Japan).

Results

To localize adipocyte cells of Japanese flounder, the cross-sectioned fillets were stained with oil red O. As expected, lipid was clearly accumulated in the inclinator muscle of ocular and blind sides of the fin (Fig. 2-1-1). Lipid accumulation was also observed around the notochord, and strongly in myosepta. Subcutaneous adipose tissue was apparent only at the blind side. Higher magnification of the inclinator muscle of fin revealed that lipid was stored in adipocytes along muscle fiber cells (Figs. 2-1-1; B and C).

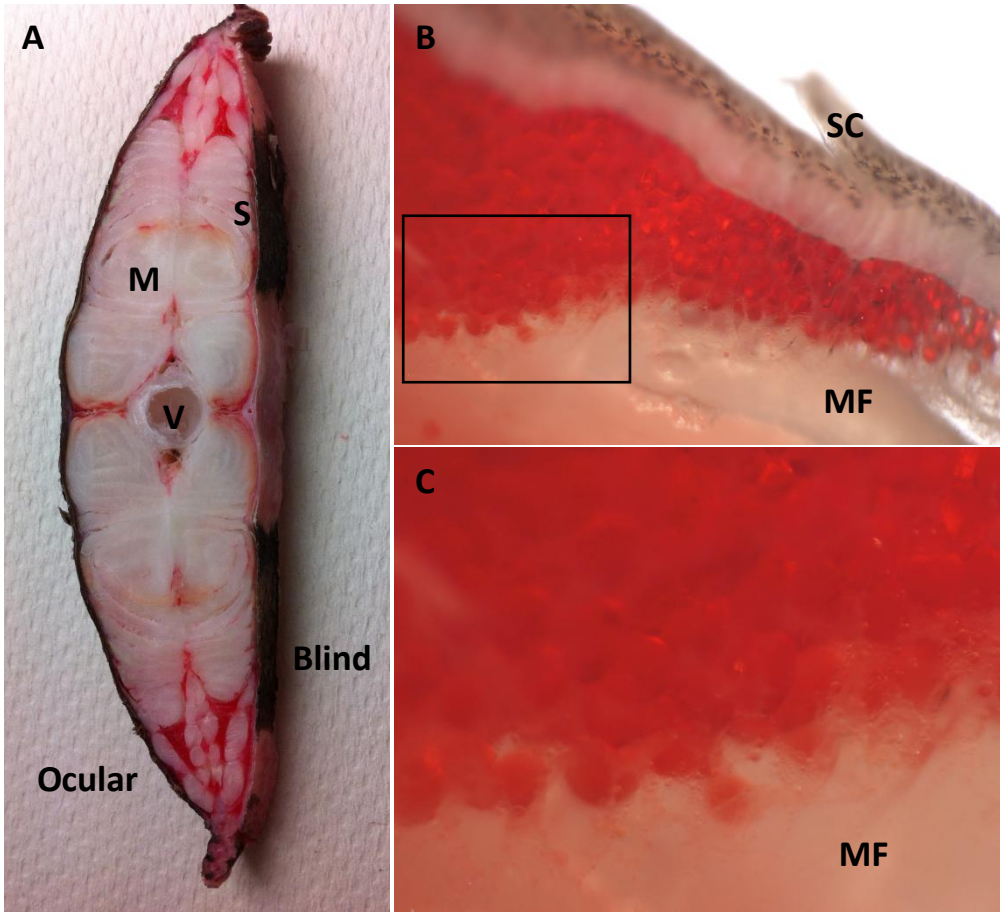

Figure 2-1-1. Representative micrographs of oil red O staining of fillet (A) and enlargement view of adipocytes around the inclinator muscle of fin (B). Enlargement of framed part in B depicts an area of stained adipocyte cells. Abbreviations: M, myosepta; S, skin; SC, scale; V, vertebra; MF muscle fiber. Original magnification: X100 (B), X200 (C).

Section 2

Tissue distribution of hormone-sensitive lipase

HSL was considered to be the rate limiting-enzyme on lipid hydrolysis and lipolysis under physiological control, by hydrolyzing stored lipid to produce free fatty and glycerol for transporting into energy requiring tissues as stated above. The molecular mass of HSL proteins in adipose tissues has been already investigated in several mammalian species. The molecular mass for bovine HSL was identified as approximately 84 kDa, a slightly lower in rat of 82 kDa, and slightly larger molecular mass was of 88 kDa for human adipose tissue HSL (Holm et al. 1989; 2000; 2003). However, little information about fish HSL is available. In this section, in order to investigate tissue distribution patterns of HSL gene and protein expressions, reverse transcription PCR (RT-PCR), quantitative real-time PCR and immunoblot analysis were carried out with Japanese flounder and red seabream.

Materials and methods

Fish

After, experimental fish was anesthetized with ice cool water, nine tissues, fin, gill, heart, intestine, liver, skeletal muscle, inclinator muscle of fin, skin and gonad, were excised out from Japanese flounder and nine tissues, adipose tissue, fin, gill, heart, intestine, liver, skeletal muscle, skin and gonad, from red

seabream. All sample tissues were immediately preserved in RNAlater (Ambion) and stored in -20^{o}C until use. Total RNAs were extracted using a RNeasy lipid tissue mini kit (Qiagen) and first-strand cDNAs were synthesized in a 10 μl reaction mixture using a Verso cDNA kit (Thermo Fisher Scientific, Epsom, UK). cDNAs of both Japanese flounder and red seabream were used for the following RT- PCR and real-time PCR analyses.

For the HSL protein distribution study, after the target tissues were excised out from both fish species, tissue samples were immediately kept at -80^{o}C until analyses.

Materials

To purify HSL-antibody, the NHS-activated agarose was purchased from Thermo Scientific. For immunoprecipitation, the protein G-Sepharose 4 Fast Flow was purchased from GE healthcare.

Japanese flounder

Reverse transcription PCR

RT-PCR was used to perform the HSL tissue distribution pattern. The HSLs genes specific primers were designed based on conserved regions aligned with others organisms as shown in Table 2-2-1. The alignment online tool, Clustal W2 (http://www.ebi.ac.uk/Tools/msa/clustalw2/), was used to determine the conserved regions between obtained sequences from Japanese flounder and

HSLs sequences from rainbow trout. The reported sequences are available in the database DDBJ/EMBL/GenBANK. Furthermore, the sizes of amplified PCR products are less than 300 bp. Designed primer pairs were considered at 3'end of each sequences due to specific site for HSL gene. The RT-PCR was carried out using Ex *taq* DNA polymerase (Takara) and specific primer pairs were used to demonstrate tissue distribution of HSL1 and HSL2 transcript (Table 2-2-1). PCR was performed in 20 µl of reaction mixture containing 1 µg of cDNA, 5 pmol each specific primers, 2 µl of 10x PCR buffer (Toyobo), 4 nmol of dNTP and 0.5 U Ex *Taq* DNA polymerase (Takara). PCR was consisted of 94^{o}C 30 s for 40 cycles with 94^{o}C for 30 s, the annealing temperatures are depending on melting temperature (Tm) of each designated primer pairs for 30 s, and 72^{o}C for 30 s, followed by a final extension at 72^{o}C for 5 min.

Amplification efficiency

To normalize the designed primer pairs, the PCR efficiency assay will determined from an amplification efficiency curves based on the cDNA serial dilution of each primer pair. Serial dilution of cDNA was diluted with dH_2O for 1, 10, 100, 1,000, and 10,000 times for the determination of the amplification curves. The reaction of real-time PCR was performed in 20 µl reaction mixtures containing 2 µl of the cDNA solution, 10 µl of SYBR Premix Ex *Taq* (Takara), 0.4 µl of 50X ROX reference dye (Takara), and 10 pmol each of gene-specific primers (Table 2-2-2). Mixed solutions were subjected and analyzed by ABI PRISM 7300 real-time PCR system (Applied Biosystems). Relative mRNA levels

were determined by the comparative Ct method. The Ct value and Log of cDNA dilution factor were plotted to calculate slope and R-square (R^2) was determined.

Quantitative real-time PCR

Real-time PCR was performed with an ABI PRISM 7300 real-time PCR system (Applied Biosystems). Total RNAs were extracted using the RNeasy lipid tissue mini kit (Qiagen) and the first-strand cDNAs were synthesized in a 10 μl reaction mixture using a Verso cDNA kit (Thermo Fisher Scientific, Epsom, UK). The gene-specific primers for the HSL and β-actin genes were designed using Primer express software v2.0 (Applied Biosystems) based on their nucleotide sequences obtained in the previous section. Real-time PCR was performed in 20 μl reaction mixtures containing 2 μl of the cDNA solution (1:100 dilution), 10 μl of SYBR Premix Ex *Taq* (Takara), 0.4 μl of 50X ROX reference dye (Takara), and 10 pmol each of gene-specific primers (Table 2-2-2). Relative mRNA levels were determined by the comparative Ct method using those of β-actin as an internal control. The data were analyzed by one-way analysis of variance (ANOVA) followed by Tukey-Kramer post-hoc test.

Red seabream

Reverse transcription PCR

HSL gene primers were designed for RT-PCR using alignment online tools as described above (Table 2-2-1). Ex *taq* DNA polymerase (Takara) and gene specific primers were used for the reverse transcription PCR (Table 2-2-

1). PCR was performed in 20 µl of reaction mixture containing as described above at 94^0C 30 s followed by 40 cycles of 94^0C for 30 s, 72^0C for 30 s, followed by a final extension at 72^0C for 5 min.

Real-time PCR

Real-time PCR was performed using TaqMan fast advanced master mix (Applied Biosystems), according to the manufacturer's protocol. Gene-specific primers and TaqMan probes were designed using Primer express software v2.0 (Applied Biosystems) from the DNA nucleotide sequences of red seabream HSL1 and HSL2 identified in the present study. β-actin was used to determine as housekeeping gene**.** We used β-actin gene from previous study which characterized by Oku et al. (2006). The relative mRNA levels were determined by the comparative Ct method using the β-actin gene as internal controls. Data were analyzed by student's *t*-test and one-way analysis of variance (ANOVA), followed by the Tukey-Kramer post hoc test using JMP 7.0.2 software (SAS Institute Inc., Cary, NC, USA).

Table 2-2-1. Oligonucleotide sequences of primers used for RT-PCR

Primer name	Sequences 5'-3'	genes
RTPCRHSLC1F_JF	CCAGTCGCCGTTAGAGAGGAG	HSL1
RTPCRHSLC1R_JF	GTTCACCAGACCTCCTCTCCTG	HSL1
RTPCRHSLC2F_JF	CGCGCAAGCACCGAAAGCTGG	HSL2
RTPCRHSLC2R_JF	CAGAATAGCACTGATGCTGGC	HSL2
β-actinF_JF	CCCATCCACCATGAAGATC	β-actin
β-actinR_JF	CATTTGCGGTGGACGATGG	β-actin
RTPCRHSLC1F_SB	GGAACCTCACAGAGTCCGGCCTTATAGC	HSL1
RTPCRHSLC1R_SB	GAGAAGGACAGGACAGTGAAGAGCTGC	HSL1
RTPCRHSLC2F_SB	CTTCTGGAACATCACAGAGACCG	HSL2
RTPCRHSLC2R_SB	CCCGGTTCAGATGAGGCTCATCTC	HSL2
β-actinF_SB	GGTTCCCTTAAAGCGAAAAGC	β-actin
β-actinR_SB	CAGTGCGGCGATTTCATCT	β-actin

Table 2-2-2. Oligonucleotide sequences of primers used for real-time PCR

Primer name	Sequences 5'-3'	genes
qPCRHSLC1F_JF	GGTGATCTCACCCAGGGAGCCTC	HSL1
qPCRHSLC1R_JF	GCAGAGGCCACGATGTATACAGG	HSL1
qPCRHSLC2F_JF	GTCTGAGCGCACTCCAGAGGATGTG	HSL2
qPCRHSLC2R_JF	GCCACTATATGTACAGGTGGCAGGCC	HSL2
β-actinF_JF	CCCATCCACCATGAAGATC	β-actin
β-actinR_JF	CATTTGCGGTGGACGATGG	β-actin
qPCRHSLC1F_SB	CCTACTGTTGGGCTCTGAATAACTG	HSL1
qPCRHSLC1R_SB	GTCCCCGGCCAGACAAA	HSL1
qPCRHSLC2F_SB	CCAGCTTTGCTTCAGTTTACCA	HSL2
qPCRHSLC2R_SB	CCAGGGAACGATATCCATTAGC	HSL2
β-actinF_SB	GGTTCCCTTAAAGCGAAAAGC	β-actin
β-actinR_SB	CAGTGCGGCGATTTCATCT	β-actin

Preparation of anti-HSL antibody

Based on the cDNA sequences, the open reading frame (ORF) sequences were determined using ORF Finder. (http://www.ncbi.nlm.nih.gov/gorf/gorf.html). Peptide sequences with high antigenicities were calculated based on the ORF sequences (Figure 2-2-3) and anti-HSL antibodies were raised in rabbit (Operon Japan, Tokyo, Japan). The anti-HSL antibodies were further subjected to purification. 0.4 g of NHS-activated agarose (Thermo Scientific) was incubated with 9 ml of 0.1 M $NaHCO_3$ buffer

(pH 8.3) containing 0.5 M NaCl and 10 mg of purified KLH at 20°C for 20 h. Excess NHS residues were blocked with 0.1 M Tris-HCl (pH 8.0) containing 0.5 M NaCl at 20°C for 2 h. The resulting KLH-agarose column was washed with 1.5 M glycine-NaOH (pH 8.9) containing 0.5 M NaCl, followed by equilibration with PBS. The HSL antibody in PBS was loaded on the column. The fraction containing antibodies was immediately stored at -20°C.

Immunoprecipitation

The supernatants were incubated with protein G Sepharose 4 Fast flow, followed by the protocol of Immunoprecipitation Starter Pack of GE Healthcare. Skeletal muscle and inclinator muscle of fin of red seabream were homogenized with tissue disruptor (Precellyse 24 Lysis and Homogenization, Brevet Bertin Technologies) with a lysis buffer containing 10 mM Tris-HCl, 10 mM sucrose, 1 mM EDTA, 1 mM dithiothreitol, 100 µl/10 ml of phosphatase inhibitor cocktail, 200 mM Na_3VO_4, and 500 mM NaF. All samples were then centrifuged at 12,000 g for 15 min. The supernatant and the purified anti-HSL antibody were incubated for 1 h at 4°C with continuous agitation. After conjugated antibody and antigen, Protein G sepharose 4 Fast Flow was added and incubated for 1 h at 4°C. The precipitation of the immune complexes was washed 3 times with the lysis buffer. The pellets were corrected and added 30 µl of sample buffer containing 1% SDS, 100 mM DTT and 50 mM Tris, pH 7.5. Samples were heat at 100°C for 3 min and centrifuged at 12,000 g for 20 s to

remove the beads. Supernatants were added 1 µl of 0.1% bromophenol blue and subjected to SDS-PAGE, and immunoblotted.

Electrophoresis and immunoblotting

Nine tissues from Japanese flounder and red seabream were excised out, rapidly frozen in liquid nitrogen and stored -80^{0}C until use. Approximately 1 g of tissues were homogenized and centrifuged as described above.The resulting supernatants were collected and used for sodium dodecyl sulfate – polyacrylamide gel electrophoresis (SDS-PAGE) and immuno blotting analyses. Protein concentration was determined using BCA protein assay reagent kit (Pierce) and bovine serum albumin as standard according to the manufacturer's instructor. Sample were mixed with loading buffer and boiled for 5 min. The resulting samples were added with a SDS-PAGE sample buffer (1:1, v/v) containing 100 mM Tris-HCl, pH 6.8, 1% SDS, 10% glycerol and 10% 2-mercaptoethanol. The solution mixtures were heated at 100^{o}C for 4 min.

The equivalent of twenty microgram of total protein in SDS loading buffer was subjected to SDS-PAGE with 10% polyacrylamide gel. After electrophoresis, the gel was rinsed with a blotting buffer containing 25 mM Tris, 150 mM glycine, and 20% methyl alcohol for 10 min. Protein were then transferred to polyvinylidene fluoride membrane (PVDF) with the blotting buffer at a stable voltage for 100 volt for 2 h. The blotting membrane was washed 3 times for 10 min each with Tris-buffered saline with Tween-20 buffer (TBST; containing 200 mM Tris, 1.5 M NaCl, 1% Tween-20). The membrane was

blocked with 3% bovine serum albumin (BSA) in TBST for 2 h at room temperature with continuous agitation. The membrane subsequently incubated with a 1:3000 diluted primary polyclonal antibody against HSL in TBST with 2.5% BSA at 4^{0}C overnight with continuous agitation. The membrane was subsequently incubated with the horseradish peroxidase anti rabbit IgG conjugate (Invitrogen) 1:10,000 dilutions in TBST with 2.5% BSA for 2 h in dark condition. Afterward, the membrane was washed 3 times with PBST for 10 min each. Visualization was carried out by incubation of the blot membrane and Immobilon Western Chemiluminescent HRP Substrate (Millipore, USA). Densitometric quantification of visualized bands was carried out in an Odyssey FC system (Li-COR BioSciences-GmbH).

Results

HSL mRNA expression

For the quantitative real-time PCR, primer pairs and probes were designed as described above. The amplification efficiency was plotted with Ct values and log of dilution factors to construct the calibration curve. The slopes of all amplification efficiency were nearly 3.3 with correlation coefficients (Fig. 2-2-1) and the obtained disassociation curve showed a symmetrical parabola like-shape.

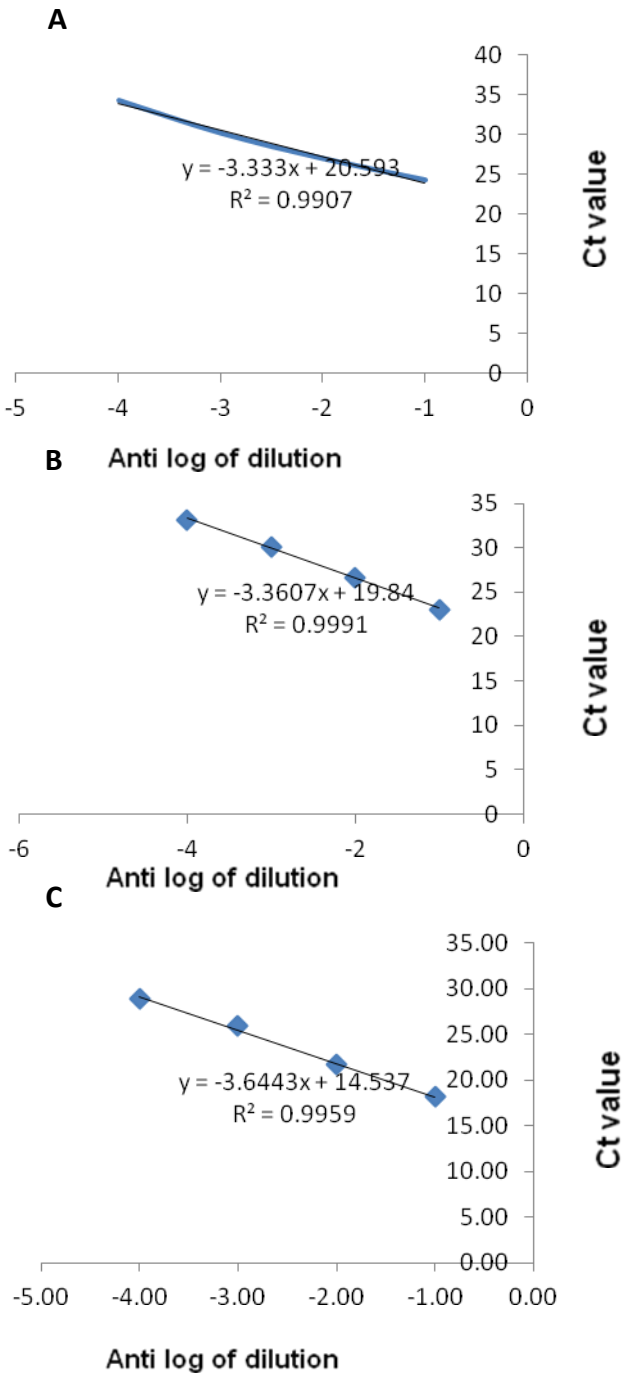

Figure 2-2-1. Amplification efficiencies for HSL1 and HSL2 of Japanese flounder. Amplificaition curves were plotted with Ct value an antilog of cDNA serial dilution of HSL1, HSL2 and β-actin genes of Japanese flounder (A, B, C, respectively).

Japanese flounder

The RT-PCR analyses showed that HSL1 mRNA was broadly expressed in all tissues examined. HSL2 mRNA was abundant in liver, skeletal muscle, and inclinator muscle of fin, followed by slightly expressed in gonad, skin, gill and heart (Fig. 2-2-2 A). The highly sensitive real-time PCR detected the HSL1 and HSL2 transcripts in all tissues examined (Fig. 2-2-2 B). Notably, HSL1 transcripts were the most abundant in the inclinator muscle of fin, followed by skeletal muscle, liver and intestine. The HSL2 mRNA levels were also the highest in the inclinator muscle of fin, and were relatively abundant in liver and skeletal muscle. The relative mRNA levels of HSL1 were 5- to 14-fold higher than those of HSL2 in skeletal muscle and inclinator muscle of fin, respectively. HSL2 mRNA levels in other examined tissues were also lower than HSL1 in Japanese flounder.

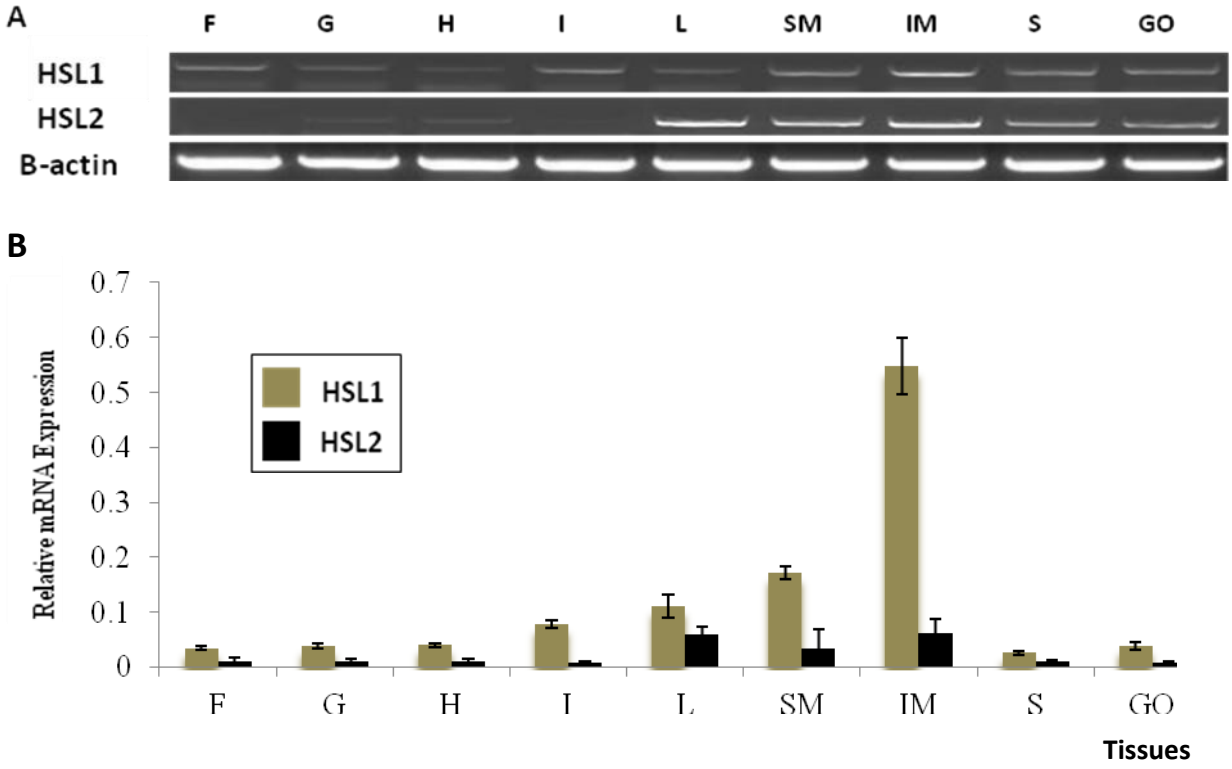

Figure 2-2-2. Tissue distribution of HSL1 and HSL2 transcripts in Japanese flounder. A; Reverse transcription-PCR. β-actin gene was used as a positive control. B; Quantitative real-time PCR. The relative mRNA levels of HSL1 (gray bar) and HSL2 (dark bar) were determined using those of β-actin as the internal control. Data are presented as mean ± SEM (n=5). Abbreviations: F, fin; G, gill; H, heart; I, intestine; L, liver; SM, skeletal muscle; IM, inclinator muscle of fin; S, skin and GO gonad.

Red seabream

The expression of HSLs performed by RT-PCR found that HSL mRNA transcripts were extremely high in both adipose tissue and gonad for

HSL1 and HSL2 of red seabream. HSL mRNA transcripts were also detected with low intensity in intestine, skeletal muscle, and skin of red seabream, whereas β-actin transcrip was found in all tissues examined (Fig. 2-2-4). In consistence with these results, HSL mRNA expressions by real-time PCR revealed that HSLs were broadly distributed in all tested tissues. HSL1 mRNA expression levels were higher than HSL2 mRNA levels in all tested tissues. HSL1 and HSL2 mRNAs were extremely abundant in adipose tissue and gonad of red seabream. HSL2 expression was 2-fold lower than HSL1 expression in these tissues. The lower expressions of HSL mRNA were observed in liver, skeletal muscle and heart, whereas HSL mRNA expressions were very low in fin, gill, heart and skin of red seabream.

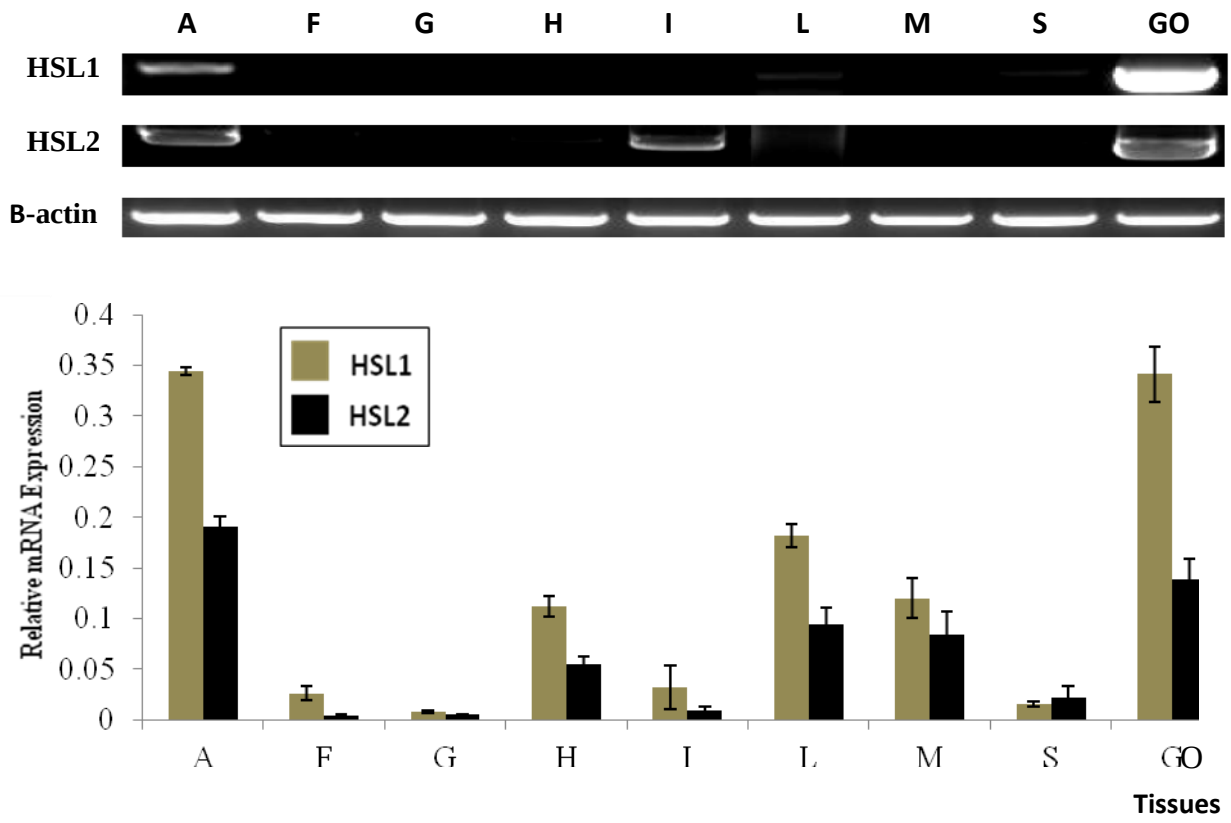

Figure 2-2-3. Tissue distribution of HSL1 and HSL2 transcripts in red seabream. A; Reverse transcription-PCR. β-actin gene was used as a positive control. B; Quantitative real-time PCR. The relative mRNA levels of HSL1 (gray bar) and HSL2 (dark bar) were determined using those of β-actin as the internal control. Data are presented as mean ± SEM (n=5). Abbreviations: A, adipose tissue; F, fin; G, gill; H, heart; I, intestine; L, liver; M, muscle; S, skin and GO, gonad.

HSL protein expression

In this section, anti-HSL antibody was affinity-purified on a column of a covalently bound KLH because polyclonal antibodies against HSLs showed much non-specific bindings. In order to identify the HSL proteins, the

immunoprecipitation was carried out, followed by immunoblotting analyses with the same purified antibody. The immunoprecipitation results showed that the migrated protein on SDS-PAGE with an apparent molecular mass of approximately 96 and 125 kDa of HSL1 and HSL2 proteins of Japanese flounder, respectively. Figure 2-2-4 and 2-2-6 shows immunoblotting analysis of Japanese flounder and red seabream using anti-HSLs. HSL1 immunoreactive bands of 96 kDa were detected in fin, gill, intestine, skeletal muscle, inclinator muscle of fin and skin of Japanese flounder. In contrast to the mRNA distributions that HSL1 mRNA was an extremely abundant in inclinator muscle of fin, the immunoblotting analyses showed that the immunoreactive bands were highly intense in skin. Whereas anti-HSL2 antibody recognized bands around 125 kDa in molecular mass in intestine, skeletal muscle and inclinator muscle of fin of Japanese flounder, which was well consistent with the results for HSL mRNA expressions as described above.

The anti-HSL1 detected around 98 kDa protein with high intensity in both adipose tissue and gonad of red seabream. Bands with lower intensity were observed in muscle and skin (Fig. 2-2-6), while no band corresponding to HSL2 was not detected in red seabream.

>HSL1_red seabream

MRVASDMDYTVVFAALETVCEDNIAIMCGPSDLPYGNVANRLVTCMRQI
QEHGRALEPVVGSFTAVYHHYDFDEQTPGNGYRTLVKVLQSCLLHIIHKG
RYIASNYNSAFFRAEHNASEMEAYCSALCQLRALLHLAQQLINDNECGQL
YSLQDRDLSRKFVQEYSSMHKACFYGRCLGFQFSPTLRPFLQTVVISMVS
YGETYGKQQSGLGMAALSLLTSGKYVMDPELRGAEFERITQNLDMQFW
KSFWNLTESGLIAGFSRIASCPVQMNFTLTLPPVTLHLPLASDPSLTATVSP
PIAHWGPGPVHMRLISHELREGQDSEELLSFSRDDPPPITASHLPWVQKQP
RSPWLLIHFHGGGFVAQTSRSHEN**YLRSWSKE**LNVPILSVDYSLSPEAPFP
RALEECFYAYCWALNNCHLLGSTAERVCLAGDSAGGNLCVTVSMKAISN
GIRVPDGIMAAYPATLLTTDASPSRLLTLIDPLLPLGVLTKCLNAYAGADC
QTVQPVVGSSSLSSLGRDTAVLLSDLTQGASNWIQSFLDPMRTSGGTRSLS
SAPMRSQSNNTRGTSTHASTPNREDHMDYPEGFEPMRSECLAFVRPTSSP
VIRNPFVSPLLSPNNLLRGLPPVHIVASALDALLDDSVMFAKKLRDMGQP
VNLTVVEDLPHGFLSLSQLAKETEVASEICVEQMRKIFQQENPTPALSKRP
KLEDTHQSTNPSG*

> HSL2_red seabream

MASNKKSSGNSRFEKSVNGRRSSKHKEGPVVMDTKAVFAALYSVCEENA
TFFSGGAKGSQGDAARRLEDVMKMIQEHARSLEPVISSFASVYHHFDFDP
HIPANGYRSLVKVVRCCLLHIIQKGRYITANRRSIFFRVAHNAGEMEAYCN
ALCQMRALLYLAQRMLHDNSHGNLFFQDESGLSESFVREYSSMHKGCFY
GRCLGFQFTPAIRPCLQTIAIGLVAFGENYRRHQSGIGVAASSFFTSGKYAI
DPELRGAEFERITQNLDVHFWKSFWNITETEVLSSLASMTSTQVKVNRAL
SVPPVPFDLPLAANHRASVTIAPPSAHIGPAPVQMRLISYDLREGQDSETLL
SLCRSEGGAISLSLGLKTKRLPSSPCLLIHIHGGSFVAHTSKSHEP**YLKSWS**
QDLGVPILSVDYSLAPEAPFPRALEECFYAYCWALRNHHLLGWTGEKVC
LAGDSAGGNLSVTTSMRAAAFGVRMPDGIVAAYPATLLTAYASPSRLLTL
MDPLLPLSVLSRCLSAYAGNEPQTETQVEKVSTLSLVRRDTALMLRDFRQ
GASNWIHSLLDSNRASASPSTAAEAPPGPPDTVRKSISEASISSPHADPPVPS
EPSEFPSRKLSVKSQTCQDLGSQHNATSHSAPLLSERTPEDVNFFLAKDAD
PFMSSNLSSVAIPPPGGEEGSEHEHPREFPLGFEPLRSVQQTEMRLQSSPVV
KDPFCSPLLAPDSMLKGLPPVHIVACALDPMLDDSVMFAKRLRNIDQPVT
LCVVDDLPHGFLSLSQLSRETREAANVLRGENSRCLHPV*

Figure 2-2-4. Deduced amino acid sequences of open reading frames of HSL1 and HSL2 used for antibody production in red seabream. Hydrophobic regions are shown in bold. Asterisk indicates stop codon.

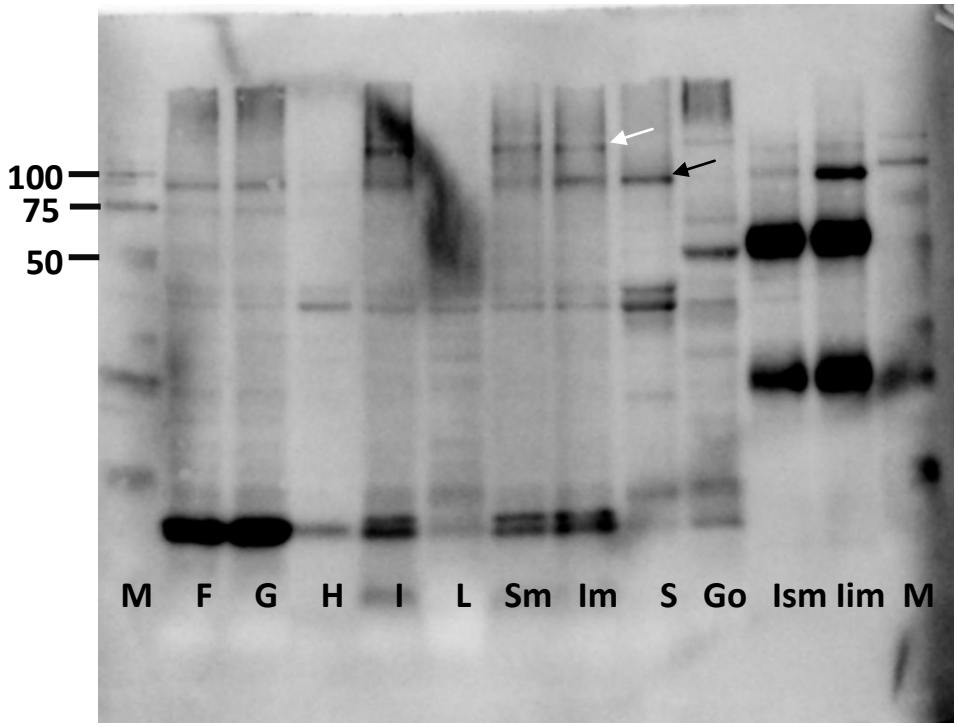

Figure 2-2-5. Immunoblot analysis of HSL in 9 tissues of Japanese flounder. Two immunoreactive bands with molecular masses of 96 and 125 kDa were observed. A black and white arrows show HSL1 and HSL2 proteins of Japnese flounder, respectively. Abbreviations: M, marker; F, fin; G, gill; H, heart; I, intestine; L, liver; Sm, skeletal muscle; Im, inclinator muscle of fin; S, skin; Go, gonad; Ism and Iim are Immunoprecipitation of skeletal muscle and inclinator muscle of fin, respectively.

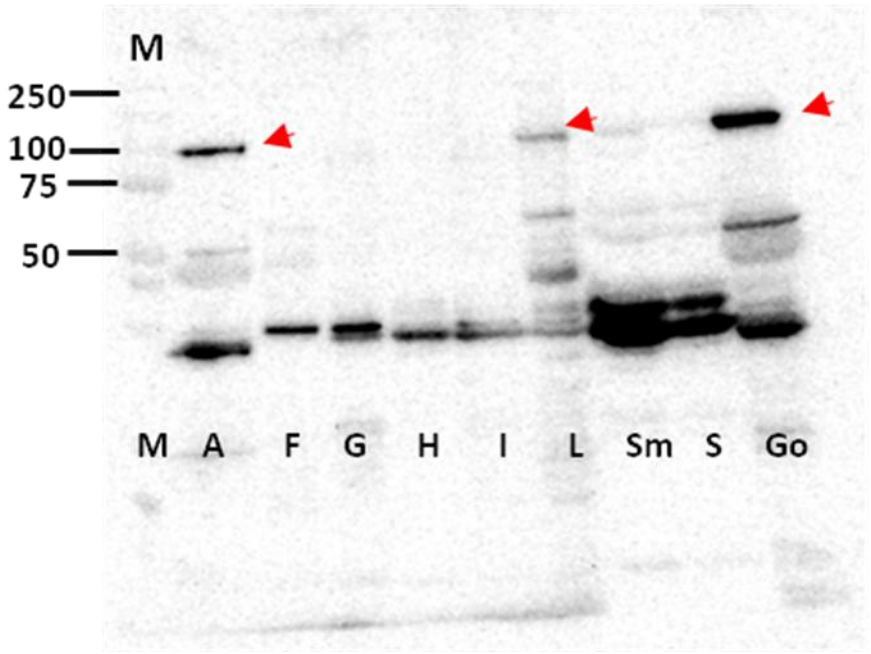

Figure 2-2-6. Immunoblot analysis of HSL in 9 tissues of red seabream. One immunoreactive band with a molecular mass of 98 was detected. Abbreviations: A, adipose tissue; F, fin; G, gill; H, heart; I, intestine; L, liver; M, muscle; S, skin and GO, gonad.

Section 3

Localization of HSL mRNAs by *in situ* hybridization

In situ hybridization is a technique to hybridize complementary DNA or RNA strand to localize a target DNA or RNA sequence in a section of tissue or muscle block. So far, HSL has been extensively investigated in testis of rat, mice and human to explore the roles on steroidogenesis and spermatogenesis. Unfortunately, there are limited studies on HSL transcripts in adipose tissue and other tissues in any mammals and no in teleost fish. To gain further insight into the function of HSL on lipid metabolism, *in situ* hybridization was performed in various tissues in both Japanese flounder and red seabream in this section. The HSL transcripts will be the first data described on HSL localization in fish tissue.

Materials and methods

Materials

Japanese flounder and red seabream were obtained from local suppliers.

Sample preparation

Sample tissues of red seabream were prepared with a cryo-sectioning method. After fixation with 4% PFA, tissue samples were pretreated

with 5, 10, 20 and 30% sucrose for 1 hour each with continuous agitation at room temperature.

Probe preparation

For the synthesis of RNA probes, 316 and 401 bp cDNA fragment of Japanese flounder and red seabream was amplified from 3'ends based on the obtained HSL sequence from previous experiment. The PCR was amplified with primers Insitu_HSL1C1_JF and Insitu_HSL1C1R_JF for Japanese flounder, and Insitu_HSLC1F_SB and Insitu_HSLC1R_SB for red seabream (Table 2-3-1). The PCR products were purified on 2% agarose gel electrophoresis. The expected cDNA fragment was purified using Qiaquick gel extraction kit (Qiagen). After gel extraction, the purified PCR products were cloned into the pGEM-T easy vector (Promega). The inserted HSL gene was amplified with primer SP6 and T7 (Table 2-3-1) by colony PCR. The plasmid was extracted and sequenced to confirm the HSL specific sequence. Then, the plasmids were used to amplify using universal primers (SP6 and T7). The purified PCR products were used as template for RNA synthesis. The Digoxigenin (DIG)-labeled antisense and sense probes for the HSL1 gene of both Japanese flounder and red seabream were synthesized using SP6 and T7 RNA polymerases (Roche, Mannheim, Germany). The probes were incubated for 2 h at 37^{o}C with the reaction mixture including 3 µg of DNA, 2 µl of DIG RNA labeling mix 10X, 2 µl transcription buffer 10X, 11 µl of sterile RNase free water and RNA polymerase. The reaction mixtures were incubated 90 min at 37^{o}C in continuous agitation. Subsequently, the probes were purified with 2

µl of 3 M sodium acetate and 50 µl of 100% ethanol and then replaced by 70% ethanol. After purification, TE buffer was added and kept at -80^{o}C until use.

In situ hybridization

In situ hybridization was performed by two methods using muscle block (Kaneko et al. 2013) and biopsy sectioning for other tissues (Koyama et al. 2012) with minor modifications. For muscle block, Japanese flounder tissue of approximately 0.5 cm in thickness were prepared from the inclinator muscle of dorsal and ventral fins. Gill, bone, intestine and testis from red seabream were cut at approximately 18 µm thicknesses using cryo-sectioning. Both samples from muscle block and tissue section samples were washed in PBS containing 0.1% Tween-20 for 30 min. Samples were fixed with 4% PFA/PBS for 10 min, pre-hybridized in hybridization buffer (50% formamide, 5X SSC, and 0.1% Tween-20) for 1 h, and hybridized with the DIG-labeled RNA probes at 51^{o}C overnight. The sample tissues were then washed twice in each of 2X saline sodium citrate with tween-20 buffer (SSCT) containing 50% formamide and 0.2X SSCT at 51^{o}C for 15 min. Subsequently, the samples were incubated with a staining buffer containing 0.1 M NaCl, 0.1 M Tris-HCl (pH 9.5), and 0.05 M $MgCl_2$ 3 times for 5 min each. Finally the samples were stained with alkaline phosphatase-conjugated anti-DIG antibody (Roche) and NBT/5-bromo-4-chloro-3-indolyl phosphate (0.375 and 0.188 mg/ml, respectively) in darkness. The photographs were taken using microscopic systems (Model MVX10, Olympus, Tokyo, Japan; BZ-9000, Keyence).

Table 2-3-1. Oligonucleotide sequences of primers used for *In situ* hybridization

Primer name	Sequences 5'-3'	genes
Insitu_HSL1C1F_JF	GTTTACCCACAGGGCTTTGAGCC	HSL1
Insitu_HSL1C1R_JF	GCGCAACGCAGATTTCTGTAGCGAC	HSL1
Insitu_HSL1C2F_JF	GACCCCATGCTGGATGACTC	HSL2
Insitu_HSL1C2R_JF	GGGTGAAGACAGCGCGAATTC	HSL2
Insitu_HSLC1F_SB	GCTTTGAGCCCATGCGCTC	HSL1
Insitu_HSLC1R_SB	GCCGGATGGATTCGTACTC	HSL1
Insitu_HSL1C2F_SB	CAGAGCCGCGCAAGCACCG	HSL2
Insitu_HSL1C2R_SB	GATGCTGCGGTATTGGAGC	HLS2

Results

In situ hybridization showed remarkable hybridization of Japanese flounder HSL1 transcripts on lipid droplet of the inclinator muscle of both dorsal (Fig. 2-3-1 A) and ventral (data not shown) fin. The strong intensity signals of HSL1 transcript were observed on the surface of the adipocyte in inclinator muscle of fin which distributed with a high number of lipid vacuoles. In this study, HSL2 transcripts were hardly observed in any tested tissues probably due to their low expression levels. No signal was observed in negative controls using sense probes (Fig. 2-3-1, B).

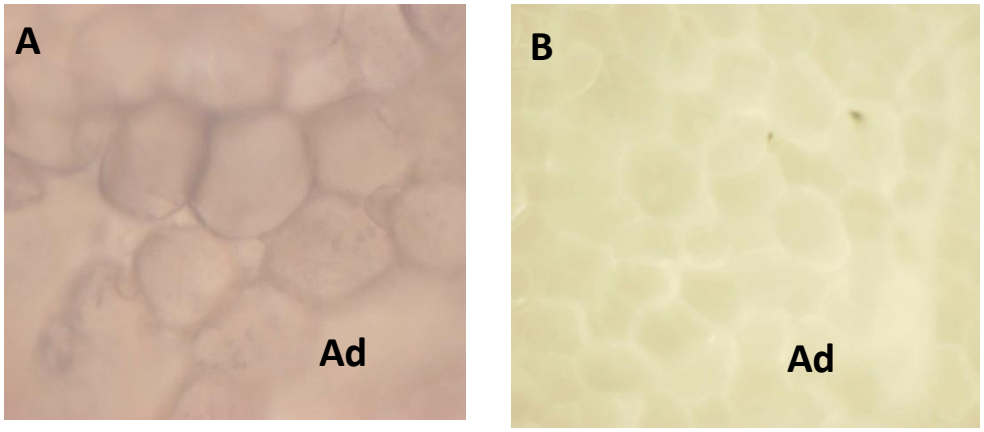

Figure 2-3-1. Localization of HSL1 transcripts in inclinator muscle of fin. Antisense probe specific to HSL1 transcripts showed hybridization signals in the peripheral region of adipocytes in the inclinator muscle of fin (A). Controls using DIG-labeled sense RNA probes were all negative (B). (Magnification; A=200, B=100). Abbreviation, Ad, adipocyte cell.

HSL1 transcripts of red seabream were detected in gill and the signals were highly intense in gill arches locating among gill filaments, though not in gill filaments (Fig. 2-3-2; A). In intestine, HSL1 transcripts were detected in the both small and large intestines. The transcripts were highly localized in villi cells nearly to goblet cell and the signal were also detected in the laminar propia (Fig. 2-3-2; B). Interestingly, HSL1 was also localized in bone, highly in newly born osteocyte cells (Fig. 2-3-2; C). So far, HSL has been extensively reported in testis of rat, mice and human testis. HSL cleaves cholesteryl ester to free cholesterol used for steroidogenesis (Vallet-Erdtmann et al. 2004), spermatogenesis and reproductive functions. In this study, HSL1 was highly localized on the seminiferous tubule of red seabream testis (Fig. 2-3-4; D).

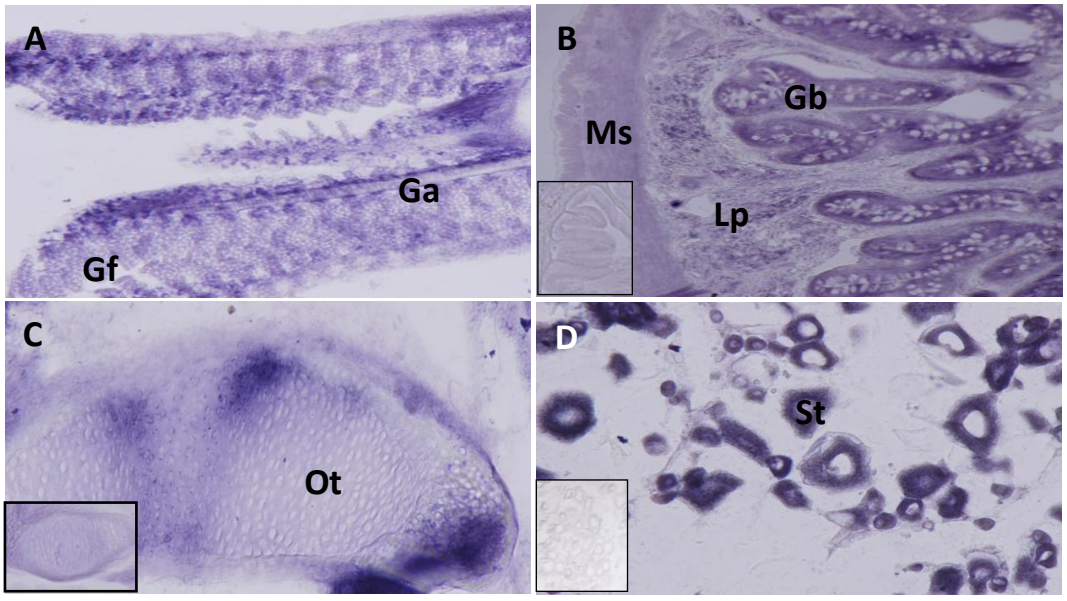

Figure 2-3-2. Localization of HSL1 transcripts in various tissues. Antisense probe specific to HSL1 transcripts showed in small frame of each organ. A shows gill; B, intestine; C, bone marrow; D, gonad. (Magnification; A; C=50, B=100, C=200). Abbreviation; Ga, gill arch; Gf, gill filament; Ms, muscularis; Lp, laminar propia; Gb, goblet cells; Ot, osteocytes; St, spermatid.

Section 4

Determination of fatty acid classification in skeletal muscle and inclinator muscle of fin from Japanese flounder *Paralichthys olivaceus*

HSL activity was considered as a hormonal-sensitive lipolytic activity in a lipid stored tissue by controlling the supply of FFA to peripheral tissues on demand for their energy metabolisms. In order to evaluate the FFA releasing through the HSL activity, the lipid class compositions in the inclinator muscle of fin and skeletal muscle were investigated by using thin layer chromatography (TLC).

Materials and methods

Total lipid extraction

Total lipids were extracted from the inclinator muscle of fin and skeletal muscle according to Bligh and Dyer (1959). Lipase inhibitor (Tocris Bioscience, Ellisville, MO, USA) was used to prevent TAG and DAG degradation. Total lipids were gravimetrically calculated.

Lipid classification

TLC was used to classify lipid class compositions in Japanese flounder tissues. Approximately 2-4 μl of each total lipid was applied on a TLC silica gel 60 glass plates (Merck Japan, Tokyo, Japan) to reach 100 μg of the total lipid. Total lipids were separated using a hexane: ether: acetic acid solution (70: 30: 1, v/v) and detected by the heat treatment with a mixture of H_2SO_4: water: ethanol (100: 95: 5, v/v).

Results

Approximately 1 mg of total lipids extracted from the inclinator muscle of fin and skeletal muscle were subjected to TLC. TAG and cholesteryl ester (CE) were detected in both tissues with a greater extent in the inclinator muscle of fin (Fig. 2-4-1). Since TAG and CE are major components of the hydrophobic ester core of lipid droplet in adipocytes (Fujimoto et al. 2008), these results, together with those of the above oil red O staining, suggest that the inclinator muscle of fin would contain typical adipocytes. Moreover, FFA was detected in the inclinator muscle of fin, but not in the skeletal muscle, in agreement with the high mRNA levels of HSL in this muscle tissue. Usually the concentration of FFA is low in fresh muscles of lean fish (Aubourg and Medina, 1999; Prego et al. 2012) and sometimes barely detectable by TLC (Chaijan et al. 2010).

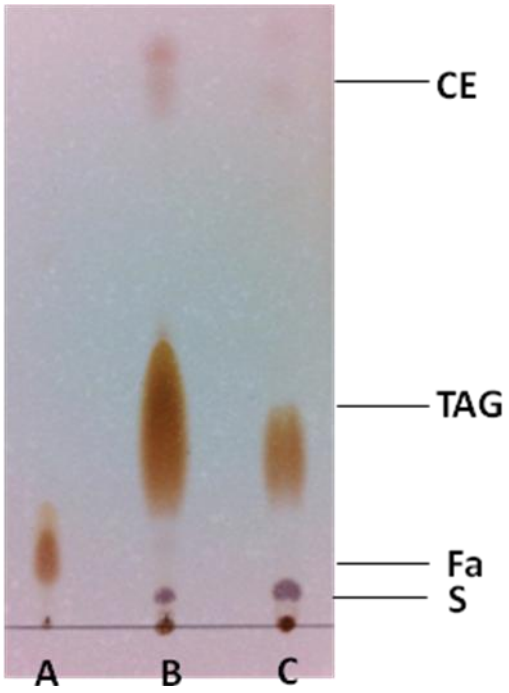

Figure 2-4-1. Thin-layer chromatography (TLC) analysis of total lipids extracted from the inclinator muscle of fin and skeletal muscle of Japanese flounder. Total lipid was subjected to TLC. Lane A, free fatty acid (control); lane B, inclinator muscle of fin; lane C, skeletal muscle. Abbreviations: CE, cholesteryl ester; FA, fatty acid; PL, phospholipid; S, sterol; TAG, triacylglycerol.

Section 5

Discussion

The HSL1 mRNAs of Japanese flounder were detected in all tissues examined as shown by RT-PCR. The highest transcripts were found in inclinator muscle and skeletal muscle of HSLs in Japanese flounder, whereas adipose tissue and gonad were most abundant in red seabream. In addition, real-time PCR indicated that both HSL mRNAs were broadly distributed as several reports have been described previously (Holm 2000; 2003; Lampidonis 2011; Kittillson 2011). The abundance of HSL mRNA was varied by tissue and species as indicated by the expressions different between Japanese flounder and red seabream. HSL1 of red seabream was the most abundant in adipose tissue and testis, followed by the lower levels heart, muscle, and liver, while the inclinator muscle of fin dominantly expressed HSL1 mRNA in Japanese flounder. The low levels of expressions were also observed in a variety of cell lines and tissues in the previous studies (Holm et al. 1988); for example, heart (Small et al. 1989), skeletal muscle (Langfort et al. 1998), macrophages (Contreras et al. 1998), pancreatic β-cells (Klannemark et al. 1998) and cultured Chinese Hamster Ovaries (CHO) cells (Osuga et al. 1997). The widespread distribution of HSL mRNAs (Fig. 2-2-2, 2-2-4) is consistent with protein expression performed by immunoblotting analysis (Fig. 2-2-3, 2-2-5) and the previous studies in which HSL activity was most pronounced in tissues with significant amount of lipid, such as adipose tissue, inclinator muscle of fin, skeletal muscles and liver

(Sheridan 1988; Sheridan and Kao 1998). The present results indicated that the expression pattern of HSLs was tissue specific as investigated in Japanese flounder and red seabream. Interestingly, HSL1 was highly expressed in gonad in red seabream but was not observed in Japanese flounder. HSL in testis has been investigated in several species including human (Arenas et al. 2004), rat (Holst et al. 1994), mice (Chung et al. 2002) and guinea pig (Kabbaj et al. 2001).

HSL molecular mass has been reported from several species of non-adipose tissues ranging from 26 to 130 kDa (Casado et al. 2012; Kraemer et al. 1993). In this study, the molecular masses of HSL1 and HSL2 were confirmed by immunoprecipitation and immunoblotting analyses. The results revealed that the molecular mass of Japanese flounder HSL1 and HSL2 were 96 and 125 kDa, respectively (Fig. 2-2-3.) and red seabream HSL1 was 98 kDa. The present study shows that HSL protein from fish are slightly larger than human adipose tissue HSL with an apparent 88 kDa, rat and bovine with 84 kDa, and the mouse and guinea-pig with 82 kDa (Holm et al. 1989; Chung, et al. 2002; Fig. 2-2-5).

The characteristics of lipid deposition pattern differ within fish species. The previous study showed that fish preferentially accumulate lipid in three tissues including liver, skeletal muscles and adipose tissues (Kaneko et al. 2013; Kitillsen et al. 2011). However, the distribution of lipid among these tissues is highly species-specific. The present oil red O staining of Japanese flounder revealed that the adipose tissues were highly stained in the inclinator muscle of fin of both ocular and blind part (Fig. 2-1-1). The oil red O staining in red seabream has been reported that lipid accumulated predominantly in its visceral adipose tissue, liver and myosepta in skeletal muscle (Kaneko et al. 2013). The transcripts

of HSL1 in Japanese flounder were observed in the peripheral region of adipocytes in inclinator muscle of fin of Japanese flounder (Fig. 2-3-1). In addition, TLC profile of total lipid FFA was detected in the inclinator muscle of fin (Fig. 2-4-1), but not in the skeletal muscle, in agreement with the high mRNA levels of HSL in the inclinator muscle. The amounts of TAG, CE and FFA per tissue are markedly higher in the inclinator muscle of fin than skeletal muscle. These observations suggest that HSL1 in the inclinator muscle adipocyte cells promote the hydrolysis of stored lipid, leading to FFA secretion, in response to some hormonal controls.

Summary

Distribution of HSL genes and HSL proteins of both Japanese flounder and red seabream were investigated by RT-PCR, real-time PCR and immonoblot analyses. The results showed that HSLs were broadly expressed in all tissues examined. The highly sensitive real-time PCR detected the HSL1 and HSL2 transcripts in all tissues examined. HSL mRNA expression of both Japanese flounder and red seabream were highly expressed in lipid stored tissues. The relative mRNA levels of HSL1 were 5- to 14-folds higher than those of HSL2 in all tissues examined. The inclinator muscle of fin of Japanese flounder also contained high amount of lipid in adipocytes aligned along the muscle fiber cells as revealed by oil red O staining and *in situ* hybridization. In addition to TAG, TLC detected considerable amounts of CE and FFA in the lipid extracted from the

inclinator muscle of fin, suggesting that the inclinator muscle of fin would be a lipid storage site which releases FFAs for the fin movement possibly through the HSL-mediated lipolysis in Japanese flounder. The immunoprecipitation results suggest the migrated proteins on SDS-PAGE with apparent molecular mass of approximately 96 and 125 kDa of HSL1 and HSL2 protein of Japanese flounder, respectively. HSL1 of 98 kDa was observed in red seabream skeletal muscle, whereas HSL2 was not detected.

Chapter 3

Effects of nutritional state and cytokines on HSL mRNA expression in red seabream *Pagrus major*

Hormone-sensitive lipase is the catalytic enzyme responsible for hydrolysis of TAG in stored lipid to produce FFA and glycerol. Recently, effects of numerous hormonal and environmental factors on HSL functions have been extensively investigated in mammals and also in fish (Holm et al. 2003; Lampidonis et al. 2011; Kitillson et al. 2011). The regulation of HSL involves several complex cytokine systems. HSL is generally regulated by cytokines, such as glucagon, epinephrine and norepinephrine. Signaling pathways received by such cytokine receptors enhance cAMP/PKA signaling pathway, leading to phosphorylation of HSL. On the other hand, HSL phosphorylation is suppressed by insulin, adenosines, and prostaglandins (Holm 2000; 2003; Kittilsen et al. 2011).

Extrinsic environmental changes also affect lipolysis activity in several species. For example, the stress from nutrition deprivation enhances lipolysis (Deng et al. 2004; Uchida et al. 2003). Under fasted state, lipolysis in adipocyte cell is mediated by several catalytic lipase enzymes, which hydrolyze stored lipid in form of TAG into FFA for energy production. Several cytokines regulates lipolysis in mammals and teleost fish (Haromon and Sheridan 1992 a; 1992b). In several organisms, FFA and growth hormone (GH) in serum were elevated after fasting, indicating that a rapid lipolysis elevated in order to supply

energy to maintain their life survival during fasting state (Straus and Takemoto, 1990; Deng et al. 2004; Daucey et al. 1994). In teleost fish, the effects of fasting state on lipid metabolisms have been extensively studied. However, the aspects of lipid mobilization remain largely controversial and unclear. In coho salmon and rainbow trout, insulin, glucagon and glucagon-like peptide in blood serum were diminished during fast indicating that several cytokines are affected in blood circulation during fasted state (Sheridan and Momsen, 1992; Bergan et al. 2013). Re-feeding attenuates the effects on lipolysis, upregulates an antilipolytic action by insulin leading to the activation of phosphodiesterase 3B (PBE 3B) and the reduction in the phosphorylation-mediated HSL and perilipin activities (Ragolia et al. 1998; Zhang et al. 2005).

Growth hormone (GH) is a complex hormonal regulator. The activity of GH is controlled under the central nervous system (CNS) to a large extent in the pituitary by several integrated intercellular signaling pathways including endocrine, neuroendocrine, and neuronal pathways (Holloway et al. 1994; Tschop et al. 2000). Currently, mediation of GH on lipolysis is interested by endocrinologists. Since 1984, the effects of GH on adipose tissue metabolism have been investigated in various species. GH stimulates adipocyte lipolysis leading to release FFA and glycerol (Carroll et al. 2004; Chavez et al. 2006). GH increases body weight and visceral fat mass in GH deficient human (Roemmich et al. 2001; Zhao et al. 2004). The observation is consistent with the previous studies in GH-deficient mice, showing that obesity was induced. In fish, information about GH regulations in nutritional deprivation and lipolysis are scarce and limited. It has been reported that serum GH levels are elevated in fasting state

black seabream (Deng et al. 2004). In coho salmon *Oncorhynchus misutch* implanted hepatic tissue incubated with GH in *ex vivo*, GH caused lower fat deposition in the liver and hepatic triacylglycerol lipase activity was elevated, leading to lipid hydrolysis (Sheridan 1986). The recent study found that GH promotes protein kinase C (PKC) and ERK through phosphorylation at Ser600 of HSL, resulting in elevating the lipolysis in rainbow trout (Bergan et al. 2013). However, the effects of GH on lipid metabolism are less studied, where especially GH function on lipid mobilization is unclear in fish. In this chapter, the effects of nutritional state and cytokine on HSL mRNA expression were investigated.

Apolipoproteins (Apo) were known to regulate on lipid utilization, lipid metabolism and homeostasis in vertebrates. APO14, the 14 kDa apolipoprotein gene, was first cloned and sequenced as a complex of HDL in Japanese eel (*Anguilla japonica*), and also have been identified from at least 14 species in fish (Kondo et al. 2001). Apo14 has been recently suggested to play significant roles during early larval development (Xia et al. 2008; Zhou et al. 2005). In situ hybridization shown that APO14 trnasciptes were highly detected in liver and brain (Kondo et al. 2005; Zhao et al. 2005). Importantly, fish Apo-14 was shown to be the homologue of mammalian ApoA-II, because phylogenetic analysis revealed 27–58% sequence similarity between internal repeats of fish Apo-14 and mammalian ApoA-II (Shen et al. 2001).

Section 1

Effects of nutritional state on HSL genes expression

Nutritional deprivation commonly occurred in mammals and fish; for example, during hibernation, reproduction, and accompanying their new born, etc. Since lipids are the predominant source of stored energy used as sparing energy. During deprivation, stored lipid in several organs is hydrolyzed to support their vital processes. In fish, many studies have been extensively investigated on the biochemical and physiological changes during food deprivation (Grigorakis and Alexis 2005). Fasted coho salmon and rainbow trout showed an elevated plasma fatty acid level concomitant with the stimulation of lipolytic activity and lipase enzymes (Harmon and Sheridan 1992; Moon et al. 1989). Most of the studies showed that fasting state leads to decreased body weight and elevated fatty acid release to generate energy for maintaining life activities. In this chapter, the effects of nutritional states on HSL functions in red seabream were investigated.

Materials and methods

Materials

Thirty individuals of red seabream (Initial body weight 7.13±2.32 g) were randomly selected from an acclimated group provided in our laboratory. All were distributed among 3,000 liters fiber glass tank and maintained with 12 h dark and 12 h light with constant water temperature (20℃). The fish were fed with a commercial diet which response to their nutritional requirement.

Feed and re-feeding procedure

Red seabream were fasted for 7 days and then fed for 3 days with continuously circulated sand filter tank. The feeding and re-feeding studies lasted totally 10 days. During feeding and re-feeding, red seabream were fed with a commercial formulated feed, which was supplied for 2 times until apparent satiation per day.

At days 0, 4, and 7 of fasting and days 10 of re-feeding, each 5 fishes were collected from the tank, fish were then killed. Adipose tissue and liver were collected and kept in RNAlater (Ambion). The sample were immediately stored in -20℃ until used. Total RNAs were extracted as described in the Section 1 of Chapter 1.

Results

HSL specific primers and TaqMan probe sets were designed for red seabream HSL1, HSL2 and β-actin as listed in Table 2-2-2. cDNA was prepared by reverse transcription as described in Chapter 2. The levels of HSL mRNAs were determined by quantitative real-time PCR methodologies. The levels of all HSL mRNAs were normalized with the expression of β-actin.

The changes in the activity and relative mRNA expression of lipid metabolism enzymes of the red seabream during fasting and re-feeding are summarized in Figure 3-1-1, A and B. During fasting stage, the mRNA expression levels of HSLs rapidly increased in adipose tissue and liver. In addition, the expressions of HSL1 mRNAs extremely increased in both tissues (Fig.3-1-1; A), and 5 times higher than HSL2 mRNA expression (Fig 3-1-1; B) especially after day 4 of fasting. Fasted fish for 7 days showed continued elevation of HSLs expression levels. After re-feeding, HSL mRNA levels were decreased after day 7 to day 10 (Fig 3-1-1; A, B). HSLs expression increased significantly after fasting for 7 days and then decreased dramatically thereafter with re-feeding of both adipose tissue and liver.

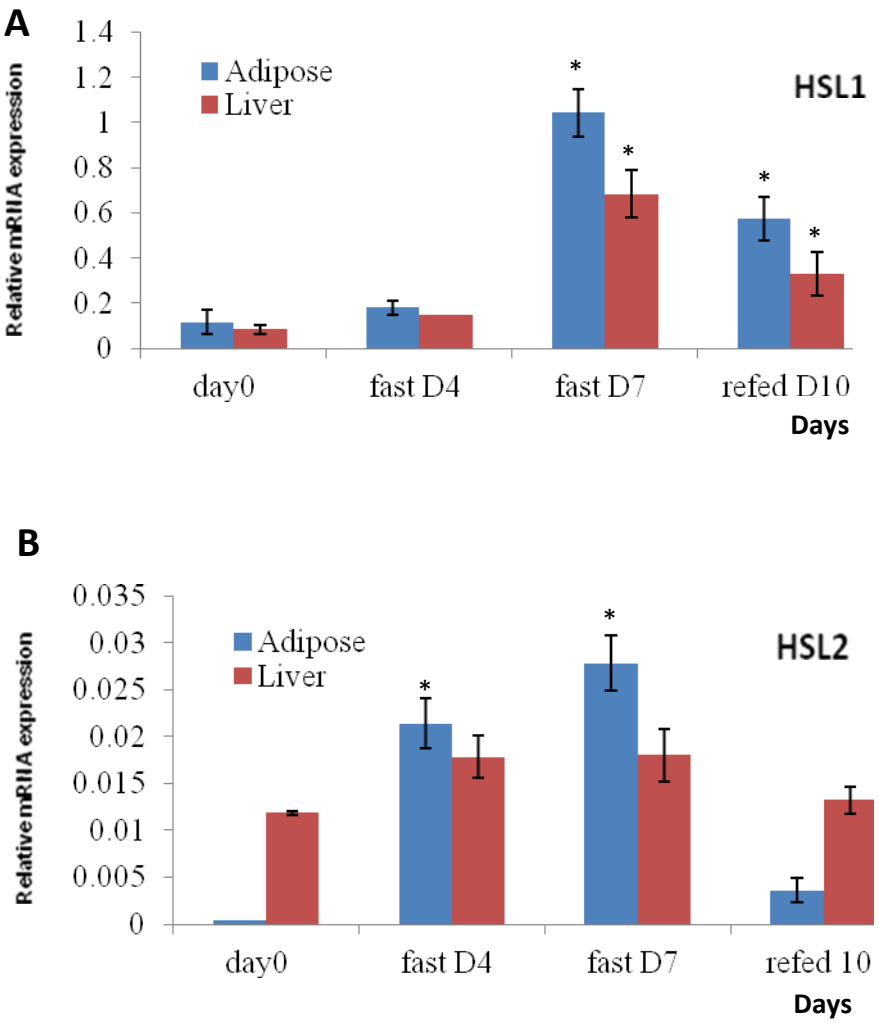

Figure 3-1-1. Effects of nutritional state on the expression of HSL1 (A) and HSL2 (B) mRNA in adipose tissue and liver of red seabream. mRNA were quantified by real-time PCR and presented as mean± SEM (n=5).

Section 2

Inhibitory action of insulin on HSL mRNA expression

Insulin is a complex regulation controlling both lipogenesis and lipolytic action in human adipose tissues (McTernan et al. 2002). One of the insulin functions is controlling lipid metabolism in mammals and fish as well as directly antilipolytic. Insulin signaling activates PDE 3B through AKT pathway leading to reduce net phosphorylation and to decrease activity of HSL and hydrolysis of TAG (Wikander et al. 1998; Eriksson et al. 1995; 1997).

In mammals, it is well know that adipose tissue is an important target for insulin. In fish, however, there are a little information regarding to the direct effects of insulin on adipose tissue and other catalytic lipase enzyme in fish. In this section, the mRNA expression levels of the HSL genes induced by different concentrations of insulin were studied.

Materials and methods

Materials

The Leibovits's L-15 Medium with L-glutamine was purchased from Gibco (Life Technology). Leibovits's L-15 Medium was prepared with 3 concentrations of insulin 1, 0.1, and 0.01 mg/ml (Wako, Tokyo, Japan).

A perfusion buffer containing 160 mM NaCl, 5.4 mM KCl, 0.44 mM KH_2PO_4, 0.34 mM $Na_2HPO_4.12H_2O$, HEPES 10 mM, 1 g/l of glucose and 0.353 g/l of $NaHCO_3$was used to remove blood in circulation.

Sample preparation

Red seabream were killed rapidly with cold ice. Liver, muscle and adipose tissue were excised out. After excision, tissues were washed with cold PBS. Liver tissue was perfused for 10 min with perfusion buffer until the blood clotting removed. Tissue explants freshly isolated from red seabream were cut with a precision-cut slice into small pieces and incubated at 37°C under agitation in Leibovitz's L-15 Medium with L-glutamine (Gibco, Life technology).

HSL mRNA expression

Sliced adipose tissue, liver and muscle were each incubated with 3 concentrations of insulin (0.01, 0.1 and 1 mg/ml). Tissue samples were incubated for 1 and 2 h at each insulin concentration with continuous shaking on the water bath, thus allowing the slices to alternate medium and incubator atmosphere. After incubation, the slice tissues were immediately stored in RNAlater (Ambion) and stored at -20°C until analyses. Total RNAs were extracted and reverse transcribed as described in Section 1 of the Chapter 1. Diluted cDNA samples were subjected to quantitative-real time PCR analysis.

Results

The effects of insulin on HSLs expression was examined in adipose tissue, liver, and skeletal muscle (Fig. 3-2-1). The sliced tissues were treated with three different concentrations of insulin 0.01, 0.1 and 1 mg/ml, for 1 and 2 h for skeletal muscle and liver. Adipose slice tissue was incubated for 30 min and 1 h at each concentration. HSL1 and HSL2 mRNAs expression levels were inhibited in concentration- and time-dependent manners in both liver and adipose tissues (Fig. 3-2-1; A-D). The suppression of HSL mRNA by insulin was highly responsible for adipose tissue of both HSL1 and HSL2, where 50% of HSL mRNA expression levels were diminished. The skeletal muscle, HSL mRNAs were not expressed and seem to elevate at 0.1 to 1 mg/ml of insulin concentration (Fig. 3-2-1; E-F). The time dependence of 0.1 mg/ml insulin shown dramatically decreased in all tissue but not in skeletal muslc of HSL2 (Fig. 3-2-2).

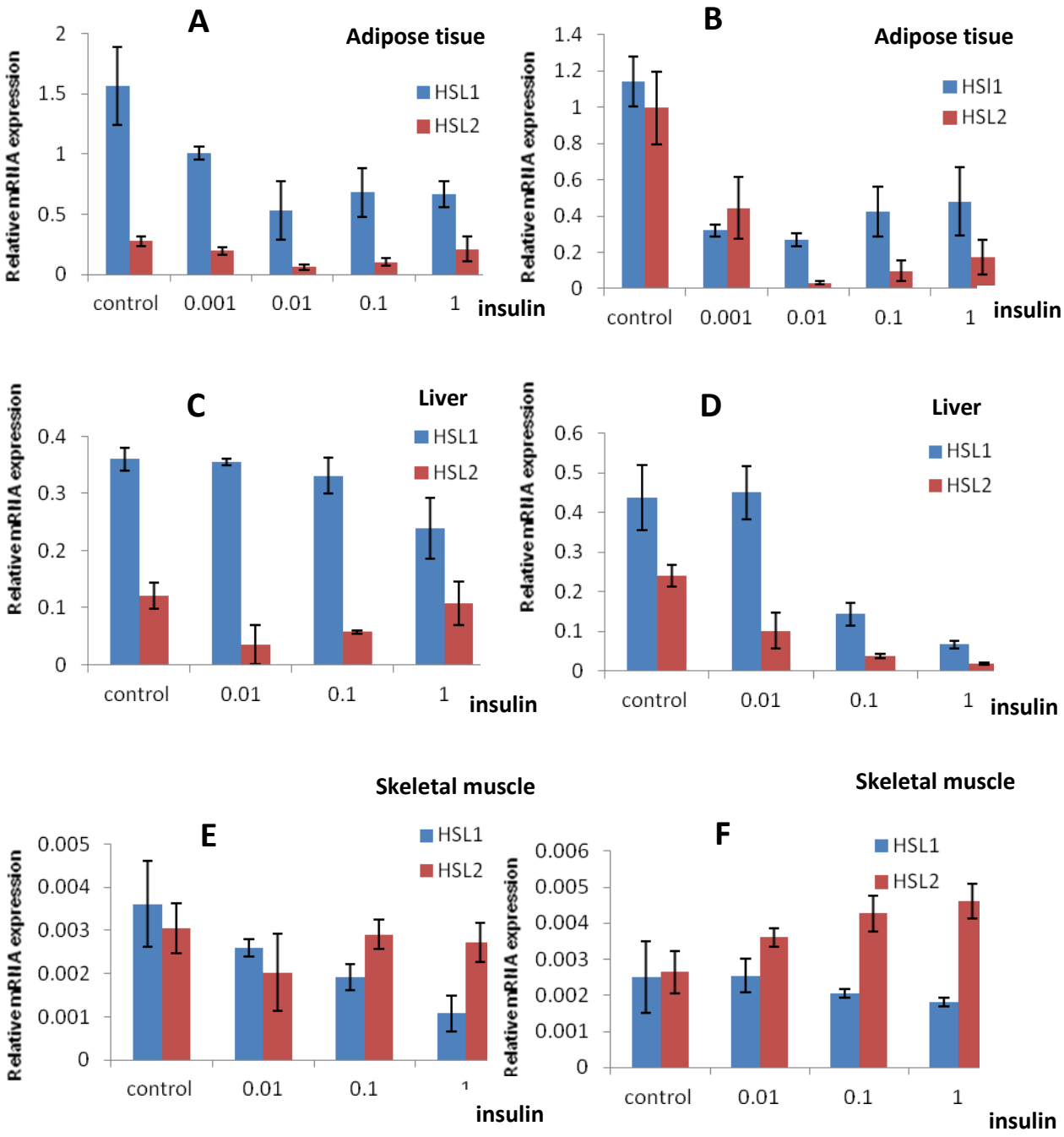

Figure 3-2-1. Suppression of HSL1 and HSL2 mRNA expression in adipose tissue, liver and skeletal muscle under insulin treatment in red seabream. Messenger RNA levels were determined by quantitative PCR. The expression levels in adipose tissue of HSLs at 30 min and 1 h incubation, respectively (A and B). The expression levels in liver and skeletal muscle of HSLs at 1 and 2 h incubation, respectively (C, D and E, F).

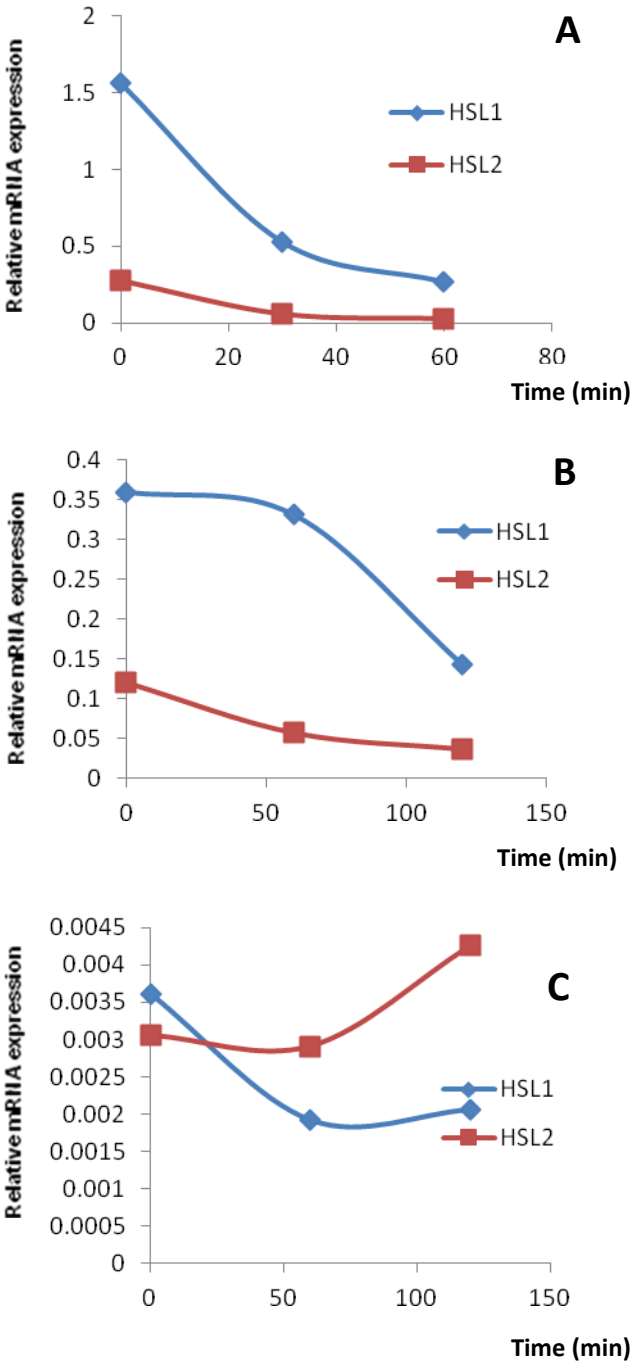

Figure 3-2-2. Time dependence of HSL1 and HSL2 mRNA expressions in adipose tissue (A), liver (B) and skeletal muscle (C) of red seabream in the incubation with 0.1 mg/ml of GH**.**

Section 3

Growth hormone mediates HSL genes expression in adipose tissue and liver using *ex vivo*

Several hormones stimulate HSL in mammals and fish, such as glucagon and catecholamine activate HSL phosphorylation leading to hydrolysis of TAG to FFA. Catecholamine activates cAMP/PKA pathway leading to phosphorylation of HSL and elevating lipolytic activity. Antilipolytic activity directly depressed the action of PKA by elevating PDE 3B, resulting in deactivation of PKA and dephosphorylation of HSL. GH was known as a regulator on lipolysis. The recent study reported the effect of GH in fish that GH mediated lipolysis through HSL activation in isolated hepatocytes from rainbow trout (Kittilsen et al. 2013).

In this chapter, sliced liver and adipose tissues were used as models to examine the mechanism of GH action on lipolysis. The mRNA expression levels of HSL genes were studied in this section.

Materials and methods

Materials

The Leibovits's L-15 medium with L-glutamine was purchased from Gibco (Life technology). This medium was added with 3 levels of growth hormone GH (Wako, Tokyo, Japan).

Sample preparation

Red seabream was anesthetized rapidly under cold ice for 30 min. Adipose tissue, and liver were excised out. Tissues were washed with cold PBS. Liver tissue was perfused with the perfusion buffer until the blood clotting removed. Tissues explants freshly isolated from red seabream were cut with a precision-cut slice into small pieces and incubated at 20°C under agitation in Leibovitz's L-15 Medium with L-glutamine (Gibco, Life technology).

HSL mRNA expression

Sliced adipose and liver tissues were incubated with 3 concentrations of growth hormone (control without GH, 50, 500 and 1,000 ng/ml of GH). Tissue samples were incubated for 1, 4, and 10 h at each GH concentration with continuous agitation in the water bath at 20°C. After incubation, the tissues were immediately stored in RNAlater (Ambion) and kept at -20°C.

Total RNAs were extracted and reversed transcribed as described previously in Section 1 of Chapter 1. Complementary DNA were diluted with dH_2O for 100 times and subjected to quantitative-real time PCR analysis.

Complementary DNA cloning of APO14

To amplify Apo14 gene, PCR was performed with a degenerate primer pair (APO14F_SB and APO14R_SB) shown in Table 3-3-1. The PCR cycle consisted at 94°C for 2 min followed by 35 cycles at 94°C for 30 s, 59°C for 30 s and 72°C for 30 s with a final extension at 72°C for 5 min. The PCR products were purified on 2% gel electrophorysis and then ligated in the pGEM-T Easy Vector (Promega) as described in Section 1 of the Chapter 2. Finally, a target gene was sequenced by ABI Prism 3130 Genetic analyzer (Applied Biosystem).

Amplification efficiency and real-time PCR

An amplification efficiency of APO14 gene were determined as described in Section 1 of the Chapter 2. The other primer pair sequences used for real-time PCR in the present study including, peroxisome proliferator-activated receptor gamma (PPARγ), fatty acid synthetase (FAS), lipoprotein lipase 1 (LPL1) were according to the previous study (Oku et al. 2002).

Table 3-3-1. Oligonucleotide sequences of primers used in GH experiment

Primers name	Sequences 5'-3'	genes	Purpose
APO14_FSB	ACAGACAACTCGCTTKCAGA	APO14	Amplification
APO14_RSB	GAACACAYTCACMCATATACATAC	APO14	Amplification
qPCRAPO_F	TCATGCCCGCTGAGTAAAGAC	APO14	Real-time PCR
qPCRAPO_R	CATTGTGCATTGCTTTTCTCAGC	APO14	Real-time PCR
PPARγ_F	GACAAGTGTGAGCGCCG	PPARγ	Real-time PCR
PPARγ_R	CATCTTTGCCACCAGGGT	PPARγ	Real-time PCR
LPL1_F	CTCAAGACCCGCGAGAT	LPL1	Real-time PCR
LPL1_R	AAGCGTCGCTCTGACC	LPL1	Real-time PCR
FAS_F	AGCTGTTCATCTGGGGAT	FAS	Real-time PCR
FAS_R	CTGGGAAGAGGGCCATC	FAS	Real-time PCR

Results

In the present study, cDNA encoding APO14 was cloned and sequenced using ABI Prism 3130, 765 bp sequence was obtained, encoding 144 amino acids of open reading frame (ORF) from APO14 gene (Fig 3-1). Based on the obtained sequence, primer pairs were designed with specificity for real-time PCR. Furthermore, the amplification efficiency was evaluated to construct the amplification curve (fig. 3-2).

```
1     ATG CAT GCA AAA TAC GCC CTG GCA CTG ATC TTC GCT CTG CAG GTC   45
1     Met His Ala Lys Tyr Ala Leu Ala Leu Ile Phe Ala Leu Gln Val   15

46    TCT GTG AGC CTG TGT GAG ATT CCT GAT CCA CCT GAG GAG CTT GTT   90
16    Ser Val Ser Leu Cys Glu Ile Pro Asp Pro Pro Glu Glu Leu Val   30

91    CAG AAA TAT AAT GAG TAC AAA GGT ACC TTC TAC AAG AGG CTG CTG   135
31    Gln Lys Tyr Asn Glu Tyr Lys Gly Thr Phe Tyr Lys Arg Leu Leu   45

136   AAT CTT CTT ACC CAG GTT CAG ACT GCT TCT GGT CCT ATG GTG GAG   180
46    Asn Leu Leu Thr Gln Val Gln Thr Ala Ser Gly Pro Met Val Glu   60

181   CAG GCC ACT CAA GAT GGG CGT GGA CAG GTT GCC AGA GAA TAC GCC   225
61    Gln Ala Thr Gln Asp Gly Arg Gly Gln Val Ala Arg Glu Tyr Ala   75

226   GAG AGT CTG CAG GCC AAG CCC GAG TTC CAA GCC ATG GTC AAG ATT   270
76    Glu Ser Leu Gln Ala Lys Pro Glu Phe Gln Ala Met Val Lys Ile   90

271   GCC ACT GCC CTG GGT GAG GAG GCA TCT CCC CTG GTG GAC AAG GCC   315
91    Ala Thr Ala Leu Gly Glu Glu Ala Ser Pro Leu Val Asp Lys Ala   105

316   CGC TTA AAA TTG CTG GGT GCT TAC CAA GCG TAC CTC CGC CCC TAC   360
106   Arg Leu Lys Leu Leu Gly Ala Tyr Gln Ala Tyr Leu Arg Pro Tyr   120

361   GTT GGC GAA TGG CTG GCT GAC ACC ATC ACC GAA GTC AAG GTC CAC   405
121   Val Gly Glu Trp Leu Ala Asp Thr Ile Thr Glu Val Lys Val His   135

406   CTG GAC AAA ATC ATG CCC GCT GAG TAA   432
136   Leu Asp Lys Ile Met Pro Ala Glu  *    144
```

Figure 3-3-1. Nucleotide and deduced amino acid sequences of cDNA encoding APO14 gene in red seabream. Bold faced letters and asterisk indicate the initiation and stop codon, respectively.

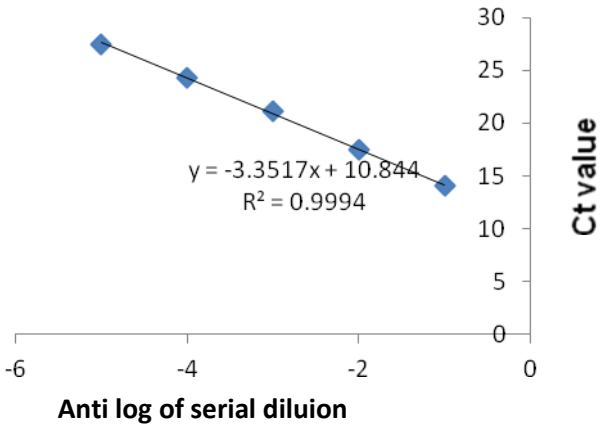

Figure 3-3-2. Amplification efficiency of APO14 gene from red seabream. Amplificaition cureves were plotted with Ct value and antilog of cDNA serial dilution of APO14.

The samples tissue slices including adipose tissue and liver were determined by quantitative real-time PCR. HSL mRNA expression levels elevated in GH incubation in both examined organs (Fig. 3-3-3) but not in HSL2 of adipose tissue after 4 h incubation. In adipose tissue, HSL1 mRNA expressions incubated with GH increased 7-13 folds after 4 h incubation and diminished after 10 h incubation (Fig.3-3-3: D). On the other hand, the induction of HSL mRNA expression in liver was 11 folds in HSL1 and 25 folds in HSL2 compared with control (Fig 3-3-3; A,B). The expression patterns of HSL1 and HSL2 mRNAs linearly increased after incubation with GH in liver and adipose tissue but not HSL2 in adipose tissue after 10 h incubation. GH also stimulated both HSL1 and HSL2 mRNA expressions in a concentration-related manner (Fig 3-3-3; A-D). The expression of HSL2 mRNA in adipose tissue was not affected by GH

treatment. HSL2 mRNA expression was activated after 1 h incubation but decreased after 4 h incubation. In addition, HSL2 mRNA expression in adipose tissue was suppressed after 4 h in all GH concentrations which may not related to GH concentration and incubation period.

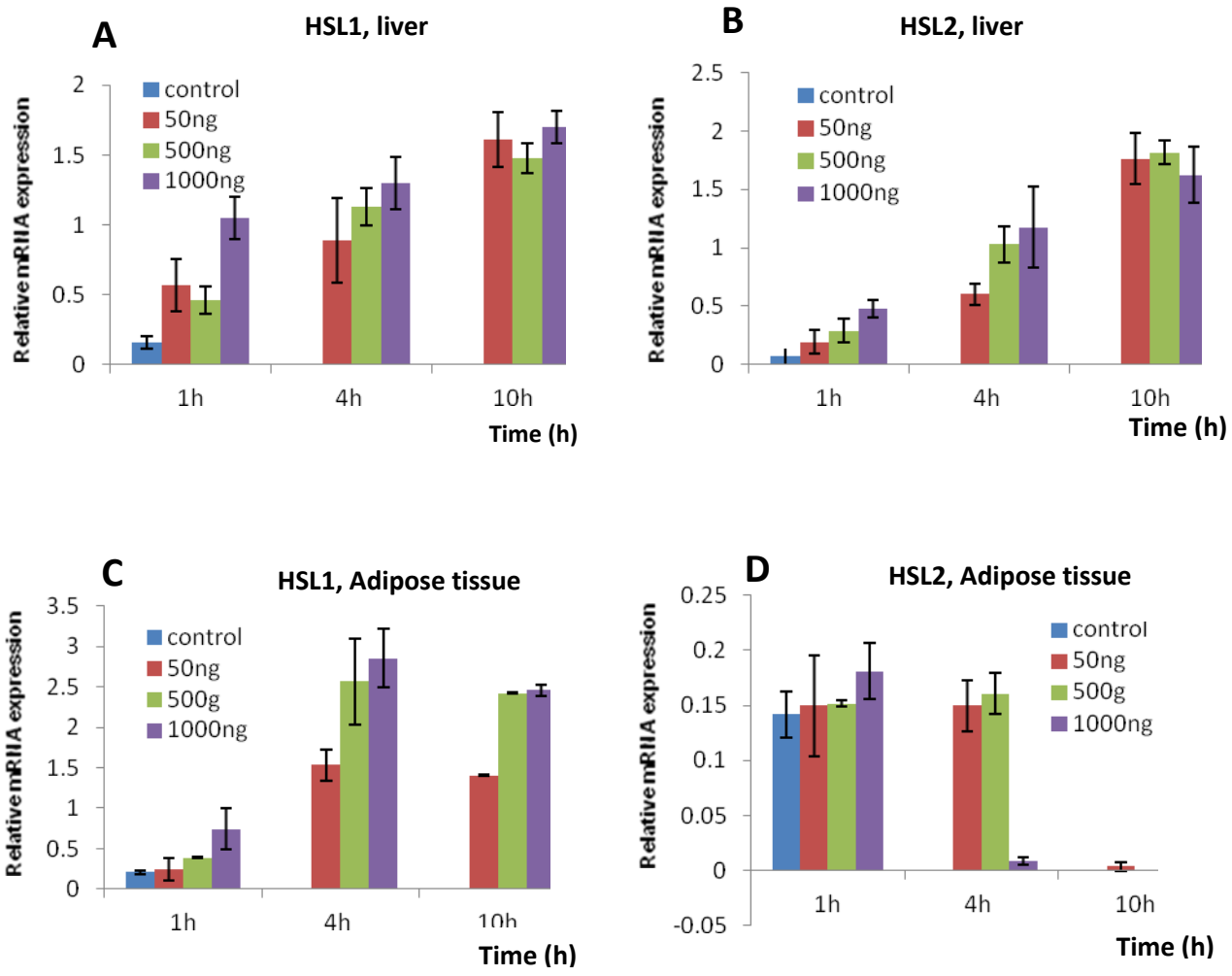

Figure 3-3-3. GH stimulated expression of HSL1 and HSL2 encoding mRNAs in slice tissues of red seabream. The expression levels in liver of HSLs at 1, 4 and 10h incubation, respectively (A and B). The expression levels in adipose tissue of HSLs at 1, 4 and 10 h incubation, respectively (C and D).

Messenger RNA expression of other genes was determined in 50 ng/ml of GH treatment for 10 h. The expression levels of PPARγ, FAS, and APO14 mRNAs extensively increased during 1 to 4 h in the presence of GH (Fig 3-3-4). The expression levels of APO14 mRNA decreased after 4 h. LPL1 genes dramatically decreased after incubated with GH (Fig 3-3-4).

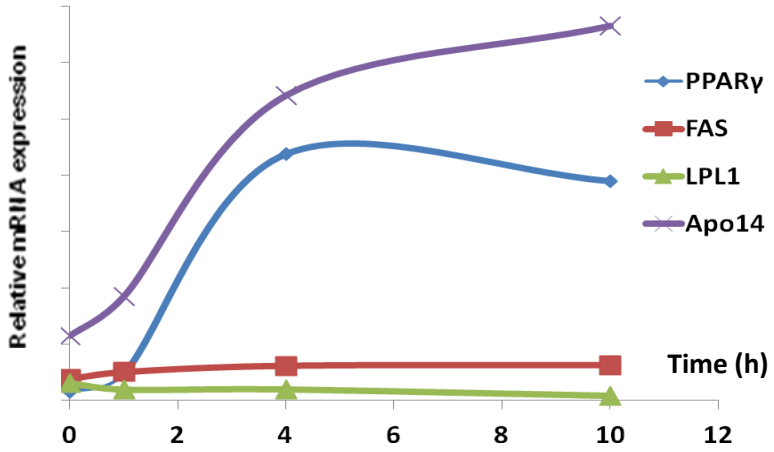

Figure 3-3-4. Time dependence of PPARγ, FAS, LPL and APO14 mRNA expressions in liver of red seabream in the incubation with 50 ng/ml of GH.

Section 4

Discussion

In response to fasting condition, animal immediately reduces their metabolism and reverses their reservoir energy using for maintaining their life activity. The nutritional state is one of the extrinsic factors which induce the metabolic changes in mammals. It has been extensively investigated on fasting state in several studies, which demonstrated that fasting is associated with growth retardation and diminished the stored lipid in several tissues but mainly in adipose tissues (Deng et al. 2004; Small et al. 2006; Uchida et al. 2003; Norbeck et al. 2007; Fox 2006). Elevated lipid depletion from lipid reservoir tissue during fasting resulted to induce an elevation of HSL activity (Sheridan, 1988; Sheridan and Mommsen, 1991; Harmon and Sheridan, 1992a). In the present study, HSL 1 and HSL2 mRNAs were elevated during fasting from day 0 to day7 in both adipose tissue and liver. This result is consistent with the previous study on rainbow trout indicating that insulin was diminished during fasting (Kitillsen et al. 2011). Furthermore, Kadowaki et al. (1996) found that insulin was suppressed leading to induce lipolytic activity. In gilthead seabream, fasting elevated lipolytic activity in adipose tissue (Albalat et al. 2001; 2005). Epinephrine has been reported with an increase during fasting and activated lipolytic activity leading to release of FFA (Finn et al. 2006; Kadowaki et al. 1996). In fasted rainbow trout and gilthead seabream, glucagon levels in plasma were elevated. These actions were manifested by increase in FFA and glycerol released by elevated

triacylglycerol lipase activity (Harmon and sheridan, 1992; Albalat et al. 2005; 2006). Jocken et al. (2007) further suggested that insulin negatively decreased not only body weight but also depressed several lipolytic protein expressions including ATGL and HSL protein.

HSL1 and HSL2 mRNA levels were determined in adipose tissue, liver and skeletal muscle using *ex vivo* study. HSL mRNA expression was suppressed by insulin. The present study suggests that insulin directly should suppress mRNA expressions of both HSL1 and HSL2 in adipose tissue and liver of red seabream. Insulin plays a crucial role in antilipolysis. Insulin activates PDE 3B, leading to decrease cAMP and HSL phosphorylation (Eriksson and Tornqvist 1997). In red seabream, HSL mRNA expressions dramatically decreased in adipose tissue and liver in the presence of insulin. On the other hand, Tashima and Cahill (1968) reported that insulin had no effect on plasma FFA levels in toadfish.

The adipose tissue and liver of teleost fish is a good model for investigating the effect on lipid mobilization and energy metabolism due to the significant lipid storage site (Sheridan 1994). Those tissues constitute with highly abundance of GH-receptor activity (Reiddl and Sheridan 2012; Holm 2000). Adipose tissue is an HSL abundant site (Holm et al. 2000; Kittillsen et al. 2011). In the present study, GH enhanced the *de novo* expressions of HSL mRNA in both adipose tissue and liver. GH stimulates lipolysis by elevating HSL mRNA expression. Norbeck et al. (2007) found that FA concentrations in circulation were higher range with GH treatment in rainbow trout. GH stimulated HSL activity and HSL mRNA expression, which mediated through the ERK and PKC signaling pathways (Bergab et al. 2013). GH stimulates the lipolysis by the activation of

HSL resulting to release the free fatty acids and glycerol in liver and adipose tissue in fishes (Sheridan 1994; Albalat et al. 2005). Langin et al. (2006) showed that GH increased the specific activity of hepatic HSL *in vivo* and *in vitro*. Lipolytic action is to increase in plasma FA in mammals and fish following by GH induction (Fain 1980; Lafontan and Langin 2009).

Accumulation of TAG has been linked to several metabolic genes. In the present study, 4 genes were used to determine the effect of GH incubation. The expression of PPARγ was largely increased in accordance with increase in HSL mRNA expression. The previous study found that HSL was upregulated by PPARγ leading to degradation of TAG stored lipid in human heptic cell cultured, suggesting that HSL is a target of PPARγ, a transcription factor (Deng et al. 2006). Lipoprotein lipase (LPL), lipoprotein and hepatic lipase decreased during GH treatment in both animal and human (Oscarsson et al. 1996; 1991). Oscarsson et al. (1999) found that GH treatment suppressed LPL mRNA expression in liver but not in adipose tissue. In the present results, LPL in liver is also suppressed by GH treatment. APO14 mRNA expression was higher than control at 7 folds, but it was depressed after 4 h with GH incubation. FAS expression was dramatically increased after GH treated in contrast to the previous studies reported that FAS expression was suppressed during GH treatment in human (Hogan and Stephen 2005), pig (Andrea et al. 2006) and sheep (Vernon and Finley, 1888).

Summary

The nutritional regulation has the effect on HSL1 and HSL2 mRNA expressions in red seabream. Fasting stimulated the expression of the two HSL mRNAs but major activation was observed in adipose tissue which is the lipid depots in a tissue-specific manner. It was found that GH promoted lipolysis by enhancing the expression of HSL-encoding mRNA. In contrast, insulin suppressed the lipolytic action.

Chapter 4

General Discussion

In the present study, the full-length cDNAs encoding HSLs were cloned, sequenced and characterized from Japanese flounder, *Paralichthys olivaceus* and red seabream, *Pagrus major*. Multiple alignments and phylogenetic tree were performed based on computational studies. The tissue distributions of HSLs were investigated based on the relationships between HSL gene and protein expression patterns on lipid metabolism. The effects of nutritional state and cytokines on HSL mRNA expression were also investigated in red seabream.

In chapter 1, the full-length HSL1 and HSL2 cDNAs from Japanese flounder and red seabream were cloned and sequenced. In fish, HSL cDNA has been documented, including partial sequence and full-length in several species such as gilthead seabream (Cruz-Garcia et al. 2009), glass carp (Li et al. 2010), grouper (Li et al. unpublished data) and rainbow trout (Kittilson et al. 2011). Adipocyte lipolysis is acutely regulated by the activity of phosphorylation HSL, activated by intracellular cAMP and PKA-dependent phosphorylation at Ser563, Ser659 and Ser660 in rat numbering HSL amino sequence (Jocken et al. 2008; Tansey et al. 2004). HSLs have a lipolytic function (Kittilson et al. 2011), which is mediated by hormonal regulations through the cAMP/PKA pathway. However, it was difficult to determine phosphorylation sites of fish HSLs based on the sequence alignment because of a sequence gap around AA530-570 in HSL1 and HSL2 of rainbow trout, 542-567 in HSL1 of Japanese flounder and

548-573 in HSL1 red seabream (Fig. 1-2-1). Putative PKA phosphorylation sites in Japanese flounder and red seabream HSLs were aligned. Although there were some candidate residues corresponding to Ser563 of rat HSL, no PKA phosphorylated consensus sequence was conserved among fish, suggesting that fish HSL would be modulate via other signaling pathways. Alternatively, we cannot rule out the possibility that fish PKA recognizes the amino acid sequence different from the mammalian PKA. Further studies on the regulatory mechanisms of fish HSLs will be required to understand the function and regulatory mechanism of fish HSLs.

In order to study on genetic evolution relationship of HSLs of Japanese flounder, red seabream and other species, phylogenetic tree was constructed using maximum-likelihood method (Fig. 1-2-2). HSL1 and HSL2 of Japanese flounder and red seabream were grouped together within the major clade of fish HSLs, but distantly separated from the mammalian HSLs. The multiple alignments showed that some basic structure including catalytic triad and phosphorylation sites were conserved in human and rat HSLs indicating that HSL from Japanese flounder and red seabream shared evolution within the HSL genes family. Interestingly, the phylogenetic analysis showed that HSL1 and HSL2 of rainbow trout were clustered at the same clade with HSL1 of fish but not observed in the previous study (Kitillson et al. 2011). The reason for this discrepancy is not clear, but it might be related to whole-genome duplication occurred at the teleost fish (Davison et al. 2010; Koop and Davidson, 2008). Whole-genome duplication was found in some fish groups such as Polypteriformes, Ancipenseriformed, and Lepisosteidae (Hoegg et al. 2004). The present study showed that both rainbow

trout has a high amino acid identity (59.9- 84.7%) of HSL1 and HSL2 to Japanese flounder and red seabream.

To study on HSLs mRNA and HSLs protein distribution, RT-PCR, real-time PCR and immunoblot analysis were also performed in Japanese flounder and red seabream in Chapter 2. Several studies have reported that HSL mRNAs were broadly expressed in several tissues. In mammalian, HSL mRNA is expressed in various tissues including the heart, liver, testis, and skeletal muscle (Holst et al. 1996; Kraemer and Shen, 2002). In accordance with the present study, HSLs mRNAs were expressed in all tissues examined. In Japanese flounder, HSL mRNAs were relatively high in the inclinator muscle of fin followed by the skeletal muscle and liver, while in red seabream HSL mRNA levels were high in the adipose tissue and gonad (Fig. 2-2-2). The results suggested that the expressions of HSLs are tissue- and specie-specific manner. The molecular masses of HSL proteins in fish were firstly determined in the present study. The molecular mass in Japanese flounder was of 96 and 125 kDa for HSL1 and HSL2, respectively (Fig. 2-2-3) while 98 kDa of HSL1 was found in red seabream (Fig 2-2-5). HSL has at least three isofomes that mainly found in adipose tissue and testis. In testis, it appears to have 2 isoforms with 120-130 kDa, which is larger than HSL protein in adipose tissue. While HSL protein in adipose tissue of human is of 88 kDa with slightly larger than rat adipose tissue HSL of an 84 kDa (Fredrikson et al, 1981; 1986; Holm et al. 1988), and mouse and guinea-pig of 82 kDa (Holm et al. 1989; Chung et al. 2001).

The function of HSL in non-adipose tissues has been studied in various tissues, for example in testis (Arenas et al. 2004; Hermo et al. 2008),

osteoblast cell (Shen et al. 2011) and skeletal muscle (Langfort et al. 2003; Jocken et al. 2008; Badin et al. 2011). Interestingly, a skeletal muscle also plays a role in lipolytic regulation controlled by HSL activity. HSL mRNAs were highly abundant in an oxidative muscle fiber in rat skeletal muscle. The HSL phosphorylation also activated through AMP dependent kinase (Langfort et al. 2003). HSL1 mRNA was highly abundant in inclinator muscle of fin of Japanese flounder (Fig. 2-3-1). Concomitantly, FFAs were detected by TLC in the inclinator muscle of fin (Fig. 2-4-1). Our present study suggest that inclinator muscle of fin in Japanese flounder is a site of depositing lipids, where HSL mediated lipolysis to provide free fatty acid in supporting aerobic movement of fins.

In Chapter 3, we studied the effects nutritional state and cytokines on HSLs mRNA expression. During periods of nutrients deprivation, adipocyte tissue is the main source for TAG stored lipid, catalyzing adipose triacylglycerol to produce FFA mobilization. In the process, FFAs are immediately liberated into blood stream to produce energy and then transported to tissues. The mobilization of FFAs are taken up by the liver and subsequently oxidized, esterified, or converted into ketone bodies (Hawkins et al. 1971). The present finding indicates that fasting-associated lipid degradation is accompanied by increasing HSL mRNA expression (Kittilsen et al. 2011). Sheridan and Mommsen (1991) and Harmon and Sheridan (1992a) have observed the pattern of fasting-associated HSL mRNA expression, lipid was firstly mobilized from mesenteric fat through the liver and red muscle in rainbow trout. Fasting also mediated lipolysis by elevating FFA circulation (Albalat et al. 2005) and further release glucagon

leading to stimulate lipolysis in liver of rainbow trout (Harmon and Sheridan, 1992b) and the adipose tissue of gilthead sea bream (Albalat et al. 2005).

Our present study shows that HSL1 and HSL2 mRNA expression levels were suppressed by insulin treatment in both adipose tissue and liver of red seabream. Insulin regulates the stimulation of PDE 3B, resulting in reduction of cAMP levels, which depress HSL phosphorylation (Shakur et al. 2001). In contrast, HSL2 mRNA expression was dramatically increased by insulin treatment. These may be caused by two possible aspects: (i) the condition of an *ex vivo* incubation at 37°C and (ii) the muscle fiber death before incubation. GH has significantly regulated several physiological processes in vertebrates, including growth activation, anabolic mechanism, lipid metabolism, lipogenesis and lipolysis. In the present study, HSLs mRNAs levels of red seabream were increased when GH was incubated in relation to time and concentration. GH has significantly regulated several physiological processes in vertebrates, including growth activation, anabolic mechanism, lipid metabolism, lipogenesis and lipolysis. In the present study, HSL mRNA levels of red seabream were increased when GH was incubated in relation to time and concentration. GH has shown to have an upregulation of lipolysis in liver and adipose tissues of rainbow trout (Albalat et al. 2005; Bergan et al. 2013).

In conclusion, the full-length cDNAs encoding HSLs were cloned, sequenced and characterized from Japanese flounder, *Paralichthys olicaceus* and red seabream *Pagrus major* Japanese flounder and red seabream. HSL of Japanese flounder and red seabream possess HSL-encoding mRNAs that expressed in different tissues. Their transcripts and HSLs protein were ubiquitously expressed in various tissues. The HSL mRNA levels were markedly high in the inclinator

muscle of fin for Japanese flounder, whereas highly expressed in the adipose tissue and gonad. The transcripts of HSL1 were localized in adipocytes of the inclinator muscle of fin. These results suggest that the inclinator muscle of fin is a supplier of FFA mobilization in Japanese flounder, and that HSL-mediated lipolysis provides FFAs for the continuous and aerobic movement of fins. Fasting condition stimulated the expression of the two HSL mRNAs in major lipid depots in a tissue-specific manner. The HSL mRNAs, HSL1 and HSL2 are differentially expressed within and among tissues, and state of nutrition would modulate the pattern of HSL expression in part via hormonal regulations such as insulin and GH.

References

Albalat, A., Gomez-Requeni, P., Rojas, P., Medale, F., Kaushik, S., Vianen, G.J., Van den Thillart, G., Gutierrez, J., Perez-Sanchez, J., Navarro, I., 2005. Nutritional and hormonal control of lipolysis in isolated gilthead seabream (*Sparus aurata*) adipocytes. Am. J. Physiol. Endocrinol. Metab. 289: 259-265.

Albalat, A., Saera-Vila, A., Cipill, E., Gutierrez, J., Perez-Sanchez, J., Navorro, I., 2007. Insulin regulation of lipoprotein lipase (LPL) activity and expression in gilthead seabream (*Sparus auratus*). Comp. Biochem. Physiol. B. 148: 151-159.

Albalat, A., Sanchez-Gumaches, J., Guierez J., Navarro, I., 2006. Regulation of lipoprotein lipase activity in rainbow trout. (*Oncorhynchus mykiss*) tissues. Gen. Comp. Endocrinol. 146: 226-235.

Albalat, A., Vianen, G., Gutierez, J., Planas, J.V., van den thillart, G., Navarro, I., 2001. Hormonal regulation of rainbow trout adipocyte lipolysis. *In* 21st conference of European Comparative Endocrinologist. Bonn, Germany, University of Bonn.

Ando, S., Mori., T., Nakamura, K., Sugawara. A., 1993. Characteristics of lipid accumulation types in 5 species of fish. Nippon Suisan Gakk. 59: 1559-1564.

Andrea, A.F.B.V.J, Lucia, E,A., Eduardo. F.D., Luiz. L.C., Dante, P.D.L, 2006. Effect of growth hormone on fatty acid synthetase gene expression in porcine adipose tissue cultures. Genet. Mol. Biol. 29: 180-186.

Arenas, M.I., Lobo, M.V., Caso, E., Huerta, L., Paniagua, R., Martín-Hidalgo, M.A., 2004. Normal and pathological human testes express hormone-sensitive lipase and the lipid receptors CLA-1/SR-BI and CD36. Hum Pathol. 35: 34-42.

Auboug, S.P., Medina, I., 1999. Influence of storage time and temperature on lipid deterioration during cod (*Gadus morhua*) and haddock (*Melanogrammus aeglefinus*) frozen storage. J. Sci. Food Agric. 79: 1943-1948.

Bergan, H.E., Kittilson, J.D., Sheridan, M.A., 2012. Nutrition-regulated lipolysis in rainbow trout (*Oncorhynchus mykiss*) is associated with alteration in the ERK, PI3K-Akt, JAK-STAT, and PKC signaling pathways. Gen. Comp. Endocrinol. 176: 367-376.

Bergan, H.E., Kittilson, J.D., Sheridan, M.A., 2013. PKC and ERK mediate GH-stimulated lipolysis. J. Mol. Endocrinol. 51: 213-224.

Bligh, E.G., Dyer, W.J., 1959. A rapid method for total lipid extraction and purification. Can. J. Biochem. Physiol. 37: 911-917.

Carroll, P.V., Drake, W.M., Maher, K.T., Metcalfe, K., Shaw, N.J., Dunger, D.B., Cheetham, T.D., Camacho-Hubner, C., Savage, M.O., Monson, J.P., 2004. Comparison of continuation or cessation of growth hormone (GH) therapy on body composition and metabolic status in adolescents with severe GH deficiency at completion of linear growth. J. Clin. Endocrinol. Metab. 89: 3890-3895.

Casado, M.E., Huerta, L., Oritz, A.I., Perez-Crespo, M., Gutierrez-Adan, A., Kraemer, F.B. Lasuncion, M.A., Busto, R., Martin-Hidalgo, A., 2012.

HSL-knockout mouse testis exhibits class B scavenger receptor upregulation and distributed lipid raft microdomains. J. Lipid Res. 53: 2586-2597.

Chaijan, M., Jongjarenorak, A., Phatcharat, S., Benjakul, S., Rawdkuen, S., 2010. Chemical compositions and characteristics of farm raised giant catfish (*Pangasianodon gigas*) muscle. Food Sci. Technol. 43: 452-457.

Chambrier, C., Picard, S., Vidal, H., Cohen, R., Riou, J.P., Beylot, M., 1990. Interactions of glucagon and free fatty acids with insulin in control of glucose metabolism. Metabolism 39: 976 – 984.

Chaves, V.E., Frasson, D., Kawashita, N.H., 2011. Several agent and pathways regulate lipolysis in adipocytes. Biochemie 10: 1631-1640.

Chavez, J.A., Gridley, S., Sano, H., Lane, W.S., Lienhard, G.E., 2006. The 47 kDa Akt substrate associates with phosphodiesterase 3B and regulates its level in adipocytes. Biochem. Biophys. Res. Commun. 324: 1218-1222.

Choo, D-W., Hurihara, T., Suzuki, T., Soda, K., Esaki, N., 1998. A cold-adapted lipase of an Alaskan phychrotroph, *Pseudomonas sp*. Strain B11-1: Gene cloning and enzyme purification and characterization. Appl. Environ. Microbiol. 64: 486-491.

Chung, S., Wang, S.P., Pan, L., Mitchell, G., Trasler, J., Hermo, L., 2001. Infertility and testicular defects in hormone-sensitive lipase–deficient mice. Endocrinology 142: 4272-4281.

Contreras, J.A., Danielsson, B., Johansson, C., Osterlund, T., Langin, D., Holm, C., 1998. Human hormone-sensitive lipase: expression and large scale purification from baculovirus/insect cell system. Protein Expr. Purif. 12: 93-99.

Contreras, J.A., Holm, C., Martin, A., Gaspar, M.L., Lasuncion, M.A., 1994. Presence of hormone-sensitive lipase mRNA in J774 macrophages. Isr. J. Med. Sci. 30: 778-781.

Contreras, J.A., Karlsson, M., Osterlund, T., Laurell, H., Svensson, A., Holm, C., 1996. Hormone-sensitive lipase is structurally related to acetylcholinesterase, bile salt-stimulated lipase, and several fungal lipases. Building of a three dimensional model for the catalytic domain of hormone-sensitive lipase. J. Biol. Chem. 271: 31426-31430.

Cordle, S.R., Colbran, R.J., Yeaman, S.J., 1986. Hormone-sensitive lipase from bovine adipose tissue. Biochim. Biophys. Acta 887: 51-57.

Cygler, M., Schrag, J.D., Sussman, J.L., Harel, M., Silman, I., Gentry, M.K., Doctor, B.P., 1993. Relationship between sequence conservation and three-dimensional structure in a large family of esterases, lipases, and related proteins. Protein Sci. 2: 366–382.

Darrin, J., Cowley., Sheridan, M.A., 1993. Insulin stimulates hepatic lipogenesis in rainbow trout, *Oncorhynchus mykiss*. Fish Physiol. Biochem. 11:1-6.

Dauncey, M.J., Burton, K.A., White, P., Harrison, A.P., Gilmour, R.S., Duchamp, C., Cattaneo, D. 1994. Nutritional regulation of growth hormone receptor gene expression. FASEB J. 8: 81-88.

Daval, M., Diot-Dupuy, F., Bazin, R., Hainault, I., Viollet, B., Vaulont, S., Hajduch, E., Ferre, P., Foufelle, F., 2005. Anti-lipolytic action of AMP-activated protein kinase in rodent adipocytes. J. Biol. Chem. 280: 25250-25257.

Davidson, W.S., Koop, B.F., Jones, S.J., Iturra, P., Vidal**, R.,** Maass**, A.,** Jonassen, I., Lien, S., Omholt**,** S.W., 2010. Sequencing the genome of the Atlantic salmon (*Salmo salar*). Genome Biol. 11: 401-410.

De Vlaming, V.L., Pardo, R.L., 1975. *In vitro* effects of insulin on liver lipid and carbohydrate metabolism in the teleost *Notemigonus crysoleucas*. Comp. Biochem. Physiol. B 51: 489-497.

Deng, L., Zhang, W.M., Lin, H.R., Chang, C.H.K., 2004. Effects of food deprivation on expression of growth hormone receptor and proximate composition in liver of black seabream *Acanthopagrus schlegeli*. Comp. Biochem. Physiol. B Biochem Mol Biol.137: 421-432.

Deng, T., Shan, S., Li, P.P., Shen, Z.F., Lu, X.P., Cheng, J., Ning, Z.Q., 2006. Peroxisome proliferator-activated receptor-γ transcriptionally up-regulates hormone-sensitive lipase via the involvement of specificity protein-1. Endocrinology 147: 875-884.

Ducharme, N.A., Bickel, P.E., 2008. Lipid droplets in lipogenesis and lipolysis. Endocrinology 149: 942-949.

Eriksson, H., Ridderstrale, M., Degerman, E.E., Ekholm, D., Smith, C.J., Manganiello, V.C., Belfrage, P., Tornqvist, H., 1995. Evidence for the role of the adipocyte cGMP-inhibited cAMP phosphodiesterase in the antilipolytic action of insulin. Biochem. Biophys. Acta. 1266: 101-107.

Ericksson, H., Tornqvist, H., 1997. Specific inhibition of the cGMP-inhibited cAMP phosphodiesterase blocks the insulin-like antilipolytic effect of growth hormone in rat adipocytes. Mol. Cell. Biochem. 169: 37-42.

Erin, E.K., Jeffrey, S.F., 2004. Adipose tissue as an endocrine organ J. Clin. Endocrinol. Metab. 89: 2548-2556.

Fain, J.N., 1980. Hormonal regulation of lipid metabolism from adipose tissue. *In* Biochemical Action of Hormones, pp 119-203. Ed. G. Litwack. New York: Academic Press.

Feller, G., Thiry, M., Arpigny, J.L., Mergeay, M., Gerday, C., 1990. Lipases from psychrotrophic Antarctic bacteria. FEMS Microbiol. Lett. 66: 239-244.

Finn, P.F., Dice, J.F., 2006. Proteolytic and lipolytic responses to starvation. Nutrition 22: 830-844.

Fortier, M., Wang, S.P., Mauriège, P., Semache, M., Mfuma, L., Li, H., Levy, E., Richard, D., Mitchell, G.A., 2004. Hormone-sensitive lipase-independent adipocyte lipolysis during beta-adrenergic stimulation, fasting, and dietary fat loading. Am. J. Physiol. Endocrinol. Metab. 287: 282-288.

Fox, B.K., Riley, L.G., Hirano, T., Grau, E.G., 2006. Effects of fating on growth hormone, growth hormone receptors, and insulin-like growth factor-I axis in seawater-acclimated tilapia, *Oreochromis mossambicus*. Gen. Comp. Endocrinol. 148: 340-347.

Fredrikson, G., Stralfors, P., Nilsson, N.O., Belfrage, P., 1981. Hormone-sensitive lipase of rat adipose tissue, Purification and some properties. J. Biol. Chem. 256: 6311-6320.

Fredrikson, G., Tornqvist, H., Belfrage, P., 1986. Hormone-sensitive lipase and monoacylglycerol lipase are both required for complete degradation of adipocyte triacylglycerol. Biochimica et Biophysica Acta 876: 288-293.

Fujimoto, T., Ohsaki, Y., Cheng, J., Suzuki, M., Shinohara, Y., 2008. Lipid droplets: a classic organelle with new outfits. Histochem. Cell. Biol. 130: 263-279.

Garton, A.J., Campbell, D.G., Carling, D., Hardie, D.G., Colbran, R.J., Yeaman, S.J., 1989. Phosphorylation of bovine hormone-sensitive lipase by the AMP-activated protein kinase. A possible antilipolytic mechanism. Eur. J. Biochem. 179: 249-254.

Garton, A.J., Campbell, D.G., Cohen, P., Yeaman, S.J., 1988. Primary structure of the site on bovine hormone-sensitive lipase phosphorylated by cyclic AMP-dependent protein kinase. FEBS Lett. 229: 68-72.

Garton, A.J., Yeaman, S.J., 1990. Identification and role of the basal phosphorylation on hormone-sensitive lipase. Eur. J. Biochem. 191: 245-250.

Geromel, E.J., Montgomery, M.W., 1980. Lipase release from lysosomes of rainbow trout (*Salmo gairdneri*) muscle subjected to low temperatures. Food Science 45: 412-415.

Golay, A., Swislocki, A,L., Chen, Y.D., Jaspan, J.B., Reaven, G.M., 1986. Effect of obesity on ambient plasma glucose, free fatty acid, insulin, growth hormone, and glucagon concentrations. J. Clin. Endocrinol. Metab. 63: 481-484.

Greenberg. A.S., Egan, J.J., Wek, S.A., Garty, N.B., Blanchette, M.E.J., Londos, C., 1991. Perilipin a major hormonally regulated adipocyte-specific phosphoprotein associated with the periphery of lipid storage droplets. J. Biol. Chem. 266: 11341-11346.

Greenberg, A.S., Egan, J.J., Wek, S.A., Moos, M.C. Jr., Londos, C., Kimmel, A.R., 1993. Isolation of cDNAs for perilipins A and B: sequence and expression of lipid droplet-associated protein of adipocytes. Proc. Natl. Acad. Sci. USA 90: 12035-12039.

Greenberg, A.S., Shen, W.J., Muliro, K., Patel, S., Souza, S.C., Roth, R.A., Kraemer, F.B., 2001. Stimulation of lipolysis and hormone-sensitive lipase via the extracellular signal-regulated kinase pathway. J. Biol. Chem. 276: 45456-45461.

Grigorakis, K., Alexis, M.N., 2005. Effects of fasting on the meat quality and fat deposition of commercial-size farmed gilthead sea bream (*Sparus aurata* L.) fed different dietary regimes. Aquacult. Nutr. 11: 341–344.

Han, C., Wen, X., Zheng, Q., Li, H., 2011. Effect of starvation on activities and mRNA expression of lipoprotein lipase and hormone-sensitive lipase in tilapia (*Oreochromis niloticus x O. areus*). Fish Physiol. Biochem. 37: 113-122.

Han, Y., Kaneko, G., Nagasaka, R., Kondo, H., Hirono, I., Takahashi, S.I., Watabe, S., Ushio, H. 2013. Distribution of adipocyte-related cells in skeletal muscle of rainbow trout *Oncorhynchus mykiss*. Fish Sci 79: 143-148.

Harbitz, I., Langset, M., Ege, A.G., Hoyheim, B., Davies, W., 1999. The porcine hormone-sensitive lipase gene: sequence, structure, polymorphisms and linkage mapping. Anim. Genet. 30: 10-15.

Harmon, J.S., Sheridan, M.A., 1992a. Effects of nutritional state, insulin, and glucagon on lipid mobilization in rainbow trout, *Oncorhynchus mykiss*. Gen. Comp. Endocrinol. 87: 214-221.

Harmon, J.S., Sheridan, M.A., 1992b. Previous nutritional state and glucose modulate glucagon-mediated hepatic lipolysis in rainbow trout, *Oncorhynchus mykiss*. Zool. Sci. 9: 275-281.

Hemila, H., Koivula, T.T., Palva, I., 1994. Hormone-sensitive lipase is closely related to several bacterial proteins, and distantly related to acetylcholinesterase and lipoprotein lipase: identification of a superfamily of esterase and lipases. Biochim. Biophys. Acta 1210: 249-253.

Hermo, L., Chung, S., Gregory, M., Smith, C.E., Wang, S.P., El-Alfy, M., Cyr, D.G., Mitchell, G.A., Trasler, J., 2008. Alterations in the testis of hormone-sensitive lipase-deficient mice is associated with decreased sperm counts, sperm motility, and fertility. Mol. Reprod. Dev. 75: 565-577.

Hoegg, S., Brinkmann, H., Taylor, J.S., Meyer, A., 2004. Phylogenetic timing of the fish-specific genome duplication correlates with the diversification of the teleost fish. J. Mol. Evol. 59: 190-203.

Hogan, J.C., Stephens, J.M., 2005. The regulation of fatty acid synthase by STAT5A. Diabetes 54: 1968-1975.

Holloway, L., Butterfield, G., Hintz, R.L., Gesundheit, N., Marcus, R., 1994 Effects of recombinant human growth hormone on metabolic indices, body composition, and bone turnover in healthy elderly women. J. Clin. Endocrinol. Metab. 79: 470-479.

Holm, C., 2003. Molecular mechanism regulating hormone-sensitive lipase and lipolysis. Biochem. Soc. Trans. 31: 1120-1124.

Holm, C., Belfrage, P., Fredrikson, G., 1989. Human adipose tissue hormone-sensitive lipase: identification and comparison with other species. Biochim. Biophys. Acta 1006: 193-197.

Holm, C., Davis, R.C., Osterlund, T., Schotz, M.C., Fredrikson, G., 1994. Identification of the active site serine of hormone-sensitive lipase by site-directed mutagenesis. FEBS Lett. 344: 234-238.

Holm, C., Fredrikson, G., Sundler, R., Belfrage, P., 1990. Incorporation of hormone-sensitive lipase into phosphatidylcholine vesicles. Lipids 25: 254-259.

Holm, C., Kirchgessner, T.G., Svenson, K.L., Lusis, A.J., Belfrage, P., Schotz, M.C., 1988. Nucleotide sequence of rat adipose tissue hormone-sensitive lipase cDNA. Nucleic Acid Res. 16: 9879.

Holm, C., Osterlund, T., Laurell, H., Contreras, J.A. 2000. Molecular mechanisms regulating hormone-sensitive lipase and lipolysis. Annu Rev Nutr. 20: 365-393.

Holst, L.S., Hoffmann, A.M., Mulder, H., Sundler, F., Holm, C., Bergh, A., Fredrikson, G., 1994. Localization of hormone-sensitive lipase to rat sertoli cells and its expression in developing and degenerating testes. FEBS Lett. 355: 125-130.

Holst, L.S., Langin, D., Mulder, H., Laurell, H., Grober, J., Bergh, A., Mohrenweiser, H.W., Edgren, G., Holm, C., 1996. Molecular cloning, genomic organization, and expression of a testicular isoform of hormone-sensitive lipase. Genomics 35: 441-447.

Ince, B.W., Thorpe, A., 1975. Hormonal and metabolism effects on plasma free fatty acids in the Northern pike, *Eso lucius*. Gen. Comp. Endocrinol. 27: 144-152.

Jocken, J.W., Langin, D., Smit, E., Saris, W.H., Valle, C., Hul, G.B., Holm, C., Arner, P., Blaak, E.E., 2007. Adipose triglyceride lipase and hormone-

sensitive lipase protein expression is decreased in the obese insulin-resistant state. J. Clin. Endocrinol. Metab. 92: 2292-2299.

Jocken, J.W., Roepstorff, C., Goossens, G.H., Baan, P., Baak, M., Saris, W.H., Kiens, B., Blaak, E.E., 2008. Hormone-sensitive lipase serine phosphorylation and glycerol exchange across skeletal muscle in lean and obese subjects. Diabetes 57: 1834–1841.

Joosten, H.F., van der Kroon, P.H., Buis, A.J., 1975. Development of the obese hyperglycemic syndrome in mice with a growth hormone deficiency. Metabolism 24: 573-579.

Kabbaj, O., Holm, C., Vitale, M.L., Pelletier, R.M., 2001. Expression, activity, and subcellular localization of testicular hormone-sensitive lipase during postnatal development in the guinea pig. Biol. Reprod. 65: 601-612.

Kadowaki, M., Kamata, T., Noguchi, T., 1996. Acute effect of epinephrine on muscle proteolysis in perfused rat hindquarters. Am. J. Physiol. 270: 961-967.

Kaneko, G., Yamada, T., Han, Y., Hirano, Y., Khieokhajonkhet, A., Shirakami, H., Nagasaka, R., Kondo, H., Hirono, I., Ushio, H., Watabe, S., 2013. Differences in lipid distribution and expression of peroxisome proliferator-activated receptor gamma and lipoprotein lipase genes in torafugu and red seabream. Gen. Comp. Endocrinol. 184: 51-60.

Kershaw, E.E., Flier, J.S., 2004. Adipose tissue as an endocrine organ. J. Clin. Endrinol. Metab. 89: 2548-2556.

Kittilson, J.D., Reindl, K.M., Sheridan, M.A., 2011. Rainbow trout (*Oncorhynchus mykiss*) process two hormone-sensitive lipase-encoding mRNAs that are differentially expressed and independently regulated by nutritional state. Comp. Biochem. Physiol. A: Comp. Physiol. 158: 52-60.

Klannemark, M., Orho, M., Langin, D., Laurell, H., Holm, C., Reynisdottir, S., Arner, P., Groop, L., 1998. The putative role of the hormone-sensitive lipase gene in the pathogenesis of type II diabetes mellitus and abdominal obesity. Diabetologia 41: 1516-1522.

Kondo, H., Kawazoe, I., Nakaya, M., Kikuchi, K., Aida, K., Watabe, S., 2001. The novel sequences of major plasma apolipoproteins in the eel Anguilla japonica. Biochim. Biphys. Acta. 1531: 132-142.

Kondo, H., Morinaga, K., Misaki, R., Nakaya, M., Watabe, S., 2005. Characterization of the pufferfish Takifugu rubripes apolipoportein multigene family. Gene 346: 257-266.

Koyama, H., Akolkar, D.B., Shiokai, T., Nakaya, M., Piyapattanakorn, S., Watabe, S., 2012. The occurrence of two types of fast skeletal myosin heavy chains from abdominal muscle of kuruma shrimp *Marsupenaeus japonicas* and their different tissue distribution. J. Exp. Biol. 215: 14-21.

Kraemer, F.B., Patel, S., Saedi, M.S., Sztalryd, C., 1993. Detection of hormone-sensitive lipase in various tissues. I. expression of an HSL/bacterial fusion protein and generation of anti-HSL antibodies. J. Lipid Res. 34: 663-671.

Kraemer, F.B., Shen, W.J., 2002. Hormone-sensitive lipase: control of intracellular tri-(di-) acylglycerol and cholesterol ester hydrolysis. J. Lipid Res. 43: 1585-1594.

Krintel, C., Klint, C., Lindvall, H., Morgelin, M., Holm, C., 2010. Quaternary structure and enzymological properties of the different hormone-sensitive lipase (HSL) isoforms. PLoS One: 2: 1-14.

Krintel, C., Morgelin, M., Logan, D.T., Holm, C., 2009. Phosphorylation of hormone-sensitive lipase by protein kinase A in vitro promotes an increase in its hydrophobic surface area. FEBS Lett. 276: 4752-4762.

Lafontan, M., Langin, D., 2009. Lipolysis and lipid mobilization in human adipose tissue. Prog. Lipid Res. 48: 275-297.

Lampidonis, A.D., Rogdakis, E., Voutsinas, G.E., Stravopodis, D.J., 2011. The resurgence of hormone-sensitive lipase (HSL) in mammalian lipolysis. Gene 477: 1-11.

Lampidonis, A.D., Stravopodis, D.J., Voutsinas, G.E., Messini-Nikolaki, N., Stefos, G.C., Margaritis, L.H., Argyrokastritis, A., Bizelis, I., Rogdakis E., 2008. Cloning and functional characterization of the 5' regulatory region of ovine hormone Sensitive Lipase (HSL) gene. Gene 427: 65-79.

Langfort, J., Ploug, T., Ihlemann, J., Enevoldsen, L.H., Stallknecht, B., Saldo, M., Kjaer, M., Holm, C., Galbo, H., 1998. Hormone-sensitive lipase (HSL) expression and regulation in skeletal muscle. Adv. Exp. Med. Biol. 441: 219-228.

Langfort, J., Ploug, T., Ihlemann, J., Holm, C., Galbo, H., 2000. Stimulation of hormone-sensitive lipase activity by contraction in rat skeletal muscle. Biochem. J. 351: 207-214.

Langfort, J., Ploug, T., Ihlemann, J., Saldo, M., Holm, C., Galbo, H., 1999. Expression of hormone-sensitive lipase and its regulation by adrenaline in skeletal muscle. Biochem. J. 340: 459-465.

Langin, D., Laurell, H., Holst, L.S., Belfrage, P., Holm, C., 1993. Gene organization and primary structure of human hormone-sensitive lipase: possible significance of a sequence homology with a lipase of *Moraxella* TA144, an antarctic bacterium. Proc. Natl. Acad. Sci. USA 90: 4897-4901.

Lanning, N.J., Carter-Su, C., 2006. Recent advances in growth hormone signaling. Rev Endocr. Metab. Disord. 7: 225–235.

Lass, A., Zimmermann, R., Oberer, M., Zechner, R., 2011. Lipolysis-a high regulated multi-enzyme complex mediates the catabolism of cellular fat stores. Prog. Lipid Res. 50: 14-27.

Li, Z., Sumida, M., Birchbauer, A., Schotz, M.C., Reue, K., 1994. Isolation and characterization of the gene for mouse hormone-sensitive lipase. Genomics 24: 259-265.

Luque, R.M., Lin, Q., Chacon, J.C., Subbaiah, P.V., Buch, T., Waisman, A., Vankelecom, H., Kineman, R.D., 2006. Metabolic impact of adult-onset, isolated, growth hormone deficiency (AOiGHD) due to destruction of pituitary somatotropes. PLoS One. 6: 1-11.

Martin, S., Okano, S., Kistler, C., Fernandez, M.A., Hill, M.M., Parton R.G., 2009. Spatiotemporal regulation of early lipolytic signaling in adipocytes. J. Biol. Chem. 248: 32097-32107.

McTernan, P.G., Harte, A.L., Anderson, L.A., Green, A., Smith, S.A., Holder, J.C., Barnett, A.H., Eggo, M.C., Kumar, S., 2002. Insulin and rosiglitazone regulation of lipolysis and lipogenesis in human adipose tissue in vitro. Diabetes 51: 1493-1498.

Meyer, C.W., Klingenspor, M., Rozman, J., Heldmaier, G., 2012. Gene or size: metabolic rate and body temperature in obese growth hormone-deficient dwarf mice. Obes Res 12: 1509-1518.

Migliorini, R.H., Lima-Verde, J.S., Machodo, C.R., Cardona G.M., Garofalo, M.A., Kettelhut, I.C., 1992. Control of adipose tissue lipolysis in ectotherm vertebrates. Am. J. Physiol. 263: 857-862.

Minick, M., Chavin, W., 1970. Effect of pituitary hormones upon serum-free fatty acid in goldfish (*Carassius auratus* L.). J. Exp. Zool. 9: 1082.

Moon, Y.S., Latasa, M.J., Griffin, M.J., Sul, H.S., 2002. Suppression of fatty acid synthethase promoter by polyunsaturated fatty acids. J. Lipid Res. 43: 691-698.

Norbeck, L.A., Kittilson, J.D., Sheridan, M.A., 2007. Resolving the growth-promoting and metabolic effects of growth hormone: Deferential regulation of the GH-IGF-I system components. Gen. Comp. Endocrinol. 151: 332-341.

Oku, H., Koizumi, N., Okumura, T., Kobayashi, T., Umino, T., 2006. Molecular characterization of lipoprotein lipase, hepatic lipase and pancreatic lipase genes: effects of fasting and refeeding on their gene expression in red seabream *Pagrus major*. Comp. Biochem. Physiol. B Biochem. Mol. Biol. 145: 168-178.

Oku, H., Ogata, H., 2000. Body lipid deposition in juveniles of red seabream *Pagus major*, yellowtail *Seriola quinqueradiata*, and Japanese flounder *Paralichthys olivaceus*. Fish. Sci. 66: 25-31.

Oscarsson, J., Ottosson, M., Johansson, J.O., Wiklund, O., Marin, P., Bjorntorp, P., Bengtsson, B.A., 1996. Two weeks of daily injections and continuous infusion of recombinant human growth hormone (GH) in GH-deficient adults. II. Effects on serum lipoproteins and lipoprotein and hepatic lipase activity. Metabolism 45: 370-377.

Oscarsson, J., Olofsson, S.O., Vikman, K., Edén, S., 1991. Growth hormone regulation of serum lipoproteins in the rat: different growth hormone regulatory principles for apolipoprotein (apo) B and the sexually dimorphic apo E concentrations. Metabolism 40: 1191-1198.

Oscarsson, J., Ottosson, M., Edén, S., 1999. Effects of growth hormone on lipoprotein lipase and hepatic lipase. J. Endocrinol. Invest. 22: 2-9.

Osterlund, T., Danielsson, B., Degerman, E., Contreras, J.A., Edgren, G., Davis, R.C., Schotz, M.C., Holm, C., 1996. Domain-structure analysis of recombinant rat hormone-sensitive lipase. Biochem. J. 319: 411-420.

Osuga, J., Ishibashi, S., Shimano, H., Inaba, T., Kawamura, M., Yazaki, Y., Yamada, N., 1997. Suppression of neutral cholesterol ester hydrolase

activity by antisense DNA of hormone-sensitive lipase. Biochem. Biophys. Res. Commun. 233: 655-657.

Planas, J.V., Mendez, E., Banos, N., Capilla, E., Navarro, I., Gutierrez, J., 2000. Insulin and IGF-I receptions in trout adipose tissue are physiologically regulated by circulating hormone levels.. J. Exp. Biol. 203: 1153-1159.

Prego, R., Pazos, M., Medina, I., Aubourg, S.P. 2012. Comparative chemical composition of different muscle zones in angler (*Lophius piscatorius*). J. Food Comp Anal. 28: 81-87.

Ragolia, L., Begum, N., 1998. Protein phosphatase-1 and insulin action. Mol Cell Biochem. 182: 49-58.

Roemmich, J.N., Huerta, M.G., Sundaresan, S.M., Rogol. A.D., 2001. Alternation in body composition and fat distribution in growth hormone-deficient perpuberta children during growth hormone therapy. Metabolism 50: 537-547.

Shakur, Y., Holst, L.S., Landstrom, T.R., Movsesian, M., Degerman, E., Manganiello, V., 2001. Regulation and function of the cyclic nucleotide phosphodiesterase (PDE3) gene family. Prog Nucleic Acid Res Mol Biol. 66: 241–277.

Shen, W-J., Liang, Y., Hong, R., Patel, S., Natu, V., Sridhar, K., Jenkins, A., Bernlohr, D.A., Kraemer, F.B. 2001. Characterization of the functional interaction of adipocyte lipid-binding protein with hormone-sensitive lipase. J. Biol. Chem. 276: 49443-49448.

Shen, Y., Lindberg, A., Olivercrona, G., 2000. Apolipoprotein CII from rainbow trout (*Oncorhynchus mykiss*) is functionally active but structureally very different from mammalian apolipoprotein CII. Gene 254: 189-198.

Sheridan, M.A., 1986. Effects of thyroxin, cortisol, growth hormone, and prolactin on lipid metabolism of coho salmon, *Onchorhynchus kisutch*, during smoltification. Gen Comp Endocrinol. 64: 220-238.

Sheridan, M.A., 1988. Lipid dynamics in fish: aspects of absorption, transportation, deposition and mobilization. Comp Biochem Physiol B. 90: 679-690.

Sheridan, M.A., 1994. Regulation of lipid metabolism in poikilothermic vertebrates. Comp. Biochem. Physiol., B: Comp. Biochem.107: 497–508.

Sheridan, M.A., Kao, Y.H. 1998. Regulation of metamorphosis-associated changes in the lipid metabolism of selected vertebrates. Integr. Comp. Biol. 38: 350-358.

Sheridan, M.A., Momsen. T.P., 1992. Effects of nutritional state on *in vivo* lipid and carbohydrate metabolism of coho salmon. *Oncorhynchus kisutch*. Gen. Comp. Endocrinol. 81: 473-483.

Small, B.C., Murdock, C.A., Waldbieser, G.C., Perterson, B.C., 2006. Reduction in channel catfish hepatic growth hormone receptor expression in response to food deprivation an exogenous cortisol. Domest Anim Endocrinol. 31: 340-356.

Small, C.A., Garton, A.J., Yeaman, S.J., 1989. The presence and role of hormone-sensitive lipase in heart muscle. Biochem J. 258: 67-72.

Smith, F.D., Samelson, B.K., Scott, J.D., 2011. Discovery of cellular substrates for protein kinase A using a peptide array screening protocol. Biochem J 438: 103-110.

Smith, G.M., Garton, A.J., Aitken, A., Yeaman, S.J., 1996. Evidence for a multi-domain structure for hormone-sensitive lipase. FEBS Lett. 396: 90-94.

Straus, D.S., Takemoto, C.D. 1990. Effect of fasting on insulin-like growth factor-I (IGF-I) and growth hormone receptor mRNA levels and IGF-I gene transcription in rat liver. Mol. Endocrinol. 4: 91–100.

Tamura, K., Peterson, D., Peterson, N., Stecher, G., Nei, M., Kumar, S. 2011. MEGA5: molecular evolutionary genetics analysis using maximum likelihood, evolutionary distance, and maximum parsimony methods. Mol. Biol. Evol. 28: 2731-2739.

Tansey, J.T., Sztalryd, C., Hlavin, E.M., Kimmel, A.R., Londos, C., 2004. The central role of perilipin A in lipid metabolism and adipocyte lipolysis. IUBMB Life 56: 379–385.

Tashima, L., Cahill, G.F., 1986. Effects of insulin in the toadfish, *Opsanus tau*. Gen. Comp. Endocrinol. 11: 262-271.

Thompson, J.D., Higgins, D.G., Gibson, T.J., 1994. CLUSTAL W: improving the sensitivity of progressive multiple sequence alignment through sequence weighting, position-specific gap penalties and weight matrix choice. Nucleic Acids Res. 22: 4673-4680.

Tschop, M., Smiley, D.L., Heiman, M.L., 2000. Ghrelin induces adipocity in rodent. Nature 470: 908-913.

Uchida, K., Kajimura, S., Riley, L.G., Hirano, T., Aida, K., Grau, E.G., 2003. Effects of fasting on growth hormone/insulin-like growth factor I axia in tilapia, *Oreochromis mossambicus*. Comp. Biochem. Physiol. A Mol Integr. Physiol. 134: 429-439.

Vallet-Erdtmann, V., Tavernier, G., Contreras, J.A., Mairal, A., Rieu, C., Touzalin, A.M., Holm, C., Jegou, B., Langin, D., 2004. The testicular form of hormone-sensitive lipase HSLtes confer rescue of male infertility in HSL-deficient mice. J. Biol. Chem. 279: 42875–42880.

Vernon, R.G., Finley, E., 1988. Roles of insulin and growth hormone in the adaptation of fatty acid synthesis in white adipose tissue during the lactation cycle in sheep. Biochem. J. 256: 873-878.

Watt, M.J., Holmes, A.G., Pinnamaneni. S.K., Garnham, A.P., Steinberg, G.R., Kemp, B.E., Febbraio, M.A., 2006. Regulation of HSL serine phosphorylation in skeletal muscle and adipose tissue. Am. J. Physiol. Endocrinol. Metab. 290: 500-508.

Wijkander, J., Landstrom, T.R., Manganiello, V., Belfrage, P., Degerman, E., 1998. Insulin-induced phosphorylation and activation of phosphodiesterase 3B in rat adiposes: Possible role for protein kinase B but not mitogen-activated protein kinase or p70 S6 kinase. Endocrinology 139: 219-227.

Xia JH, Liu JX, Zhou L, Li Z, Gui JF. 2008. Apo-14 is required for digestive system organogenesis during fish embryogenesis and larval development. Int J Dev Biol. 2008; 52(8): 1089-1098.

Yang, X., Zhang, X., Heckmann, B.L., Lu, X., Liu, J., 2011. Relative contribution of adipose triglyceride lipase and hormone-sensitive lipase to tumor necrosis factor-alpha (TNF-alpha) induced lipolysis in adipocytes. J. Biol. Chem. 286: 40477-40485.

Yeaman, S.J., 2004. Hormone-sensitive lipase - new roles for an old enzyme. Biochem. J. 379: 11-22.

Zhou, L., Wang, Y., Yao, B., Li, C., Ji, G., Gui, J., 2005. Molecular cloning and expression pattern of 14 kDa apolipoprotein in orange-spotted grouper, Epinephelus coioides. Comp. Biochem. Physiol., B: Comp. Biochem. 142: 432-437.

Zhao, J.T., Cowley, M.J., Lee, P., Birzniece, V., Kaplan, W., Ho, K.K.., 2011. Identification of novel GH-regulated pathway of lipid metabolism in adipose tissue: a gene expression study in hypopituitary men. J. Clin. Endocrinol. Metab. 96: 1188-1196.

Zhang, J., Hupfeld, C.J., Taylor, S.S., Olesky, J.M., Tsien, R.Y. 2005. Insulin disrupts beta-adrenergic signalling to protein kinase A in adipocytes. Nature 437: 569-573.